INRS
UNIVERSITÉ DE RECHERCHE

Université du Québec
Institut National de la Recherche Scientifique
Center Institut Armand-Frappier
Laval, Québec

MODELLING CHARGE SYNDROME IN THE ZEBRAFISH : A ROBUST TOOL FOR DRUG DISCOVERY

Betelhem Kassa

Report submitted to obtain a
Masters of Science (M.Sc.) degree
in Experimental Health Sciences

Examinators

Jury president and Internal examinator	Dr. Charles Ramassamy INRS-Institut Armand-Frappier
External examinator	Dr. Zoha Kibar Centre du recherche CHU Sainte Justine
Director of research	Dr. Kessen Patten INRS-Institut Armand-Frappier

ACKNOWLEDGEMENT

First, I would like to thank my heavenly Father, my Creator and my Greatest support, God. He has been opening all the doors of opportunity to me and helped me to accomplish what I could not even have dreamed of! Second, I would like to thank Dr. Kessen Patten for entrusting me this great and meaningful project. Thank you for all the guidance and for having patience with my sometimes slow progress. You were not only my supervisor, but also my mentor and advisor. I cannot thank you enough for all the support and kindness you showed me!

Third, I would like to thank the most caring and compassionate person in my life, my mom Hana Getachew and the most loving person in my life, my husband Abebe Mamo. They were always there to encourage me through all the ups and downs!

I would like to express my gratitude to the Fondation Armand-Frappier and Bell Canada for the invaluable financial support and sponsorship that helped me pay for my living expenses and tuition.

I would like to say thank you to the whole *C. elegans* team of Dr. Alex Parker for the collaboration and in specific Dr. Kathrin Schmeisser for the co-authorship of the drug discovery project. I am also grateful for my current and former lab mates, Priyanka Jamadagni, Zoé Butti, Maximilian Breuer, Marilou Préville; summer students Pierre-Alexandre Piec, Valentin Lemoine and Gabrielle Fortier; and Charlotte Zaouter who has taught me histological techniques and Jessy Tremblay for his invaluable guidance with the confocal imaging.

To all the people I got acquainted with at the institute, who made this journey enjoyable. Thank you all for the fun and for all the French you have taught me!

For the people who became so dear to me, Rita-Audrey Gouessé, Sarra Landri, Ilona Gdovinona and Lorenna Fernandes, thank you so much for being such good friends and I hope we will keep in touch!

DEDICATION

I would like to dedicate my work and my thesis to all the CHARGE syndrome patients around the world. I truly hope it can contribute to their well-being!

ABSTRACT

CHARGE Syndrome (CS) is a genetic disorder characterized by a complex array of birth defects, for which there is no treatment or cure. The majority of CS is caused by mutations in the gene *CHD7,* which encodes a chromatin remodeling protein. We have developed *C. elegans* and zebrafish mutants of *chd7* to model CS. Both simple genetic models were characterized and the defects related to CS were exploited for screening of potential therapeutic compounds. The *C. elegans* carrying a deletion mutation in the gene *chd-7,* have a pronounced impaired movement phenotype, and are short-lived. Our stable *chd7*$^{-/-}$ mutant zebrafish larvae exhibit a small head phenotype which was measured using the software, imageJ. Alcian blue staining displayed defects in craniofacial cartilage development and pericardial edema indicated heart defects in the mutant zebrafish. Moreover the *chd7*$^{-/-}$ zebrafish consistently lacked a swimbladder. The swimbladder development was studied in more detail. H&E staining showed hypoplastic swimbladder formation in the mutants and qRT-PCR results indicated downregulation of the gene *ctnnb1* and upregulation of the *Hh* related gene *wif1* in the *chd7*$^{-/-}$ zebrafish embryos. We also found that *chd7*$^{-/-}$ fish display hyperactivity, particularly in dark and immuno-fluorescence of acetylated α-tubulin could show aberrant axonal network development. The *C. elegans chd-7* mutants were initially used for a phenotypic drug screen of 3850 FDA-approved molecules. The motor phenotype of mutant *chd-7 C. elegans* was exploited in the context of a high-throughput *in vivo* drug screen to identify suppressors of the motor deficit. Fourty-nine compounds were found to be capable of rescuing the motor defects. Two of the 49 hits were most potent in rescuing the survival and motor abnormalities in the *C. elegans.* The two lead compounds were further validated in the zebrafish *chd7*-mutant. They were found to be potent in rescuing the hyperactivity phenotype and the neuronal developmental defects in the zebrafish mutant. We aspire that our study contributes to the acceleration of drug discovery to treat CS.

Key words: CHARGE syndrome, genetic models, zebrafish, *C. elegans, CHD7,* characterization, drug screening, CNS, drug discovery, swimbladder

RÉSUMÉ

Le syndrome de CHARGE (SC) est une maladie génétique caractérisée par un ensemble complexe de malformations congénitales, pour lesquelles il n'existe aucun traitement. La majorité du CS est causée par des mutations dans le gène *CHD7*, qui encode une protéine de remodelage de la chromatine. Nous avons développé des *C. elegans* et poisson zèbre pour modeler SC. Les deux modèles génétiques simples ont été caractérisés et les défauts liés au CS ont été exploités pour le dépistage de composés thérapeutiques potentiels. Les vers porteurs d'une mutation par délétion chez le gène *chd-7* présentent une altération de locomotion et une courte durée de vie. Nos larves de poisson zèbre mutantes (*chd7*$^{-/-}$) présentent une microcéphalie, mesuré par imageJ, des défauts de développement du cartilage crânio-facial ont démontrer par le cartilage coloration Alcian blue. Des mutantes poisson zèbre des défauts cardiaques et ne développent pas de vessie natatoire. De plus, le développement de la vessie natatoire a été étudié plus en détail, car il s'agissait d'un phénotype cohérent dans notre modèle. La coloration H&E indique une formation de vessie natatoire hypoplasique chez les mutants et l'analyse par qRT-PCR a indiqué une expression réduite du gène *ctnnb1* et une expression augmentée du gène *wif1* dans les *chd7*$^{-/-}$ embryons de poisson zèbre. Nous avons également constaté que les poissons *chd7*$^{-/-}$ présentent une hyperactivité, en particulier dans l'obscurité et l'immuno-fluorescence de l'acétyle α-tubulin pourrait montrer le développement aberrant de réseau axonal. Les mutants *chd-7* de *C. elegans* ont été initialement utilisés pour un criblage de médicaments de 3850 molécules approuvées par la FDA. Le phénotype moteur de *C. elegans* mutant a été exploité dans le cadre d'un criblage *in vivo* à haut débit de petites molécules afin d'identifier les suppresseurs du déficit moteur. Quarante-neuf composés se sont révélés capables de remédier à la déficience motrice. Deux des 49 molécules ont été les plus efficaces pour améliorer la survie et les anomalies motrices chez les *C. elegans*. Les deux composés principaux ont été validés chez le poisson zèbre *chd7*$^{-/-}$. Les deux composes améliorent le phénotype d'hyperactivité et les anomalies du développement neuronal chez le mutant *chd7*$^{-/-}$. Nous aspirons à ce que notre étude contribuera à accélérer la découverte de médicaments pour traiter la SC.

Mots clés: Syndrome CHARGE, modèles génétiques, poisson zèbre, *C. elegans, CHD7,* caractérisation, dépistage de drogues, CNS, découverte de médicaments, vessie natatoire

FRENCH SYNOPSIS

Introduction

Le syndrome CHARGE (SC) est un trouble génétique rare, caractérisé par une combinaison unique de multiples anomalies des organes. La majorité des patients atteints de SC présentent certains types de défauts du système nerveux central (SNC), qui entraînent des défauts structuraux du cerveau et des anomalies vestibulaires. Environ 92 % des patients atteints ont des anomalies dans au moins un nerf crânien. Les anomalies du SNC se manifestent notamment par une déficience intellectuelle et un comportement semblable à celui d'un autiste (Yu et al., 2013; Donna M. Martin, 2010; Kim D. Blake, Hartshorne, Lawand, Dailor, & Thelin, 2008).

La principale cause du SC est des mutations dans le gène Chromodomain Helicase DNA binding protein 7 (*CHD7*), qui encode un facteur de remodelage de la chromatine dépendant de l'ATP (Vissers et al., 2004a). Le CHD7 joue un rôle primordial dans la répression et l'activation des gènes du développement de manière temporel et tissulaire (Woodage, Basrai, Baxevanis, Hieter, & Collins, 1997a). De plus, ce gène est nécessaire pour une régulation épigénétique normale de l'expression des gènes du développement neuronal et cérébral, ainsi que pour un développement normal de la crête neurale (K. H. Kim & Roberts, 2013b; Feng et al., 2013; Bajpai et al., 2010). Le CHD7 joue aussi un rôle clé dans la prolifération et la différenciation des cellules souches, ainsi que des cellules progénitrices des organes fréquemment affectés dans le SC (Donna M. Martin, 2010).

L'expression et la fonction du CHD7 ont été étudiées dans diverses espèces, notamment : *Drosophila melanogaster*, *Xenopus laevis,* poisson zèbre (*Danio rerio*) et la souris (*Mus musculus*) (Steffen & Ringrose, 2014; Bajpai et al., 2010; Patten et al., 2012; Bosman et al., 2005). Le CHD7 est l'un des quatre homologues de la protéine Kismet dans la *Drosophila melanogaster.* Kismet est une famille de protéine de *trithorax* (*trx*) que favorisent l'allongement de la transcription par polymérase de l'ARN II (Srinivasan, Dorighi, & Tamkun, 2008). Les souris hétérozygotes Ethylnitrosourea (ENU) mutantes de *Chd7* possèdent la plupart des phénotypes observés chez les patients atteints du SC, incluant des troubles de l'équilibre, l'hyperactivité, une perturbation des canaux semi-circulaires latéraux, une croissance postnatale réduite, une fente palatine, une atrésie des choanes, des anomalies cardiaques et des défauts olfactifs (Bosman et al., 2005). La perte de la fonction du *Chd7,* chez les souris, est létale au stade embryonnaire, et les souris présentent de graves défauts dans de nombreux tissus et organes en développement (Elizabeth A. Hurd et al., 2007). Cette perte de fonction chez la souris montre des phénotypes semblables aux patients humains atteints de SC, cela pourrait suggérer une conservation du Chd7 entre les différentes espèces.

De plus, chez le poisson zèbre, l'expression embryonnaire et la fonction du Chd7 est conservée. (Patten et al., 2012; Bosman et al., 2005). Le gène *chd7* du poisson zèbre est situé sur le chromosome 2 et les domaines fonctionnels de la protéine sont conservés entre le poisson zèbre et l'humain. Les domaines de protéines du poisson-zèbre comprennent des chromodomaines en tandem N-terminal, un domaine central de type SNF2 ATPase/helicase et un domaine BRK C-terminal (Balow et al., 2013). Dans l'ensemble, l'alignement de la séquence *Chd7* du poisson zèbre avec celui du CHD7 humain montre une similitude de 69 % au niveau de l'acide aminé. La **Figure 1.5**, montre une image schématique des domaines CHD7 chez l'humain par rapport aux domaines *Chd7* chez le poisson zèbre, avec les emplacements envisagés des domaines protéiques (Balow et al., 2013).

Objectifs et hypothèses

Étant donné que le SC est un trouble du développement très complexe et que l'étude du gène causal *CHD7* est toujours en cours, un dépistage génétique rapide est une approche prometteuse vers la découverte de médicaments. Ainsi, les premiers objectifs de cette étude étaient d'établir une lignée stable de poissons zèbres mutants *chd7*. Deuxièmement, caractériser toutes anomalies de phénotype/locomoteur dans cette lignée transgénique et troisièmement, dépister et valider les composés potentiels, découverts dans le système *C. elegans*, dans le poisson zèbre mutant *chd7*. En ce qui concerne les objectifs, notre hypothèse était d'abord que nos poissons stables et mutants développeront les phénotypes principaux et les défauts liés au SC. Après la caractérisation des phénotypes pertinents, nous avons émis l'hypothèse que nous pouvons identifier le potentiel d'amélioration des deux molécules cibles (Fisetin et éphédrine), ou au moins l'une d'entre elles.

Résultats et méthodes : génération et caractérisation de la ligne mutante du *chd7*

La technique relativement nouvelle de modification génomique CRISPR/Cas9 a été utilisée pour établir notre lignée stable de mutants du *chd7*. L'ARN guide ('ARNg) et le Cas9 ont été injectés dans des œufs de poisson-zèbre à un stade des cellules et l'ARNg ciblait la séquence du domaine hélicase de la région de codage du *chd7*. L'analyse qPCR pourrait montrer une diminution significative de l'expression du *chd7* dans les poissons hétérozygotes (Chd7 +/-) et homozygotes (Chd7 -/-), voir la **Figure 3.1D**. Toutefois, les poissons hétérozygotes n'ont pas montrés de différence morphologique ou de survie significative en comparaison avec des poissons wildtypes. Ainsi, une caractérisation plus poussée a été effectuée uniquement pour les embryons/larves mutants homozygotes.

Nous avons observés plusieurs défauts chez le poisson chd7$^{-/-}$ qui correspondent aux phénotypes du SC chez les patients humains. Nous avons suivi la survie des mutants par rapport aux wildtypes, et observé leur développement morphologique au moyen de la brightfield microscopy (Leica S6E). La durée de vie des mutants homozygotes a été considérablement réduite, notamment de 9 jours post fertilisation (jpf), comparativement à la durée de vie des mutants hétérozygotes et des wildtypes (**Figure 3.2D**). Les larves de *chd7*$^{-/-}$ présentaient une forme (grave ou légère) de courbure du corps, voir la **Figure 3.2A**. Les défauts de la physiologie cardiaque sont clairement observables à partir du taux plus élevé d'œdème dans le mutant comparativement aux témoins (**Figures 23.C** et 3.**2F**). De plus, la taille de la tête a été mesurée dans des larves de 3 jpf à l'aide du logiciel ImageJ et était beaucoup plus petite chez les mutants (**Figure 3.2E**). Les colorations du cartilage avec Alcian bleu pouvaient rendre visible la structure cranio-facial, qui a également été évaluée puisque les mutants semblaient avoir une tête et une face plus petites et malformées. La coloration bleue du cartilage a montré que la structure cranio-faciale des mutants était légèrement ou gravement déformée dans les larves de *chd7*$^{-/-}$. La mesure du cartilage du Meckel, qui correspond à la mâchoire inférieure chez les humains, a révélé une augmentation significative chez des mutants (**Figure 3.3**). Cela correspond à la malformation cranio-faciale chez les patients humains (Bajpai et al., 2010). La majorité des patients atteints du SC ont un visage carré en plus de la paralysie faciale et de l'asymétrie (Sanlaville & Verloes, 2007).

De plus, nous nous sommes concentrés sur un autre phénotype du SC - le retard de développement et l'inflammation de la vessie natatoire chez les poissons mutants (**Figure 3.4**).

La coloration H&E (Hematoxylin & Eosin) a été effectuée afin d'évaluer l'histologie de la vessie natatoire, qui s'est révélée hypoplasique chez les mutants *chd7*. De plus, certains gènes importants qui sont liés au développement de la vessie natatoire, comme la signalisation de *Wnt* et *Hh*, ont été analysés par qRT-PCR (**Figure 3.5**). Le niveau d'expression des gènes *sox2*, *wif1* et *ctnnb1* a été analysé. Ce dernier est l'un des gènes principal de la voie de signalisation de *Wnt*. Il est souvent utilisé comme mesure de l'activité de signalisation de *Wnt*. En effet, l'accumulation de *ctnnb1* et de sa translocation au noyau, active la signalisation de *Wnt* (Reya & Clevers, 2005). Le gène *sox2* est le premier marqueur épithélial de la vessie natatoire, et de nombreux gènes de la famille SOX sont connus pour moduler la signalisation canonique WNT/Beta-catenin dans le développement normal ainsi que dans certaines maladies (Yin et al., 2011; Kormish, Sinner, & Zorn, 2009). De plus, on sait que le facteur de transcription Sox2 interagit physiquement avec le Chd7 (Engelen et al., 2011). Le gène *wif1* est un gène cible de *Hh* et un inhibiteur de la voie *Wnt* (Yin, Korzh, & Gong, 2012a). Nos résultats qRT-PCR ont montré que l'expression de *wif1* est considérablement régulée et que l'expression de bêta-caténin (*ctnnb1*) est significativement réduite dans les embryons *chd7*$^{-/-}$ (**Figure 3.5B** et **3.C),** indiquant que le *Chd7* pourrait affecter les gènes impliqués dans le *Wnt* ainsi que la signalisation *Hh*.

Une autre caractéristique majeure, était l'observation du comportement de la nage. Ceci a été fait, car les troubles du sommeil, l'hyperactivité nocturne, l'OCD et les comportements autistes sont présents chez la plupart des patients atteints de SC (Hartshorne et al., 2009; Hartshorne, Hefner, et al., 2005). La distance de nage a été quantifiée en heures données. Il a été surveillé par deux cycles du lumière-obscurité de 4h-4h dans la chambre d'enregistrement de DanioVision (Noldus) couplée à la caméra Basler GenIcam. L'analyse a été effectuée à l'aide du logiciel EthoVision XT12 (Noldus). Les résultats ont montrés que les larves de *chd7*$^{-/-}$ sont très hyperactives comparativement aux larves de *chd7*$^{+/-}$ et aux wildtypes (**Figure 3.6A**). Leur hyperactivité était plus marquée pendant les cycles nocturnes (**Figure 3.6B**). L'hyperactivité pendant la nuit était également observé dans les modèles poisson zèbres de troubles du spectre autistique (TSA) dans une autre étude (Hoffman et al., 2016).

Ensuite, le développement du réseau neuronal a été évalué en effectuant l'immunofluorescence acétyl-tubulin. Les embryons ont été montés dans les positions correspondantes (latéralement pour 28 jpf et dorsalement pour 48 jpf) et imagés au microscope confocal (Zeiss LSM780). Cela a révélé plusieurs défauts dans le réseau et l'organisation des nerfs crâniens et de la région du cerveau du tectum optique (**Figure 3.7**). Plus précisément, l'organisation des nerfs trijumeaux est déformée et la ramification axonale est aberrante dans les régions cérébrales évaluées.

Les résultats du criblage de médicaments

En combinant les avantages des organismes simples, le *C. elegans* et le poisson zèbre. Ces modèles animaux se sont révélés prometteurs comme outil pour une découverte rapide de médicaments suite à des collaborations entre le Dr. Patten et le Dr. Parker (Patten et al., 2016; Patten et al., 2017). La même approche a été utilisée pour découvrir des composés qui pourraient sauver/améliorer les phénotypes liés aux SC. Dans le cadre d'un projet de collaboration, le laboratoire du Dr. Parker a décrit une délétion d'environ 700 pb dans le gène *chd-7* de *C. elegans* (**Figure 4.1A**), dans la ligne mutante *chd-7*(*gk290*) acquise du *Caenorhabditis* Genetics Center. Les homozygote mutants *C. elegans* avaient une durée de vie plus courte que les wildtypes (**Figure 4.1C**) et ils présentaient un défaut de locomotion à la nage (**Figure 4.1B**). L'affaiblissement de la locomotion a été exploité comme mesure de résultat pour un examen rapide de 3850 petits produits chimiques approuvés par la FDA. De

ce nombre, quarante-neuf composés avaient un potentiel afin d'améliorer partiellement la locomotion des vers *chd-7* (*gk290*). En particulier, deux composés, Fisetin et Ephedrine, étaient particulièrement efficaces pour améliorer le mouvement de nage du *C. elegans* mutant (**Figure 4.2A**). Ces composés ont également augmenté considérablement la durée de vie des vers *chd-7* (*gk290*) (**Figure 4.2B**).Dans mon mémoire, Fisetine et Éphédrine ont été validé dans le *chd7*-mutant du poisson zèbre, établi par le Dr. Patten.

Le comportement anormal de la nage des larves de *chd7*$^{-/-}$ poisson zèbre a d'abord été utilisé comme dépistage principal. Les *chd7* mutants traité avec de la Fisetine ou de l'éphédrine ont montrés une réponse de nage d'hyperactivité réduite, évaluée par la distance de nage pendant les cycles de obscurité (**Figure 4.3**). Les composés n'ont eu aucun effet sur les poissons *chd7*$^{+/+}$ (WT). Ensuite, les deux composés ont été testés sur les défauts de développement du réseau neuronal, l'œdème, le développement de la vessie natatoire et la survie. Les deux étaient puissants dans l'atténuation des défauts neuronaux. Le réseau de groupement des ganglions trijumeaux ainsi que la migration axonale semblent avoir été améliorés après traitement à la Fisetine ou à l'Éphédrine (**Figure 4.4A**). Le développement du réseau des commissural axones a été partiellement amélioré dans les deux groupes de traitement (**Figure 4.4B**). Et la région du tectum optique était plus dense et plus grande dans les groupes de traitement (**Figure 4.4C**). Dans l'ensemble, Fisetin et Éphédrine semblent avoir un effet positif sur les défauts du SNC. De plus, les composés ont également réduit le taux d'œdème péricardiaque. Plus précisément, l'œdème dans le groupe de l'éphédrine était aussi faible que dans les wildtypes (**Figure 4.5A**). Cependant, elles ne pouvaient pas entraîner une augmentation de la durée de vie et du développement de la vessie natatoire (**Figure 4.5B** et **4.5C**). Nous pensons que leur mécanisme pourrait être limité à la voie de développement neuronal, ce qui exige une étude plus approfondie.

Discussion et conclusion

Dans cette étude, nous avons réussi à établir une lignée mutante *chd7* chez le poisson zèbre, et à notre connaissance, c'est la première. Cette lignée possède les défauts de développement liés au SC et en utilisant cette dernière, nous avons examinés les composés cibles comme remèdes potentiels pour améliorer ou sauver les caractéristiques liées au SC. De plus, cette lignée sera très utile pour étudier le rôle du CHD7 dans la pathogenèse du SC ainsi que le développement neuronal normal. Les produits chimiques approuvés par la FDA, l'éphédrine et la Fisetin, semblent efficaces pour supprimer l'hyperactivité et améliorer les connexions ainsi que le réseau neuronales dans les mutants chd7$^{-/-}$ du poisson zèbre. Ainsi, en plus d'être un remède possible aux symptômes neuronaux du SC, ils pourraient aussi bien être réorientés pour traiter d'autres troubles neurocomportementaux comme le TSA (Trouble du Spectre de l'Autisme). Dans l'ensemble, mon projet a pour but de mieux comprendre la pathogenèse du SC et d'accélérer le développement thérapeutique. Mon aspiration est que les composés principaux puissent être utilisés pour traiter les phénotypes liés au SC ou même les anomalies neurocomportementales liées au TSA, un jour.

TABLE OF CONTENTS

LIST OF TABLES

CHAPTER 1: LITERATURE REVIEW AND INTRODUCTION

CHAPTER 2: MATERIALS AND METHODS

LIST OF FIGURES

CHAPTER 1: INTRODUCTION

CHAPTER 2: MATERIALS AND METHODS

CHAPTER 3: RESULTS

CHAPTER 4: SCREENING OF SMALL MOLECULES THAT POTENTIALLY AMELIORATE CHARGE SYNDROME PHENOTYPES

LIST OF ABBREVIATIONS

µm	micro molar
ABC	Autism Behavior Checklist
AD	Alzheimer's disease
AMO	Antisense Morpholino Oligonucleotide
ASD	Autism spectrum disorder
ATP	Adenosine Triphosphate
BAF	Brg/Brahma-Associated Factor
BMP	Bone Morphogenic Protein
BRK	Brahma and Kismet
C. elegans	Caenorhabditis elegans
cAMP	Cyclic Adenosine Monophosphate
Cas9	CRISR associated protein 9
CHD	Chromodomain Helicase DNA-binding protein
CHD7	Chromodomain Helicase DNA-binding protein 7
CMS	Congenital Myasthenic Syndromes
CN	Cranial Nerve
CNS	Central Nervous System
CRF	Chromatin Remodeling Factor
CRISPR	Clustered Regularly Interspaced Short Palindromic Repeats
CS	CHARGE syndrome
Ctnnb1	catenin β-1
DKK3	Dickkopfs-3
Dpf	Day(s) post fertilization
DRC	Dorsolateral Cluster
e.g	example
EMT	Epithelial Mesenchymal Transition
ENU	Ethylnitrosourea
ERK	Extracellular signal-Regulated Kinase
ESC	Embryonic Stem Cell
FAM124B	Family with sequence similarity 124 member B

FDA	Food and Drug Administration
FGF8	Fibroblast Growth Factor 8
GABA	Gamma-Aminobutyric Acid
Gabra1	γ-aminobutyric acid receptor subunit1
GFP	green fluorescence protein
Hh	Hedgehog
HMB	High Mobility Group box
Hpf	hour(s) post fertilization
iPSC	induced Pluripotent Stem Cells
NCC	Neural Crest Cell
NMJ	Neuromuscular Junction
NSF	N-ethylmaleimide Sensitive Factor
O/N	Over Night
OCD	Obsessive Compulsive Disorders
PBAF	Polybromo BRG1- associated Factor containing complex
PcG	Polycomb group
rDNA	ribosomal DNA
rRNA	ribosomal RNA
SANT	Swi3, Ada2, N-cor, and TFIIIB
SEMA3E	Semaphorine 3E
SGZ	Sub Granular Zone
SOT	Supra-Optic Tract
SOX2	Sry-related HMG bOX-2
SVZ	Sub ventricular Zone
SWI/SNF	SWItch/sucrose Non-Fermentable
TALEN	Transcription Activator-Like Effector Nuclease
TBX1	T-box transcription factor-1
TCF-2	T-cell Factor-2
Trx	trithorax
Wif1	*Wnt* Inhibitory factor-1
Wnt	Wingless/integrated
ZFN	Zinc Finger Nuclease

CHAPTER 1: INTRODUCTION

1.1 CHARGE syndrome

CHARGE syndrome (CS) is a complex genetic disorder marked by a wide range of organs and organ systems defects (Balow et al., 2013). The CHARGE acronym stands for and includes most of the major clinical features observed in CS patients, which are **C**oloboma of the eye, congenital **H**eart defect, **A**tresia of the choanae, **R**etardation of growth and development, **G**enital abnormalities, and outer and inner **E**ar anomalies (Seema R Lalani, Hefner, Belmont, & Davenport, 1993a). Even though the acronym covers most cardinal outcomes of CS, there are other defects which are also observed in a relatively high percentage of patients but are not included in the acronym, for instance abnormalities of the Central Nervous System (CNS) form one of the major challenges in CS and have been correlated to poor life expectancy (Tellier et al., 1998). They are manifested among others, in swallowing problems, delay of the motor development and autistic-like behavior (Seema R Lalani et al., 1993a; D. Brown, 2005; Zentner, Layman, Martin, & Scacheri, 2010b). The CNS abnormalities in CS will be discussed in more detail in the next section.

Nearly all of the CS patients have a characteristic dysmorphism of the facial and external ear structures. They have a square-shaped face, a narrow forehead, broad nasal bridge, small and inverted V-shaped upper lip. Facial paralysis and dysplasia of the outer ears often lead to a pronounced asymmetrical face. Between 15 % to 20 % of CS patients also have cleft lip or palate, which leads to deformed facial structure (Damien Sanlaville & Verloes, 2007). The structures that make up the inner, outer ear as well as the bones that make up the facial structure such as the jaw are affected in more than 90% of CHARGE patients. The external ear is cup-shaped and asymmetrical. The concha space is triangular and the antihelix does not connect to the antiragus as in normally developed outer ear. Additionally some parts of the helix can be snipped off. These distinctive external ear characteristics by themselves can lead to consideration of CHARGE diagnosis (Davenport, Hefner, & Thelin, 1986). Inner ear anomalies include, hypoplasia or aplasia of the three semicircular canals (Guyot, Gacek, & DiRaddo, 1987) which are connected to the cochlea and also function as hearing and balance sensory structures. In addition the cochlea itself can also be affected in CS, which is referred as mondini malformation, where the cochlea is less coiled than normal (Morgan et al., 1993). Moreover, the dental development can also be affected in CS. Reported dental anomalies include oligodontia, where there are six or more primary or permanent teeth are missing and a delayed eruption of the teeth (Al, Cottrell, & Hughes, n.d.).

The developmental defects and dysfunctions arising from CS show variable percentages of penetration, where some of them are present in almost all of the patients and some occur in a fraction of the CS cases (W. S. Layman, Hurd, & Martin, 2010). The variable penetration of the CS features makes diagnosis very challenging. Ravenswaaij-Arts and colleagues calculated averages of the frequency of the most important defects in CHARGE after reviewing at least three independent publication of cases (van Ravenswaaij-Arts & Martin, 2017). According to their summary the incidence of each anomaly is as follows: coloboma of the eye is present in 80% of CHARGE patients, where the development of the structures that make up the eye, such as the iris and retina is affected leading to blindness and microphthalmia in some cases. Congenital heart defects are found in 78% of CHARGE cases (van Ravenswaaij-Arts & Martin, 2017). The most frequently observed heart defects involve conotruncal malformations, which are a group of cardiac outflow tract anomalies that include tetralogy of fallot, pulmonary atresia

with ventricular septa defect, interrupted aortic arch, double-outlet right ventricle and truncus arteriosus. Also atrioventricular canal defects have been observed (Seema R Lalani, Hefner, Belmont, & Davenport, 1993b). Bilateral or unilateral atresia of the choanae is observed in 49% of CHARGE patients. Choanal atresia or stenosis, is the failure of the oro-nasal cavity to recanalize well, where a membranous or bony structure remains (Zentner, Layman, et al., 2010b; Bergman et al., 2011). Additionally, Some fraction of the patients (50-60%) also have genital abnormalities, which result in cryptorchidism or micropenis in males, hypoplastic labia in females and hypogonadotropic hypogonadism in both males and females (Seema R Lalani et al., 1993b).

Pathogenic variable mutations of Chromodomain Helicase DNA binding protein 7 (*CHD7*) were found to be responsible for CS pathogenesis in 2004 (Vissers et al., 2004a). There is to date no medical treatment or alleviation for this complex developmental disorder. The incidence of CS is estimated to be 0.1-1.2 in 10,000 live births, depending on the professional recognition and classification of the associations as CS (Kim D Blake & Prasad, 2006). The incidence rate also differs regionally. For instance in Canada the highest provincial prevalence over three years is estimated to be 1 in 8500 live births, in the maritime provinces New Brunswick, Nova Scotia, and Prince Edward Island (Issekutz, Graham, Prasad, Smith, & Blake, 2005). The life expectancy of CS patients can range between 5 days (Issekutz et al., 2005) to 46 years (M C J Jongmans et al., 2006). The mortality rate is highest in the group having combination of choanal atresia and heart defects or trachea-esophageal fistula. The high prevalence of swallowing and feeding difficulties in combination with gastro-esophageal reflux are also associated with overall mortality in infants and other patients of CS (K. D. Blake et al., 1998).

The heterogeneity and variable penetration of the organs affected in CS makes diagnosis a complex process. However, because of the non-random combination of the defects and the distinct facial/ear dysmorphisms, CS can be recognized clinically (Kim D Blake & Prasad, 2006). Molecular confirmation is also possible since the discovery of the causative gene *CHD7*, which has been found to have pathogenic mutations in most CS patients. This gene encodes Chromodomain Helicase DNA binding protein 7 (Vissers et al., 2004a). A pathogenic variant mutation of *CHD7* have been found in 70-90% of suspected cases of CHARGE (Zentner, Layman, et al., 2010b). However, when strict diagnostic is applied, a mutated *CHD7* is found in more than 90% of the cases (J. E. H. Bergman et al., 2011a). Mutations that lead to loss of function of CHD7 are found to result in CS. The most reported mutations from a big cohort study of 360 *CHD7* mutations in the Netherlands, were either frameshift or nonsense with 70% occurrence, 13 % missense and 17% splice site. Deletion mutations were rare with less than 1% occurrence (J. E. H. Bergman et al., 2011b). The structure, function and interaction partners of protein CHD7 discussed in more detail in following sections.

1.1.2 Diagnosis of CHARGE syndrome

The diagnosis of Cs is based on combination of major and minor characteristics. The major features of CS are those that are most commonly observed in CS and less commonly observed in other syndromes. Minor characteristics are common in CS but are either less specific, like heart defect, or they are hard to evaluate consistently (e.g. Facial dysmorphia). Moreover, the minor criteria are less clear to be conclusive about during infancy (Seema R Lalani et al., 1993b). All the major and minor features in CS are summarized in **Table 1.1.** Definite CS can be diagnosed if the individual presents with all four major or three major and three minor characteristics. Possible or probable CS can be diagnosed when a person presents with one or two major or several minor characteristics (Seema R Lalani et al., 1993b). Prenatal detection of CS is also possible. In case of CS suspicion or polyhydramnios, focused ultrasound could be used to detect external ear anomalies, choanal atresia, semicircular canal agenesis and arhinencephaly, which leads to a high detection rate (Busa et al., 2016).

Table 1.1: The major and minor clinical criteria for CHARGE syndrome diagnosis

Major criterion	**Features/manifestations**	**Frequency**
Coloboma	Coloboma of iris, retina, choroid or disc leading to microphthalmia or anophthalmia	80-90%
Choanal atresia	Unilateral (UL) or Bilateral (BL); bony or membranous; Stenosis or atresia	50-60%
Cranial nerve dysfunction	I: lack of smell VII: facial palsy (UL or BL) VIII: sensorineuronal hearing loss or vestibular problems IX/X: swallowing dysfunction	Frequent >40% 70-85% 70-90%
Characteristic CHARGE ears**	External ear: short, wide and asymmetrical ears with little to no lobe, snipped off helix, prominent antihelix discontinuous with tragus, triangular concha, decreased cartilage and often laterally protruding ears.	90%
Minor criterion	**Features/manifestations**	**frequency**
Characteristic CHARGE face	Square shaped head with broad prominent forehead, big eyes, prominent nasal bridge, flat midface, small mouth, occasional small chin which becomes larger with age, facial asymmetry even if there is no facial palsy	>50%
Characteristic CHARGE hands	Small thumb, broad palm with "hocky stick" shaped palmar line, short fingers	50%
Genital hypoplasia	Males: cryptorchidism, micropenis Females: small labia Both: delayed or incomplete pubertal development	70-85% Frequent 50% ?
Congenital heart defects	Most common: tetralogy of fallot, VSD, AV canal, Aortic arch anomalies	70-85%
Cleft lip/cleft palate	UL or BL cleft lip +/- cleft palate	20-30%
TEF	Tracheo-esophageal atresia or fistula Esophageal atresia	20% 15%
Middle ear	Frequent ear infections	>80%
hypotonia	Upper body hypotonia, sloping shoulders	Frequent
Renal anomalies	Hydronephrosis or reflux; horse shoe shaped kidney; small or absent kidney	40%
Growth deficiency	Short stature Growth hormone deficiency	Common Rare

** The external ear features are so specific that it is possible to suggest CHARGE diagnosis based on the ears alone. Modified from Meg Hefner's report (Hefner, 1999).

Moreover, since the discovery of *CHD7* mutations as the major cause of CS, there is a routine screening of this gene in possible CHARGE patients. The DNA of patients is isolated from peripheral blood and *CHD7* is amplified by PCR using primers that target the 37 coding exons (exons 2-38, RefseqNM_017780-02) and their flanking intron sequences (M C J Jongmans et al., 2006).

The management of CS requires a well-coordinated multidisciplinary approach. This is necessary for a good life quality of a CS patient and for an improved survival, since there is no medical treatment available (Seema R Lalani et al., 1993a). The primary focus of early management should be on airway stabilization and circulatory support in case of combined heart defect and choanal atresia. Additionally, choanal atresia can be surgically corrected (K. D. Blake et al., 1998). Management of feeding difficulties is also crucial, which often means gastrostomy feeding. Eye examination by an ophthalmologist as well as hearing examination by an audiologist are also required (Kim D Blake & Prasad, 2006). Adapted education and therapeutic services to help the patient adapt to dual auditory and visual sensory impairment should be introduced as early as possible in the child's life (BLAKE & BROWN, 1993; Tellier et al., 1996).

1.1.3 Brain and cranial nerve involvements in CHARGE

The CNS is affected in CS and has been regarded as one of the major criterion of CS diagnosis for a while. Children and adults with CS have many CNS dysfunctions that are manifested in intellectual disabilities, cranial nerve impairments and autistic-like behaviors among others. The majority of CS patients have some (mild to severe) form of intellectual disability and exhibit structural abnormalities of cerebellar vermis and corpus collosum (Yu et al., 2013; Donna M. Martin, 2010). Intellectual ability is affected in around 79% of the CS case (Zentner, Layman, et al., 2010b; Bergman et al., 2011). Up to 99% of CS patients show retardation of the cognitive development and/or motor development, that might be partially due to general illness, dual sensory impairment and vestibular dysfunction (J. E. H. Bergman et al., 2011a). Other developmental abnormalities include delayed motor milestones. A British survey found that on average CS patients start walking independently at the age of 4 (D. Brown, 2005).

There are also many reports of CS patients with white matter defects in their brains (Gregory et al., 2013a; Liu, Yu, Wang, Mo, & Yu, 2014). In a review of 47 CS patients with post mortem examination or a computerized axial tomography scan, 55% were shown to have CNS malformations. The malformations were manifested in archinencephaly; which is incomplete development of the forebrain structures, such as the olfactory bulb and its nerve tracts, holoprosencephaly, hindbrain defects and other defects (Lin, Siebert, & Graham, 1990). Last but not least, CS has also been associated to a structurally abnormal pituitary gland (Gregory et al., 2013b). The presence of CNS involvement was most strongly correlated with choanal atresia (Lin et al., 1990).

From a total of 99 CS cases that were analyzed in the study of Blake and colleagues, 92% had symptoms of at least one Cranial nerve (CN) involvement and 77% reported one or two CN impairment. Symptoms recorded by clinicians as evidence for CN involvement are Weak chewing and/or sucking (CN V) facial palsy (CN VII), sensorineural hearing loss (CN VIII), balance vestibular problems (CN VIII), and swallowing problems (CN IX/ X). The highest correlation with diagnosis certainty is CN IX/X involvement and involvement of vestibular nerve CN VIII is the weakest predictor of CS (Kim D. Blake, Hartshorne, Lawand, Dailor, & Thelin,

2008). Accordingly, feeding difficulties because of the swallowing problems are the major cause of morbidity among CS patients in all age groups (Seema R Lalani et al., 1993a).

Other specific CNS anomalies linked to CS are auditory nerve anomalies (cranial nerve VIII), that connect the cochlea to the brainstem and the brainstem to the brain. These anomalies may lead to Central Auditory Processing Disorder (CAPD) (Thelin & Fussner, 2005). Most frequently observed manifestations of CAPD are difficulties of filtering out significant information from all other noises, and difficulties to process/understand speech (D. Brown, 2005).

The CNS effects are also manifested in olfaction defects. In a case study of 10 CS patients, high resolution Magnetic Resonance Imaging (MRI) showed that all the patients had either hypoplasia or absence of the olfactory bulbs and the olfactory sulci (Blustajn, Kirsch, Panigrahy, & Netchine, 2008). Other important manifestation of the CNS anomalies are hyperactivity and autistic-like behaviors, which will be discussed in detail in the following sub-sections (Zentner, Layman, Martin, & Scacheri, 2010a).

1.1.4 Behavioral features of CHARGE syndrome patients

As stated before, the eyes and ears are often affected in CS. Thus, deafness and blindness can occur in combination or independently, in severe or mild forms in 80-90% of the individuals with CS (Hartshorne, Hefner, & Davenport, 2005). This can affect the children's ability to receive any sensory information or adjust their behavior to their environment. It can also be a big barrier for learning and communication. Although some behavioral issues might be due to loss or decrease of sensory input, others might be integral part of the CNS defects as many researchers have shown (Blake & Brown, 1993).

Individuals with CS indeed have many behavioral abnormalities which are distinct from children affected with other syndromes with or without deaf-blindness. An anecdote of two highly educated women in their 40's who independently diagnosed themselves with CS proves this point. They reported that they struggle with Obsessive-Compulsive Disorder (OCD). One of the women is nearly blind and had hearing loss, the other had severe hearing loss but a good vision. This OCD tendency observed in many children and young adults with CS might be one of the concrete behavioral features of CS. Many parents of children with CS have also reported autistic-like, attention deficit as well as tic disorders (Hartshorne, Hefner, et al., 2005).

Furthermore, sleep disorder was represented in 57.5% of CS patients according to a cohort study of Hartshorne and colleagues (Hartshorne et al., 2009). Analysis of anecdotal reports from 87 patients between the age of 6 and 18 years indicated the presence of sleep disturbances. Most commonly the patients had problems initiating sleep and maintaining it as well as sleep breathing and sleep-wake transition. Sleep disturbances seemed to be significantly correlated to a later age onset of walking, but not to craniofacial anomalies, which might point out its neuronal origin (Hartshorne et al., 2009).

1.1.5 Autistic-like behavior in CHARGE syndrome patients

Part of the behavioral outcomes in CS are very similar to behavioral and cognitive anomalies in Autistic Spectrum Disorder (ASD). For this reason 27,5% of CS patient can be classified as autistic (Hartshorne, Grialou, & Parker, 2005). Children with CS show many autism spectrum related behaviors such as Obsessive Compulsive Disorders (OCD), social interaction abnormalities, self- stimulation as well as self-abuse among others.

Hartshorne and his colleagues (Hartshorne, Grialou, et al., 2005) set out to study characteristics of autistic-like behaviors in CS patients. To do this, they had 160 useful surveys back from families of 204 children with CS. The results showed that the total score of CS group on Autism Behavior Checklist (ABC) significantly differs from the autism and deaf-blind groups. Higher scores of autism-like behaviors in CS patients were significantly correlated with walking at older age. CS patients who were deaf-blind had more challenging behavior than those without deaf-blindness. This is understandable regarding that coping with multisensory defect makes life very challenging. However, the deaf-blindness in CS cannot be labeled as the only cause of autism-like behavior in CS, as the other deaf-blind group had a distinct score on the ABC from CS deaf-blind patients (Hartshorne, Grialou, et al., 2005). Another study suggested that neuro-endocrine dysfunctions might underly autistic-like behavior in CS (Fernell et al., 2007).

1.1.5.1 CHD7 and CHD8 mutations elevate the risk on Autism Spectrum Disorder

ASDs are believed to be caused by combination of genetic and environmental factors. However, specific causes could be identified in only small fraction of individuals with ASD. Many studies, focused on performing whole exome sequencing combined with protein-protein interaction bioinformatics data as well as case-control studies, could isolate a number of risk genes related to ASD (Jiang et al., 2013; Neale et al., 2012). A study that coupled *de novo* mutation events to a case-control study could prove that mutations in *CHD8* are among the genuine autism risk factors (Neale et al., 2012).

In another study, *de novo* mutations in *CHD7* and *CHD8* were discovered to be responsible for ASD pathogenesis among many other genes. As mentioned earlier, ASD-like behaviors have been found in two third of the CS patients, indicating that *CHD7* might play a role in the syndromic subtype of ASD (O'Roak et al., 2012)

1.2 The genetics of CHARGE syndrome

The primary cause of CS is mutation of the gene Chromodomain Helicase DNA binding protein 7 (*CHD7*), which encodes an ATP-dependent chromatin remodeling factor (Vissers et al., 2004a). Vissers et al identified a 2.3-Mb de novo overlapping microdeletion on chromosome 8q12 by array comparative genomic hybridization in two individuals with CHARGE syndrome. Sequence analysis of genes located in this region detected mutations in the gene CHD7 and mutations in CHD7 was further confirmed in several individuals with CHARGE syndrome.

CHD7 plays a crucial role in repressing and activating developmental genes in a time- and tissue-specific manner (Woodage, Basrai, Baxevanis, Hieter, & Collins, 1997a). While most *CHD7* mutations are unique and sporadic, there have been some reports of familial germline mosaicism cases, with a 2-3% chance of recurrence risk for parents with children that have *de novo* mutations (M. Albert Basson & van Ravenswaaij-Arts, 2015). CS patients have 50% chance of transmitting the dominant mutation to their offsprings (S Pauli et al., 2009).

Woodage and colleagues found that the CHD proteins can alter gene expression by affecting chromatin structure, which alters the access of the transcriptional apparatus to its DNA template (Woodage, Basrai, Baxevanis, Hieter, & Collins, 1997b). CHD7 seems to be required for the proper development of the cell-types that give rise to organs and tissues affected in CS, where it regulates the expression of genes involved in cell proliferation, differentiation, and migration (Zentner, Layman, et al., 2010a).

1.2.1 Genotype-phenotype correlations

Since the discovery of *CHD7* as the causative gene for CS in the year 2004, 528 different mutations of the gene have been described. However, a clear correlation between the genotype or the kind of mutation and the phenotype has not been established (www.CHD7.org) (Janssen et al., 2012). From what is known, most common features in *CHD7* mutation-positive patients are, external ear malformations (91%) temporal bone anomalies (98%) and hearing loss (89%) (Zentner, Layman, et al., 2010b).

The penetrance of all the defects in CS is so variable that even rare familial cases of CS with identical *CHD7* mutations display striking differences in phenotype (Marjolijn C.J. Jongmans et al., 2008). Missense variant mutations are in general correlated with milder phenotypes, and lower frequency of congenital heart defects, choanal atresia, cleft lip and/or palate (M C J Jongmans et al., 2006; Jorieke E.H. Bergman et al., 2012). In the rare familial cases with parent-to-child transmission, the children often display atypical CS phenotypes (J. E. H. Bergman et al., 2011a). Except these two correlations, there is no other established correlation of the genotype with the phenotype of CS patients (M. Albert Basson & van Ravenswaaij-Arts, 2015). All in all, the great variability of the CS associated features suggests a pleiotropic developmental defect arising from the *CHD7* mutations. However, clear mechanisms of pathogenesis and in particular the expression of the variable phenotypes are yet to be discovered (W. Layman, Hurd, & Martin, 2010).

1.2.2 Functional domains of the CHD protein family

The human *CHD7* gene is located on the short arm of chromosome 8 (8q12). It consists of 37 coding exons that encode 2997 amino acids and one non-coding exon (Vissers et al., 2004b). CHD7 belongs to the third sub-type of chromodomain super family of the Chromodomain Helicase DNA binding proteins. This sub-group has a unique combination of functional domains. The domains include two N-terminal chromodomain, a Sucrose Non-Fermentable 2/Adenosine Tri-Phosphate (SNF-2/ATPase) like domain in the middle and at the C-terminal end protein-protein interaction and/or DNA binding domains (see **Figure 1.1**).

The three most common and cardinal domains of the CHD proteins are: a chromodomain, a DNA-binding domain and an SNF2-like helicase domain with ATP-hydrolysing activity (Hall & Georgel, 2007). The chromodomain, which is named after its function as a chromatin organizer, is known to be conserved among diverse species and mammals (Eissenberg, 2001). The second conserved domain is the SNF2-like helicase ATP-ase domain, which is very similar to the earlier described yeast SWItch/Sucrose-Non-Fermentable 2 (SWI2/SNF2) catalytic subunit of the SWI/SNF complex (Peterson, Dingwall, & Scott, 1994). Proteins that contain the SWI2/SNF2-ATPase are often involved in multiple processes including, transcriptional regulation, mitotic chromosomal stability maintenance as well as DNA recombination and repair (Hall & Georgel, 2007). The third common domain is the more obscure and less conserved DNA-binding domain. This was the domain that set apart the CHD proteins as unique sub-families of proteins that comprise of both an SNF2-helicase-ATPase activity and a DNA-binding ability (Stokes & Perry, 1995).

The ATP hydrolysis energy is converted to conformational stress necessary for chromatin remodeling. Some of the ways to do so are histone displacement or histone octamer sliding (Pazin & Kadonaga, 1997; Dürr, Flaus, Owen-Hughes, & Hopfner, 2006). Some of the CHD protein families have distinct domains. For instance, the Swi3, Ada2, N-cor, and TFIIIB (SANT) domain, which is involved in association of DNA and chromatin, has only been observed in the CHD subfamily III members, CHD5, CHD7 and kismet, a drosophila homologue of the human CHDIII subfamily (Daubresse et al., 1999). This domain has also been found to recognize the nucleosome through the facilitation of histone tail binding (Dürr et al., 2006). Onother not so well defined domains of CHD subfamily-III members are the Conserved Region (CR1-3) and the Brahma and Kismet (BRK) domain which is found in CHD7, CHD8 and CHD9 (Daubresse et al., 1999). They are believed to have a potential interaction or activity with the replication or transcription machinery (Hall & Georgel, 2007). And last but not least, at the C-terminal, there is Leucine zipper domain that might be involved in recognition of highly conserved DNA regions (H.-G. Kim et al., 2008).

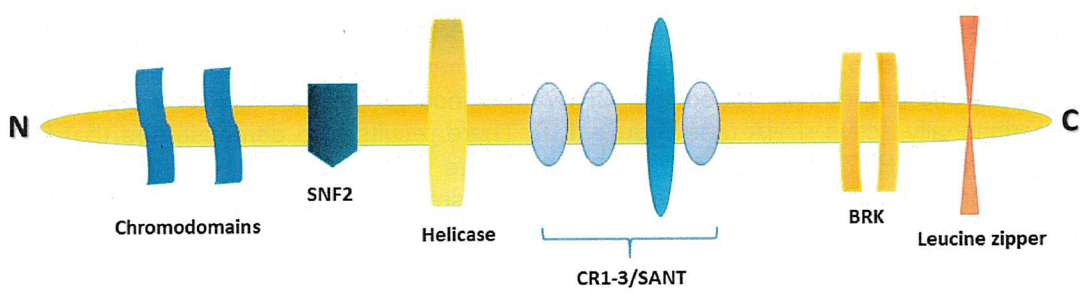

Figure 1.1: The schematic structure of the functional domains of CHD7 protein. The main characterized domains of CHD7 protein are: two chromodomains at the N-terminal followed by SNF2 and ATP-lysing helicase, three Conserved Regions (CR1-3); the SANT and BRK domains of largely unknown function and Leucine zipper domain at the end of the C-terminal. Adapted form (Gregory et al., 2013b) (H.-G. Kim et al., 2008).

1.2.3 The functions of protein CHD7

CHD7 plays a crucial role during embryonic development of many different species (Patten et al., 2012; Bosman et al., 2005; D Sanlaville et al., 2006). It functions as a chromatin remodeler during early development and makes way for epigenetic control of gene expression in mesenchymal cells that originate from cephalic neural crest (D Sanlaville et al., 2006). From this notion, the testable hypothesis can be derived that CHD7 targets paired domain- or homeobox domain- containing transcription factors that are important in the development of organs affected in CS, such as *Hesx1*, *Pitx2*, *Otx1*, *Prop1*, *Krox20* and *Titf1*/*Nkx2a*. Transcription factor genes such as *Pax2* or *Tbx1* that are widely expressed in affected organs in CS are also possible targets of CHD7 (D Sanlaville et al., 2006). The third subgroup of the CHD proteins, that includes CHD5, CHD6, CHD7, CHD8 and CHD9, has been much less studied than the members of the first two subgroups. However, the overall function of all the CHD proteins is not much different and shows the same trend of development and transcription regulation (Hall & Georgel, 2007).

Schnetz and colleagues performed an extensive research to elucidate the function of CHD7 by using Chromatin Immunoprecipitation coupled with massive parallel DNA sequencing (CHIP-seq). Using this approach, they could map CHD7 bound genomic sites in mouse Embryonic Stem cells (ESCs). They could identify 10,483 sites that were associated with CHD7. These regions seem to be enhancer elements of distinct genes. More specifically, CHD7 was localized distal to transcription start sites, that contain high amount of mono-methylated Lysine number 4 on Histone 3 (H3K4me), which marks an open chromatin. For these reason, CHD7 is believed to be involved in enhancer-mediated fine tuning of the expression level of ESC specific genes. It possibly modulates gene expression in both positive (activation) or negative (repression) directions (Schnetz et al., 2009a; Schnetz et al., 2010a).

A research of nucleolar proteome database demonstrated that virtually CHD proteins localize in the nucleoplasm. The database shows that all nine CHD proteins have been detected in the nucleolus (Ahmad, Boisvert, Gregor, Cobley, & Lamond, 2009). These findings imply that beside functioning as regulators of nuclear gene expression, CHD proteins might simultaneously regulate ribosomal RNA (rRNA) biogenesis (Zentner, Hurd, et al., 2010). Confirming this hypothesis, CHD4 which is a repressor of nuclear gene transcription was demonstrated to be bound to ribosomal DNA (rDNA) and activate rRNA transcription (Shimono, Shimono, Shimokata, Ishiguro, & Takahashi, 2005). Zentner and colleagues confirmed this further and added that CHD7 also localizes in the nucleolus and binds to transcriptionally active rDNA (see **Figure 1.2**). There results also demonstrated that ESCs derived from CHD7 heterozygote and homozygote mutant mice have increased DNA methylation of the rRNA promoter, leading to decreased rRNA expression (Zentner, Hurd, et al., 2010).

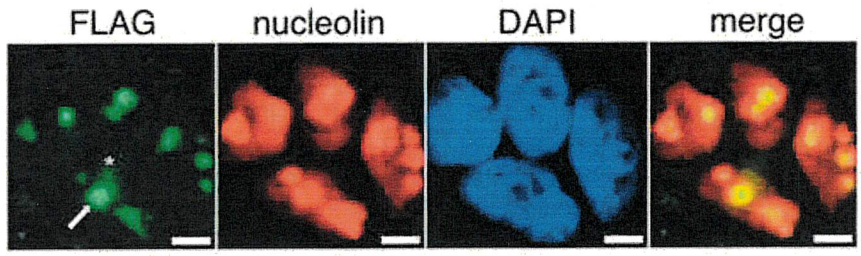

Figure 1.2: CHD7 is localized in the nucleoplasm and nucleolus. Immunofluorescent staining of DLD1-A2 cells labeled with FLAG and nucleolin antibodies. Arrow indicates presence of CHD7 in nucleolus and Asterix indicates CHD7 in the nucleoplasm. Scale bar=4 μm. (Zentner, Hurd, et al., 2010).

1.2.3.1 Epigenetic regulation

DNA is tightly wrapped and organized around histones octamers to form nucleosomes and higher-order chromatin structures. This compaction, however, forms a barrier to gene expression, because then there is no access for the transcription machinery to the DNA. Therefore, chromatin remodeling complexes play a crucial role in dynamic modulation of DNA accessibility, which is an important mechanism of controlling cell fate during development and can lead to diseases when dysregulated (K. H. Kim & Roberts, 2013b). Additionally, recent studies have shown that distinct chromatin states are associated with maintained or restricted differentiation potentials (Okuno et al., 2017). A study of mouse trunk neural crest cells demonstrated that Bone Morphogenic Protein (BMP)/WNT activates the expression of CHD7. This interaction is linked to maintenance of multipotency of the neural crest cells leading to the formation of mouse neural crest-derived stem cells (Fujita, Ogawa, Kawawaki, & Ito, 2014).

The Chromatin Organization Domain (Chromo) domain of the CHD protein family is a conserved domain consisting of 50 amino acids that are involved in functional structure of the eukaryotic nucleus (Hall & Georgel, 2007). Many experimental data point out that the chromodomain is involved in binding certain proteins to DNA (histones) and probably RNA. The helicase domain of CHD7 protein functions as an ATP-dependent unwinder of DNA and RNA duplexes as well as histone deacetylation (Woodage et al., 1997a; Wade et al., 1998). Additionally, many in vitro studies indicate that most *CHD7* mutations leading to CS affect the ATP-dependent chromatin remodeling activity of the protein product (Schnetz et al., 2009b).

1.2.3.2 The role of CHD7 in neuronal and brain development

Feng and colleagues investigated the involvement of CHD7 in regulation of developmental and adult neurogenesis (Feng et al., 2013). They first made the observation from Allen brain atlas that expression of *CHD7* is highly enriched in sub ventricular zone (SVZ) and sub granular zone (SGZ) of the brain, two regions where adult neurogenesis takes place. In this study they demonstrated that CHD7 expression is low in quiescent neural stem cells (NSCs), but is highly expressed in active NSCs, reaches a peak in transit-amplifying cells and is persistently expressed in neuroblasts. To understand the mechanism by which CHD7 contributes to NSC differentiation, they looked at genes with similar expression levels as CHD7, thus genes that show the highest correlation with CHD7 expression. The expression of two important transcription factors involved in neuronal identity, SOX4 and SOX11 showed the highest correlation with CHD7. Furthermore, CHD7 seemed to occupy the promotor region of this genes to make the chromatin less compact. This study implies that CHD7 is a regulator of

neurogenesis which directly controls the acquisition of neural fate by controlling the expression of transcriptional factors (Feng et al., 2013; K. H. Kim & Roberts, 2013a).

In a more recent study, the same research group showed that CHD7 is indispensable for mammalian brain development. They showed that CHD7 controls granule neuron differentiation in the cerebellum. Inactivation of CHD7 in the mice cerebellum replicated clinical features similar to cerebellum in CS patients, due to impaired granule neuron differentiation, increased apoptosis, and aberrant localization of purkinje cells (Feng et al., 2017).

As mentioned before, CHD7 interacts with tissue specific factors to regulate the expression of downstream target genes. Research in mice, regarding the genome-occupancy of CHD7 combined with transcriptomic profiling in the CNS revealed that CHD7 interacts with SOX10 to control the onset of myelination and remyelination. The interaction of these two transcription factors occupies the enhancer regions of important myelinogenic genes. This study identified previously unidentified targets of CHD7, including the bone formation regulators Osterix, which are known as Sp7 and Creb312, factors important for oligodendrocyte maturation; oligodendrocytes are glial cells that are involved in myelinations of the CNS. The results of this research provided evidence for the function of Chd7 in white matter pathogenesis observed in CS (He et al., 2016).

1.2.3.3 The role of CHD7 in neural crest cell development

Abnormal development or migration or interaction of the cephalic neural crest cells has been proposed as the major mechanism for CS pathogenesis. The tissues affected in CS have their precursor cells from the neural crest origin during the embryonic development (Siebert, Graham, & MacDonald, 1985). This hypothesis is partly supported by the involvement of CHD7 in the neural crest cell development. CHD7 is expressed in diverse cell types, including pluripotent stem cells of the neural tube and placode (Aramaki et al., 2007). The neural crest cells migrate within the embryo to give rise to the major Neural Crest Cell (NCC) derived organs, after delaminating from the neural tube (Steventon, Mayor, & Streit, 2014; Kim D. Blake et al., 2008). The migratory NCCs contribute to the formation and development of numerous tissue lineages, which include craniofacial skeleton, cranial nerves (VII, VIII, IX and X), ears, eyes and heart (Okuno et al., 2017).

Recent studies show that knockdown (KD) of *CHD7* indeed affects NCC development. Knocking down *CHD7* in human embryonic stem cells results in migrational defects in the neural crest development (Bajpai et al., 2010). Furthermore, KD of *chd7* in zebrafish and *Xenopus laevis* caused aberrant neural crest specification and migration (Asad et al., 2016a; Bajpai et al., 2010). In the *Xenopus laevis,* pharyngeal arch development was abolished upon *chd7* morpholino KD. This defect was partially rescued by co-microinjection of the human *CHD7* mRNA (Bajpai et al., 2010).

The *in vitro* characterization of CS in the study of Okuno et al. (Okuno et al., 2017) additionally demonstrated that CHD7 is not necessarily involved in the differentiation of NCCs, because the patient-derived induce Pluripotent Stem Cells (iPSC)-NCCs were able to differentiate into adipocytes, chondrocytes, osteocytes, myofibroblasts and peripheral neurons. However, compared to control iPSCS-NCCs, the patients derived iPSC-NCCs show defective delamination, migration, and motility.

1.2.4 The expression pattern of *CHD7* in human embryo and fetus

The expression of CHD7 in early human development was studied following electively terminated pregnancies. Seven embryonic stages and fetal stages were used for *in situ* hybridization studies of *CHD7* RNA expression. In the earliest stages, 20-24 days post conception (dpc), CHD7 is ubiquitously expressed, with a more marked signal in the neural tube. At 26 dpc, CHD7 is expressed in CNS and neural crest-containing mesenchyme of the pharyngeal arches. Further in the embryonic development at 33 dpc, the expression is maintained in the brain, cephalic mesenchyme and pharyngeal arches. Some expression was also observed in otic vesicle and limb bud mesenchyme with more strong intensity in the spinal cord and dorsal root ganglia. By 34 dpc, strong expression remains within the CNS, but is now restricted to the dorsal part of the otic vesicle. Furthermore in the embryonic development, at 47 dpc, intense expression is maintained in neural retina and rhombencephalon and moderate expression is observed in the semicircular canal, forebrain, pituitary gland, and olfactory bud and nerves. At the fetal stage, gestational week 9, *CHD7* is expressed in the nasal epithelia, the neural retina, the optic nerve sheath and the anterior and median lobes of the pituitary gland. The expression pattern correlates with most of the organ defects and dysfunctions observed in CHARGE syndrome (D Sanlaville et al., 2006). **Figure 1.3** gives a broad overview of the ubiquitous expression of *CHD7* during early development in ESCs and further in embryonic development in progenitor cells of the various organs affected in CS. This schematic diagram shows that CHD7 plays a key role in proliferation and differentiation of the Stem cells as well as progenitor cells of the organs that are frequently affected in CS. The expression of *CHD7* is very low or absent in progenitor cells that give rise to the lungs, liver and the muscles (Donna M. Martin, 2010).

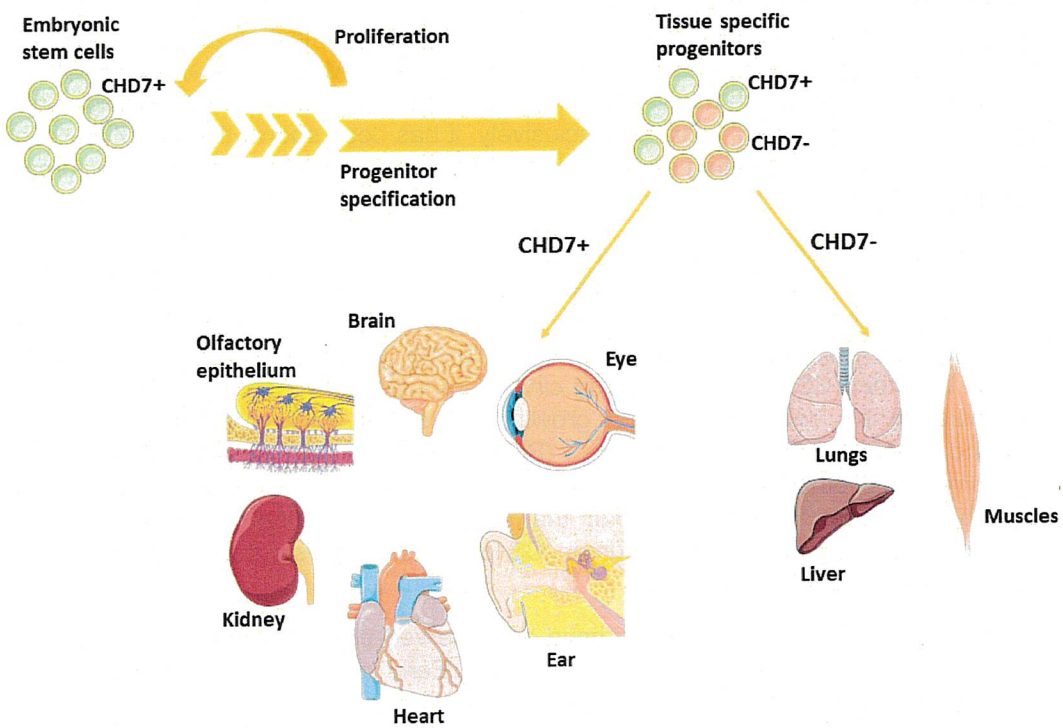

Figure 1.3: Overview of CHD7 expression in embryonic stem cells and progenitor cells and organs, during embryonic development. CHD7 is ubiquitously expressed during early embryogenesis in the ESC. The robust expression is maintained throughout development in most organs and central and peripheral nervous system (ganglia) which are affected in CS. CHD7 expression is very low or absent in other organs such lungs, skeletal muscles and liver. Adapted from (Donna M. Martin, 2010).

1.2.5 Conservation of CHD7 among different species

The expression and the function of CHD7 has been studied in diverse species including, *Drosophila melanogaster*, *Xenopus laevis,* zebrafish (*Danio rerio*) and mouse (*Mus musculus*) (Steffen & Ringrose, 2014; Bajpai et al., 2010; Patten et al., 2012; Bosman et al., 2005). CHD7 is one of the four homologues of the protein kismet in *Drosophila melanogaster*. Kismet is a family of *trithorax* (*trx*) proteins believed to promote transcription elongation by RNA polymerase II (Srinivasan, Dorighi, & Tamkun, 2008). The *Drosophila trx* was discovered because spontaneous mutations in this gene led to head, thoracic and body segment defects (Ingham, 1983). The gene *trx* encodes methyltransferase protein in the fly and this protein functions as a suppressor of the Polycomb group (*PcG*) genes. These genes are highly conserved among species and generally *trx* genes are activators of gene expression while the *PcG* genes are repressors (Steffen & Ringrose, 2014).

During *Xenopus* embryogenesis, *chd7* is expressed in the neural crest, neural and preplacode ectodermal tissues. The latter are thickenings of the ectodermal layer in the cranial region, from which the special sensory and other systems develop (Bajpai et al., 2010). The *chd7* morpholino knock-down in *Xenopus laevis* had defects in the circuitry of multipotent neural crest formation and recapitulated many CS features. The expression of key regulators of this transcriptional reprogramming process was severely affected in the *Xenopus* morpholino model of CS. Defects in the of genes important for Epithelial Mesenchymal Transition (EMT) of the neural crest cells, such as *slug* and *twist,* was partially or completely rescued upon co-injection of the human *CHD7* mRNA. Conclusively, it has been shown that *Chd7* in *Xenopus* plays a crucial role in regulating gene expression during multipotent neural crest formation (Bajpai et al., 2010)

In the mouse, Chd7 is made of 2985 amino acids, 38 exons and similar exon-intron structure as the human CHD7 protein. On the protein level, the mouse Chd7 is 94.7% identical to the human protein, which corresponds to 89.7% similarity at the nucleotide sequence level. Heterozygous Ethylnitrosourea (ENU) *chd7*-mutant mice recapitulate most of the phenotypes observed in human CS patients including circling behaviour, hyperactivity, disrupted lateral semi-circular canals, reduced postnatal growth, cleft palate, choanal atresia, cardiac septa defect and olfactory defects among others (Bosman et al., 2005). Loss of *Chd7* function in mice is embryonic lethal and the mice have severe defects in many developing organ tissues (Elizabeth A. Hurd et al., 2007). The fact that *Chd7* loss-of-function in the different species produces similar phenotypes as in human CS patients, suggests that it has a conserved function between the species.

Similarly, in zebrafish, *chd7* shows to have a conserved embryonic expression as well as function (Patten et al., 2012; Bosman et al., 2005). Early in zebrafish development, *chd7* is ubiquitously expressed, but later in development the expression becomes restricted to the brain region, retina, the eye, somites and tailbud. The morpholino *chd7* KD zebrafish model of CS displays many of the features in human patients including heart defect, retinal defects,

abnormal swimming behavior and aberrant development of the cranial motor neurons (Patten et al., 2012).

The zebrafish *chd7* gene is located on chromosome 2. Of the 5 annotated transcripts, two are full-length and encode the zebrafish homolog of the human *CHD7*. They both seem to have similar coding sequences and exon-intron structure to that of the human *CHD7*. These full-length transcripts code for 3140 amino acids, which is slightly longer than the human homolog with 2997 amino acids. Furthermore, the functional domains of the protein are conserved between zebrafish and human. The zebrafish protein domains include tandem N-terminal chromodomains, a central located SNF2-like ATPase/helicase domain and a C-terminal BRK domain. Overall the alignment of the zebrafish chd7 sequence to that of the human CHD7 shows 69% similarity at the amino acid level. **Figure 1.4** shows a schematic image of the human CHD7 versus zebrafish chd7 domains, with the envisioned locations of the protein domains (Balow et al., 2013).

Figure 1.4: Illustration of the human CHD7 and zebrafish chd7 domains with their predicted locations of functional domains. Adapted from (Balow et al., 2013).

1.2.6 CHD7 interacting partners

A study that combined co-immunoprecipitation with ChIP-seq showed that CHD7 co-localizes and physically interacts with the High Mobility Group box (HMG-box) transcription factor Sry-related HMG bOX (SOX2). This transcription factor is crucial for *in vivo* survival of mouse embryonic and adult NSCs. It also plays important roles in neurogenesis (Engelen et al., 2011). In addition, several set of genes were discovered to be targets of the SOX2-CHD7 complex. These genes are members of the Notch pathways (*Jag1*, *Rbpj* and *He5*) and of the Sonic Hedge Hog (shh) pathway (*Gli2*, *Gli3*, *Mycn* and *Tulp3*). Downregulation of these genes was observed upon *Sox2* or *Chd7* KD. A similar trend has been shown in human NSCs, indicating that regulation of these sets of genes by CHD7-SOX2 is conserved between human and mice (Engelen et al., 2011).

The genomic occupation of 13 ESC transcription factors was compared to *CHD7* genomic location, specifically at the enhancer elements (Chen et al., 2008; Schnetz et al., 2010b). Pairwise comparison was executed between CHD7 binding sites to that of P300 and other 12 transcription factors. Each combination of CHD7 with the other factors was tested for enhancer activity using luciferase reporter assay. The data indicates that CHD7 co-localizes with the

core transcriptional machinery in ESCs, that includes, SOX2, NANOG, and OCT4. These factors are known to be involved in self-renewal and pluripotency of ESCs (Schnetz et al., 2010b).

Additionally, this extensive study points out that the interaction of CHD7 with these factors does not necessarily affect self-renewal and pluripotency, bus does however function as transcriptional modulator of tissue specific gene expression (Schnetz et al., 2010b). **Figure 1.5** demonstrates the putative CHD7 complexes and the proposed functions of the complexes in different cell lines and lineages. This figure further explains the role of BRG/Brahma-associated (BAF) complexes during early embryogenesis. Distinct combination of the BAFs is required for ESC maintenance and pluripotency. Proteomic analysis could demonstrate that BAF-CHD7 complexes in ESCs directly interact with key regulators of pluripotency transcription circuitry (Ho et al., 2009).

Additionally, CHD7 is known to cooperate with PBAF (Polybromo BRG1- associated factor containing complex) to control the formation of multipotent neural crest cells (Bajpai et al., 2010). There was since the discovery of CS already the assumption that abnormal development of the multipotent neural crest cells is the basis of CS pathogenesis. Neural crest cells give rise to diverse cell and tissue types such as cartilage, bone, smooth muscles, pigment, endocrine cells, neurons and glia (Siebert et al., 1985; Silke Pauli, Bajpai, & Borchers, 2017). Recent research of iPSC cells derived from CS patients suggested that these cells exhibit migrational defects compared to control iPSC neural crest cells (Okuno et al., 2017).

CHD7 also interacts with CHD8, a protein from the same sub-family. As mentioned earlier, *de novo* mutations of *CHD8* have been found to be involved in ASD pathogenesis (Neale et al., 2012). CHD8 was found to negatively regulate β-catenin target genes by directly binding to it (B. A. Thompson, Tremblay, Lin, & Bochar, 2008).

Cell type	Combination of CHD7 interacting partners	Proposed function	Reference (s)
Mouse embryonic ES cells	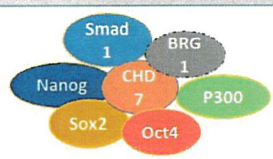	Unknown	Schnetz et al. 2010
Mouse bone marrow mesenchymal stem cells		Wnt-induced osteoblast formation	Takada et al. 2008
Human differentiated ES cells	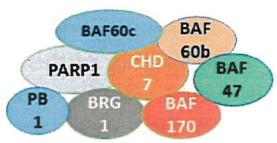	Cell motility	Bajpai et al. 2010
Human differentiated teratocarcinoma cells		Unknown	Bajpai et al. 2010

Figure 1.5: Schematic summary of tissue specific CHD7 interacting partners and their known and unknown functions. CHD7 might form different complexes with tissue specific transcription factors to act as a transcriptional modulator. Adapted from (Donna M. Martin, 2010).

1.2.6.1 Other proteins known to interact with CHD7 and/or are implicated with certain CS phenotypes

Since the discovery of *CHD7* as the responsible gene for the majority of CS cases, many other genes have been found to cause CS-like phenotypes in different model systems. Individual mutations in different genes either downstream of CHD7 or not have been found to reproduce distinct feature in CS. Among them are, *FAM124B*, *22q11* deletion, *FBXL10*, *SEMA3E*, and *FGF8* (Batsukh et al., 2012; Schnetz et al., 2010; Balow et al., 2013; S R Lalani, Safiullah, Molinari, Fernbach, & Martin, 2004; M. A. Basson et al., 2008) . The latter is a specifically important factor for cerebellar vermis hypoplasia, which is occasionally observed in CS. Mice with total knockout of *Fgf8* are not able to survive post-natally, but the conditional knockdown of the gene causes cerebellar vermis hypoplasia (M. A. Basson et al., 2008). Mice having only a heterozygous mutation of either *Chd7* or *Fgf8* showed no clear sign of cerebellar vermis hypoplasia. But in double heterozygotes, the cerebellar vermis hypoplasia was evident, implying genetic synergy between *Chd7* and *Fgf8*. Mice with heterozygous *Chd7* mutations had downregulated expression of *Fgf8* and the downstream gene *Etv5.* This indicates that a reduced level of *Fgf8* expression possibly underlies the CS-related cerebellar vermis hypoplasia (Haldipur & Millen, 2013).

Family with sequence similarity 124B (FAM124B) was discovered to be an interacting partner of both CHD7 and CHD8 following the discovery of the interaction of both CHD proteins. The study aimed to find another possible interacting protein of the CHD7-CHD8 complex. Comparison of *Fam124B* expression in both adult and embryonic mouse tissues with the known expression patterns of *Chd7* showed correlations. *Fam124B* was demonstrated to be expressed in most tissues affected in CS. At mouse embryonic stage E12.5, the expression of *Fam124B* was observed in several brain regions, spinal cord, dorsal root ganglia, developing cochlea, and surrounding tissue, lung, heart and kidneys (Batsukh et al., 2012).

Patients of *22q11.2* deletion syndrome and CHARGE syndrome show a great phenotypic overlap. The *22q11.2* deletion syndrome is caused by haploinsufficiency of T-box transcription factor (*TBX1*). A cohort study combined with a literature study of 5 clinically diagnosed CS patients led to the discovery that the patients had deletion of *22q11.2*. Possible explanation for the clinical overlap is that both CHD7 and TBX1 have a role in the same developmental pathway or act in pathways with a shared target gene(s). The known function of TBX1 is in regulating the expression of growth and transcription factors that are involved in the development of the heart, palate, thymus and parathyroid. It is also known to interact with SMAD1, interfering with its binding ability to SMAD4, which influences the further TGF beta signaling transduction (Fulcoli, Huynh, Scambler, & Baldini, 2009). Similarly, CHD7 was found to be colocalized with SMAD1 and many other transcription factors at enhancer elements that are located near repressed genes (Schnetz et al., 2010b).

Jumonji domain-containing histone demethylase (FBXL10) is a repressor of ribosomal RNA genes. Morpholino-mediated knock down of *Fbxl10/kdm2bb* in the zebrafish could rescue most of the *chd7* morphant phenotypes, including cell proliferation and cartilage defects. As mentioned earlier, CHD7 localizes on the nucleolus rDNA and is involved in activation of rRNA transcription (Balow et al., 2013; Zentner, Hurd, et al., 2010). During early zebrafish embryogenesis, *fbxl10/kdm2bb* is ubiquitously expressed like *chd7*. The expression is restricted to the anterior side of the embryo, such as the retina and CNS by 4 days post ferilization (dpf). The *chd7/fbxl10* zebrafish double morphants had better development of the ceratobranchial arches, meckel's cartilage and generally better craniofacial cartilage than single *chd7* morphants. Furthermore, the double morphants had amelioration of cell

proliferation and other morphological defects observed in the single *chd7* morphants (Balow et al., 2013).

Different types of mutations involving the gene semaphorin 3E (*SEMA3E*) gene were discovered in CS patients, even before *CHD7* was described as the causative gene. *De novo* mutations of *SEMA3E* were discovered in two unrelated CS patients. One of the mutations was a balanced translocation between chromosome 2 and 7, where the *SEMA3E* gene is located within 200 kb of the translocation breakpoint on 7q21.11. In the second patient, the mutation was a substitution of the conserved serine residue at 703 by Leucine (S703L) (S R Lalani, Safiullah, Molinari, Fernbach, & Martin, 2004).

The phenotypes of the child with the balanced translocation were bilateral choanal atresia, absence of semicircular canals, cranial nerve dysfunction, genital hypoplasia, developmental delay and growth retardation. The translocation is believed to cause a deletion or disruption of the genes within the involved region (D M Martin, Sheldon, & Gorski, 2001). The phenotypes of the child with the missense mutation were coloboma, choanal atresia, ear malformation, severe deafness, tetralogy of Fallot, developmental delay and growth retardation (S R Lalani et al., 2004). Semaphoring proteins have crucial functions in many cellular pathways implicated in axon guidance and cell migration. For instance, semaphoring signaling interacts with *plexinA* in neural-crest mediated heart development (C. B. Brown et al., 2001).

All in all, it seems that CS does not only exhibit a big spectrum of phenotypes but also a spectrum of affected genes that are possibly involved in its pathogenesis. This all adds to the complexity of this developmental disorder and makes *CHD7* an important gene to study. **Figure 1.6** depicts possible interaction of CHD7 with its protein partners in multiple developmental and pathogenesis related pathways. Defects in those interactions are believed to result in the specific disorders or malformations mentioned in the diagram (M. Albert Basson & van Ravenswaaij-Arts, 2015) .

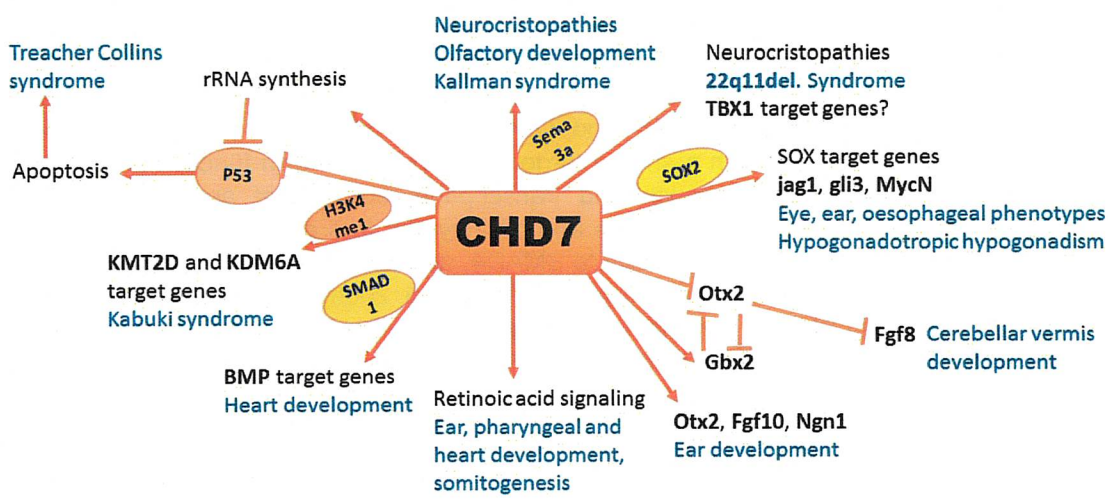

Figure 1.6: Development and disease-related pathways regulated by CHD7. Summarizing scheme of the interaction/cooperation of CHD7 with other proteins and the role of the defect in this interaction in pathogenesis of diverse CHARGE-like developmental disorders. Adapted from (M. Albert Basson & van Ravenswaaij-Arts, 2015).

1.2.7 Mutations of *CHD7* are also involved in other disorders

Beside CS, mutation of *CHD7* have been found in many other syndromes and disorders. CHD7 is found to play important role in pathogenesis of other developmental disorders such as Treacher Collins syndrome, Kallmann syndrome and Digeorge syndrome (Zentner, Hurd, et al., 2010; M. Jongmans et al., 2009; Kaliakatsos et al., 2010) (**Figure 1.6**).

CHD7 was associated with treacle, the causative protein of Treacher Collins syndrome. Even though both syndromes have distinct phenotypes, there is often overlap of affected systems including the eye and the ears. Surprisingly, treacle is a nucleolar protein which can associate with CHD7 at rDNA to positively regulate rRNA synthesis. The ability of treacle to bind to rDNA was compromised in *Chd7*-mutant cells as compared to wildtype cells. This findings show that the ability of treacle to bind to rDNA is partially dependent on CHD7 (Zentner, Hurd, et al., 2010).

Another syndrome connected to CHD7 is Kallmann syndrome (KS), a genetic disorder marked by loss of sense of smell and hypogonadotropic hypogonadism. These two features are also occasionally observed in CS patients. The defects arise due to migrational defects of gonadotropin releasing hormone (GnRH) producing cells and olfactory neurons, when they travel towards the olfactory placode, hypothalamus and the olfactory bulb (Dodé & Hardelin, 2010; Van Battum, Brignani, & Pasterkamp, 2015). Not surprisingly, most Kallman syndrome patients have a mutation in the axonal guidance and growth involved genes like semaphorin 3A (*SEMA3A*) (Hanchate et al., 2012; Känsäkoski et al., 2014). *CHD7* heterozygous mutations have been discovered in some Kallmann syndrome patients, who also have more CS related phenotypes such as hearing loss. For this reason it has been proposed that Kallmann syndrome is a mild form of CS (M. Jongmans et al., 2009). Furthermore, a genome-wide study of *Chd7* conditional knock-out mice, demonstrated that Chd7 is an epigenetic regulator of class 3 semaphorins. *Chd7* is namely enriched at the promotor region of *Sema3a* in NCCs and Chd7 loss-of-functions results in inhibition of *Sema3a* expression (Payne et al., 2015; Ufartes et al., 2018).

CHD7 could also be involved in immunodeficiency syndromes like Digeorge syndrome that is characterized by hypoplastic or aplastic thymus, hypocalcemia and T-cell immunodeficiency. A small fraction of CS patients shows overlapping phenotype with DiGeorge syndrome, but very few DiGeorge patients have been tested for *CHD7* mutation. Comparative genome-wide array hybridization of a CS patient with Digeorge phenotypes and *CHD7* mutations indicated that there is genomic disruption near regions containing immune system specific genes (Kaliakatsos et al., 2010).

All in all, the studies in different species and cell lineages as well as the diverse syndromes caused by *CHD7* mutations demonstrate that CHD7 has multiple distinct interacting partners, depending on cell type and developmental stage (Janssen et al., 2012). Also this phenomena adds onto the complexity of the pathogenesis mechanisms in CS as well as other developmental defects where CHD7 is involved in.

1.3 The zebrafish as a model organism

Zebrafish (*Danio rerio*) is a powerful organism for the study of vertebrate biology, physiology and human diseases. Its advantages include the conservation of genome and of physiological processes and applicable *in vivo* tools, including easy imaging, loss or gain of function genetic methods, and the amenability to perform rapid chemical/drug testing on large numbers of animals. Additionally, raising and maintaining zebrafish lines takes less space than other model organisms like mice and rat. An adult zebrafish is only 2.5 cm big- and is relatively cheap to maintain (Bailey, Oliveri, & Levin, 2013). Another important advantage of the zebrafish as a disease model is their quick development. Several of these advantages make this simple vertebrate model favorable above other models. The advantages of the zebrafish are discussed in more detail in the following sub-sections.

1.3.1 Ease of genetic manipulation and availability of transgenics

The zebrafish genome is fully sequenced and amenable to genetic manipulation, making it a good genetic vertebrate model for studying certain human diseases (Kabashi, Brustein, Champagne, & Drapeau, 2011). There has been an explosion of mutagenesis methods and most of them are attainable in the zebrafish. The first targeted zebrafish knock-out line was created in 2008 using Zinc Finger Nuclease (ZFN) method (Chang et al., 2013). After that, many other mutagenesis techniques were applied on the zebrafish genome, among them are Transcription Activator-Like Effector Nuclease (TALEN) genome editing and Clustered Regularly Interspaced Short Palindromic Repeats-Cas9 (CRISPR-Cas9). The CRISPR- Cas9 system can effectively be used to target a gene and introduce random mutations by homology DNA repair or non homologous end-joining (Chang et al., 2013). The mutation is efficiently transmitted through the germline (Hwang et al., 2013). Knockout lines seem to offer more advantages over a morpholino KD, which is still being widely performed (Ata, Clark, & Ekker, 2016). Gain of function is easy to model by mRNA injection to study phenotypes induced by mutant alleles that are dominant negative or lead to a toxic gain of function (Patten et al., 2014). Overexpression of genes by retroviral insertions is also applicable in the zebrafish (Jao, Maddison, Chen, & Burgess, 2008). Embryonic translucency of the zebrafish makes it possible to visualise fluorescent reporters that allow for a detailed sub-cellular visualisation studies (Karlsson, von Hofsten, & Olsson, 2001; White et al., 2008). Furthermore, incorporation of a fluorescent reporter with the inserted DNA-sequence can serve as a good screening tool to ascertain incorporation of the mutation and for the visualisation of affected cell types. There are many fluorescent proteins that excite by a specific spectrum of light and emit fluorescence. Green Fluorescent protein (GFP) is the most often used one, but there are other options now across the color spectrum (Rafferty & Quinn, 2018).

Most developmental pathways are conserved between mammals and the zebrafish and around 70% of the zebrafish genes are orthologous to human genes. Most zebrafish organs are also structurally and physiological similar to their human counterparts. Often the orthology between zebrafish and human genes is unequivocal, making it possible to translate genetic findings in the zebrafish to human biology (Braasch et al., 2016). Zebrafish embryos/larvae are transparent and without any pigmentation, which makes it easy to perform *in vivo* imaging and to assess morphological changes during development. Furthermore, there are numerous antibodies available for immuno-histochemistry and there are several automated tracking devices on the market for the study of motor as well as social behaviours (Bailey et al., 2013).

1.3.2 Useful model for the study of early brain development and pharmacology

Other features that make the zebrafish an attractive model include a rapid development. In fact, within 3 months, the adult fish acquire reproductive maturity and can give between 100-200 embryos during each mating. The nervous system starts to develop by 6-7 hours post fertilization and functional neurons are formed by 1-day post fertilization. Apart from being much smaller in size, the zebrafish brain has similar development, structure and function as the human counterpart. For this reason, neuroscience is a research field that is benefitting from this model (Tropepe & Sive, 2003). Moreover, brain neurochemistry is highly conserved in vertebrates. Zebrafish possess the main systems of neuromediation similar to humans and rodents including, neurotransmitters, their receptors, transporters and enzymes that synthesise and metabolize them (Chen, Priyadarshini, & Panula, 2009; Anichtchik, Sallinen, Peitsaro, & Panula, 2006; Panula et al., 2006). Growing evidence suggests that genetics and physiology of major brain processes and behavioral traits are conserved among rodents and zebrafish. Additionally, zebrafish are responsive to most neurotropic drugs in the same way as humans, which makes them very useful for neuropharmacological research (Kalueff, Stewart, & Gerlai, 2014).

This model has also proven to be very useful to study the early brain development. In both larval and adult stages the use of the zebrafish to study complex brain development and dysfunction is rapidly growing. Thus the zebrafish is becoming a widely used model organism in neuropharmacology and pharmacogenetics. The zebrafish has been used to understand pathology of depression, autism, cognitive deficits and drug abuse among others (Kalueff et al., 2014). For instance, the zebrafish has been successfully used to simulate Alzheimer's disease (AD) and Tauopathy. The zebrafish is also suitable for ca^{2+} imaging, which permits a non-invasive study of neuronal activity as well as axonal dystrophy. Moreover, the possibility of high-throughput screening, makes the zebrafish an excellent model for screening neurotropic compounds that possibly treat AD (Saleem & Kannan, 2018). Another example is the recent and first mutant zebrafish model that allows for the study of epilepsy pathogenesis as well as normal brain development. This mutant line exhibits a homozygous mutation of the gene γ-aminobutyric acid receptor subunit1 (*gabra1*) (Samarut et al., 2018).

1.3.3 Modelling CHARGE syndrome in the zebrafish

Patten et al. previously evaluated the role of *chd7* in zebrafish using an antisense morpholino oligonucleotide (AMO) (Patten et al., 2012). First, the expression pattern of the zebrafish homolog of the mammalian *CHD7* was assessed. The results pointed out that the zebrafish *chd7* is expressed robustly in whole embryo during early development. Later in the development the expression is restricted to some organs and parts of the zebrafish embryo/larvae. At advanced somitogenesis stages, the expression level of *chd7* remains high in the retina, brain, somites and the tailbud of the embryo. After 48 hpf the expression stays high only in the brain and the eye. This shows the dynamics in the spatio-temporal expression of this important chromatin remodeling factor.

The morphant larvae displayed many developmental defects compared to wildtypes larvae and control morpholinos. Among the defects, were severe pericardial edema, defects in otolith formation (asymmetric size or just one otolith), curvature of the body axis and circling swimming behavior. Moreover, the organization of the cranial motor neurons was disrupted in the morphants and their facial branchiomotor neurons were reduced in number; reflecting the

neurological disorders observed in CS patients. Similar phenotypes were observed in a subsequent independent study of *chd7* morphant zebrafish (Balow et al., 2013). Cranial cartilage abnormalities were also observed and morphant embryos had decreased cell proliferation combined with elevated levels of cell cycle inhibitors including, *p21* and *p27* as well as reduced level of rRNA (Balow et al., 2013). Although the zebrafish *chd7* morphants recapitulated most of the CS related features, they are not suitable for drug screenings due to the several drawbacks including transient KD of a gene not being relevant to disease mechanisms in humans as they are not transmitted through the germline (Patten, Parker, Wen, & Drapeau, 2016). To circumvent this, a stable *chd7* mutant line is needed.

1.4 The power of chemical genetic screening using the zebrafish and *C. elegans*

The zebrafish embryo is an ideal *in vivo* tool for high-throughput screening of compounds due to its small size and the ease of waterborne exposure among others (Murphey, Stern, Straub, & Zon, 2006). This can greatly contribute to the acceleration of the process of neuroactive drug discovery (Kokel et al., 2010). The zebrafish model can be utilized to screen compounds for disease-rescuing activity, time- and cost-effectively (Goldsmith & Jobin, 2012). Moreover, using chemical libraries of FDA-approved drugs further accelerates the translation of hits or leads in the zebrafish, to clinical trials (Tamplin et al., 2012).

The nematode worm *C. elegans* has proven to be an ideal model to study mechanisms of neurological disorders, such as Amyotrophic Lateral Sclerosis (ALS) (Patten et al., 2016) and CS in the current study. This nematode is reproductive in 3.5 days post fertilization and it has a life span of about 3 weeks. The whole nervous system of the *C. elegans* is composed of only 302 neurons, which use most of the known neurotransmitters in the mammalian nervous system. Genome sequencing has revealed that 43% of the *C. elegans* genes are similar to human genes (Markaki & Tavernarakis, 2010) and 60-80% of the genes have human counterparts (Harris et al., 2004). A single *C. elegans* hermaphrodite can self-fertilize and yield around 300 progeny and give even more progeny if it mates with male, making high-throughput drug screening feasible. The body of the *C. elegans* is transparent throughout its development, which allows for tracking cells of interest (Sulston, Schierenberg, White, & Thomson, 1983). An important advantages of this type of phenotype-based chemical screens in the *C. elegans* and the zebrafish is that they provide assessment of targeted effects as well as adverse effects of the screened compounds at the whole organism level, as opposed to the widely used cell-culture model (Markaki & Tavernarakis, 2010).

A phenotype-based chemical genetic screening is a promising approach to find medical treatment for complex disease like CS, for which the disease mechanism is still being elucidated (Tamplin et al., 2012). In the Amyotrophic Lateral Sclerosis (ALS) research, combining the advantages of both *C. elegans* and zebrafish models has revealed the synergistic potential of using tractable organisms for drug discovery (Patten et al., 2017). The discovery of a compound pimozide as a potential treatment for ALS was accelerated by utilizing the advantages of both models. Pimozide restored motility defects in the *C. elegans* and zebrafish models of ALS. Initially, a large chemical library was screened on the *C. elegans* model and hits were validated in the zebrafish. Following the validation in the zebrafish, pimozide was tested in mice and in a small clinical trial (Patten et al., 2017). This is a perfect example of how integrating these simple models can accelerate the drug discovery process.

1.5 Hypotheses and objectives

Our first hypothesis was that the stable *chd7*-mutant fish will display the cardinal phenotypes and defects related to CS. Following the characterization of relevant phenotypes, we hypothesized that we were able to identify the rescuing or ameliorating potentials of both target molecules (Fisetin and Ephedrine) or at least one of them.

With the complex disease mechanism of CS still being widely elusive, chemical genetic screening is a promising path for a rapid drug discovery. Therefore, the objectives of my MSc project consisted of:

i) Generating a stable *chd7*-mutant line to model CS features using the zebrafish
ii) Characterizing any defects arising from the *chd7* mutation
iii) Screening the two lead compounds for their potential to ameliorate or possibly rescue the defects.

The ultimate goal of the study was validating the two lead compounds from the *C. elegans* project. Following this, it is possible that they will be tested on mammalian models of CS and get rapidly translated in the clinical trials for treating the symptoms of CS.

CHAPTER 2: MATERIALS AND METHODS

2.1 Animal husbandry

Adult zebrafish (*Danio rerio*) were maintained following standard procedures ("ZFIN The Zebrafish Information Network," n.d.) at the facility of the Institut national de la recherche scientifique – Institut Armand Frappier. Eggs were collected through adult crosses and incubated at 28.5 °C. All experiments were performed in compliances with the guidelines of the Canadian Council for Animal Care and local ethic committee.

2.2 Generation and genotyping of the *chd7* zebrafish mutant

A guide RNA (gRNA) targeting the helicase domain of the *chd7* gene was designed using the online tool CRISPRscan (http://www.crisprscan.org/) (TGTATTCCTGCTGTGCACAAGGG; PAM site underlined). Cas9 mRNA was synthesized using the mMESSAGE mMACHINE T3 kit from pT3TS-nCas9n plasmid (Addgene #46757) linearized with Xba1. A volume of 1nl containing a mix of 100 ng/µl Cas9 mRNA and 30 ng/µl gRNA was injected into one-cell stage embryos using the Picospritzer III pressure ejector. Genotyping was performed by high resolution melting (HRM) analysis using genomic DNA extracted by boiling larva/clipped caudal fin in 50 mM NaOH for 10 minutes and then neutralized in 0.1 M Tris HCl (pH8).

2.3 Gross morphology and survival assessment

The *chd7*$^{+/+}$, *chd7*$^{+/-}$ and *chd7*$^{-/-}$ larvae were assessed for their survival rate and morphological phenotypes. The sample sizes for the different genotypes were as follows: five different batches (N=5) each batch containing 30 larvae (n=30) for *chd7*$^{+/+}$, *chd7*$^{-/-}$ larvae and N=3, n=18-19 for *chd7*$^{+/-}$ larvae. Gross morphology was observed under a stereomicroscope (Leica S6E).

2.4 Head size measurements

The head size was measured using the software imageJ. For the length a straight line was drawn between the lowest point of the otolith and the anterior end of the brain, around the upper jaw area. The line was measured by comparing it to a calibrated scale, which was set up from a picture of a ruler at the same magnification as the larvae images. All the measurements were done in a lateral position (**Figure 2.1**). A total of 12 *chd7*$^{+/+}$and 15 *chd7*$^{-/-}$ larvae were measured at the age of 3 dpf.

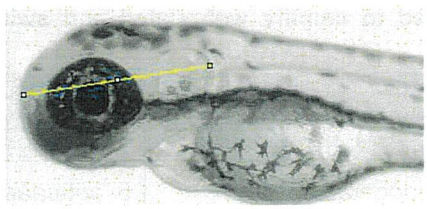

Figure 2.1: Zebrafish head length measurement using ImageJ

2.5 Study of the swimbladder development

Zebrafish of 3, 4 and 5 dpf were fixed in 4% PFA in PBS either O/N at 4°C or 5 hours at RT. The fish were then rinsed in PBS (3X 5 minutes) and put in 70% Ethanol (EtOH). Following this, the whole fish was embedded in paraffin and sectioned on a semi-manual microtome (Leitz 1512 Rotary Microtome) in 7 µm slices until we could get a clear view of the swimbladder. The sections were then put on glass slides, deparaffinized in xylene and then rehydrated in decreasing concentrations of EtOH (100%, 95%, 75% and 50%) for 5 minutes in each. At the end, the samples were washed in H2O for 2 minutes. For the coloration, the glasses were put in hematoxylin (StatLab Vintage) for 4 minutes. They were then washed in H2O, acid alcohol and lithium carbonate before being put in eosin (StatLab Vintage) for 2 minutes. Finally the samples were dehydrated in 100% EtOH and covered with glass cover slips. The staining was visualized on bight field microscope (AmScope , B020C). The pictures were taken with a 10X magnification.

2.5.1 Expression of swimbladder related genes by qRT-PCR

A selection of several wingless/integrated (*Wnt*) and hedgehog (*Hh*) pathway related genes that are expressed in the swimbladder was made, prior to the experiment. The genes implicated in the *wnt* signaling as well as the proper development of the swimbladder that were chosen for this experiment were: Sry-related HMG bOX-2 (*sox2)*, catenin β-1 (*ctnnb1*) and *Wnt* Inhibitory factor-1 (*wif1*). The forward and reverse primers were ordered from eurofins genomics. The sequences were amplified with the primers listed in the following table (**Table 2.1**). First, total RNA was extracted from fourteen 48hpf embryos ($chd7^{+/+}$ and $chd7^{-/-}$) using TRI reagent (Sigma-Aldrich, Canada) according to the manufacturer's protocol. The quality and quantity of RNA was measured on Nanodrop. A260/280 ratio was under 2 and the quantities of RNA were above 300 ng/µL. Then the RNA was reverse transcribed to cDNA using the VILO kit (Invitrogen). The cDNA was diluted to 1 in 10 and used for qPCR with SYBR Green Supermix (Biorad) on a LightCycle96 (Roche). Gene *elfα4* was used as a housekeeping gene for normalization and all the genes were run in technical triplicates.

Table 2.1: The primer sequences used to amplify *wnt*-related and swimbladder expressed candidate genes.

Candidate gene	Sequence of forward primer	Sequence of reverse primer
sox2	5' tggaccaacggaggctac 3'	5' cgttcaaactcgggtgct 3'
ctnnb1	5' tcaacactattccactctttgttca 3'	5' agccagttcacacagcactc 3'
wif1	5' gtcaacttcacctggcaagc 3'	5' caaagaacgcagagtctgaaac 3'

2.6 Locomotor behavior characterization

Larval locomotor activity was monitored at 5-6 days postfertilization over two 4h-4h light-dark cycles using Basler GenIcam camera and a DanioVision recording chamber (Noldus). Analysis was performed using the Ethovision XT12 software (Noldus) to quantify the total swimming distance in given hours/minutes.

2.7 Assessment of the neuronal network by anti-acetyl tubulin immuno- histochemistry

To visualize neuronal axonal tracts, in specific the trigeminal neurons, the optic tectum region axonal scaffolds and the commissural axons, fluorescent immunohistochemistry was performed using the marker acetylated α-tubulin (Sigma-Aldrich). Prior to the staining, the embryos were put in 0.003 % PTU in zebrafish medium to prevent pigmentation as in other studies (King Heiden, Spitsbergen, Heideman, & Peterson, 2009). Then 28 hpf and 48 hpf larvae were fixed in Dent's fixation (80% methanol and 20% DMSO) overnight (O/N) at 4 °C. Samples were rehydrated in 75 %, 50 % and 25 % Methanol in PBST for 30 minutes each. Then washed 4 times in PBST for 30 minutes (twice under agitation and twice without followed by blocking in 10 % normal goat serum (NGS) and 2 % bovine serum albumin (BSA) in PBST for 1 hour at room temperature (RT), under agitation. Primary acetyl-tubulin monoclonal mouse antibody was added to the blocking solution (1:500) and incubated O/N at 4 °C. After washing the primary at least 6 times 30 minutes in PBST and blocking for 1 hour, the secondary antibody Alexa 488 goat anti-mouse (Sigma-Aldrich) was added O/N at a ratio of 1:1000. Secondary antibody was washed and samples were mounted laterally for 28hpf and dorsally for 48hpf. Images were taken on a confocal microscope (Zeiss LSM780).

2.8 Visualization of the cranial cartilage development by Alcian blue staining

To visualize the cranio-pharyngeal cartilage, the acidic staining Alcian blue staining was applied (Mork & Crump, 2015). Larvae were fixed in 4% PFA in PBST (1 pellet in 200ml dH2O and 0,1 % Tween); Three batches with at least 10 larvae in each, were used for each genotype (*chd7*$^{+/+}$ and *chd7*$^{-/-}$). The larvae were fixed at 6dpf for 5 hours at RT. Then the samples were dehydrated in methanol solution with increasing concentrations; 25 %, 50 % and 75 % in PBST (10-15 minutes each) and stored at -20 °C until use. Before the staining was started, the samples were rehydrated in the reverse order of methanol concentrations for 15 minutes each. After 3 quick washes in PBST, the samples were incubated in 0.1 % Alcian blue solution with 70 % ethanol (EtOH) and 0,37 % HCl for two hours, under agitation. Then they were washed in EtOH and HCl solution; 3 quick washes and then twice 15 minutes. The larvae were digested in 10 % trypsin in 30 % saturated borax water which was prewarmed a 42 °C. At the end, the samples were washed overnight at 4 °C in 0.1 % KOH in H2O. The following day, they were washed in 0.25 % KOH for 1h and stored in 80 % glycerol and 0.25 % KOH solution at 4 °C until being imaged. Imaging was done on the Leica stereomicroscope (Leica S6E).

2.9 Initial high-throughput screening of FDA approved small chemicals

Initial high-through put screening was performed in collaboration with the *C. elegans* lab of Dr. Alex Parker. Initially 3850 FDA-approved chemical compounds was screened on a *C. elegans* model of CS. This model carrying a homozygous deletion mutation of gene *chd-7* was provided by the international *C. elegans* Gene Knockout Consortium. The large selection of FDA-approved compounds form chemical libraries Pretwick, biomol, Sigma Lopac and Microsource was tested on the locomotion behavior of the mutants. Of 49 hits, two compounds were discovered to be most potent and were further validated in this study on zebrafish *chd7*-mutants.

2.9.1 Drug screening in *C. Elegans*

The *C. elegans* part of the study was performed by the Dr. Alex Parker lab. A chd7 mutant (*gk290*) strain carrying a homozygous deletion mutation of gene *chd-7* was provided by the *Caenorhabditis* Genetics Center at the University of Minnesota and backcrossed four times to N2 wildtype. Worms were kept on NGM agar with an E. coli OP50 lawn at 15°C for maintenance and 20°C for assays. A worm tracking machine (Wmicrotracker, Phylum Tech) was used to track the swimming locomotion of *C. elegans*. Assays were performed in 96-well-microtiter plates with approximately 30 worms and 100 µl M9 buffer per well. *E. coli* OP50 were added to the wells to prevent worms from starving. Each microtiter well was crossed by two infrared light rays from top to bottom and a detector determined interruptions of these light rays by worms moving in the well. From the signal a movement score was calculated, which is defined as animal movement in a fixed time period. Movement was tracked for 10 hours. The assay was performed in triplicates and movement scores of chd-7(gk290) over time were compared to WT in three independent experiments using two-tailed t-test to determine significance.

FDA-approved compounds were provided by Sigma-Adrich (Sigma Aldrich's Library of Pharmacologically Active Compounds (Lopac) 1280 library, containing compounds as of July 2015, Oakville/Canada), Prestwick Chemicals (Prestwick Chemical Library; containing compounds as of March 2015, Illkirch/France), Microsource (880 compounds, Gaylordsville, CT/USA), Enzo Life Science, Inc. (BML-2865 Natural Products Library, containing compounds as of April 2015, Farmingdale, NY/USA). All compounds were dissolved in DMSO and tested at a concentration of 20 µM. Chd-7(gk290) nematodes were exposed to the drugs from the libraries in microtiter wells at a concentration of 20 µM in M9 buffer with OP50 and movement was tracked for at least 4 hours. The average movement score of *C. elegans* treated with a specific drug was compared to the DMSO control and the average movement score of the whole plate. If values for a drug were higher than the respective controls, a second screen to validate the increased movement due to the specific drug was performed. Compounds that increased locomotion of chd-7(gk290) significantly according to a two-tailed t-test in the second screen were counted as positive.

2.9.2 Validation of hit compounds in the *chd7*-mutant zebrafish

First, the lead compounds were tested for toxicity/dose responses in zebrafish embryos/larvae. Five different concentrations were tested in order to determine the safest and most potent concentration. The drugs were dissolved in negligible amount of DMSO (<0.01%) from an initial concentration of 20 mM. They were diluted in zebrafish water to make the test concentrations. The concentrations tested were 2, 5, 10, 20 and 40 µM. The 10 µM concentration was found to be potent and safe for both compounds. The two candidate lead compounds were tested for their ability to ameliorate survival rate, gross morphology, locomotor phenotype and neuronal network of the zebrafish *chd7*-mutants.

2.9.3 Statistical analysis

Data are presented as mean ± standard error of the mean (SEM). Statistical analysis was done using sigmaplot 11.0 and the graph prism 6 software. Either one way ANOVA or student's t-test were run on the datasets. For the significances; * denotes $P<0.05$, ** $P<0.01$, *** $P<0.001$, **** $P<0.0001$. N represents batch numbers and n represents number of embryos/larvae per batch.

CHAPTER 3: RESULTS OF THE CHARACTERIZATION

3.1 Generation of a *chd7*-mutant zebrafish line

Using CRISPR/Cas9 genome editing, the 17th exon of *chd7* gene encoding the helicase domain was targeted for disruption. Wild-type zebrafish embryos (F0) were injected with *chd7*-specific guide RNA (gRNA) and Cas9 mRNA at the 1-cell stage. The resulting F0 zebrafish were raised to adulthood and outcrossed to individual wild-type adults to obtain F1 embryos. The F1 embryos were screened for germline transmission of *chd7* mutations by High Resolution Melting (HRM) technique analysis (Samarut et al., 2016). F0 adults carrying potential mutations in the germline were selected and outcrossed to individual wild-type adults. F1 embryos obtained from this second outcross were raised to adulthood and individually screened for *chd7* mutations by HRM (**Figure 3.1A**) and Sanger sequencing (**Figure 3.1B**). A positive founder transmitting a 1-nucleotide insertion causing a frame-shifting mutation was identified and selected (**Figure 3.1B**). More precisely, the 1-nucleotide insertion resulted in a frameshift and the formation of a premature stop codon 8 amino acids after the mutation site, which would express a prematurely terminated protein after translation (1419 amino-acid long instead of 3140 for the wild-type protein; (**Figure 3.1C**). Quantification of mRNA expression showed a significant reduction in heterozygous and homozygous larvae (**Figure 3.1D**).

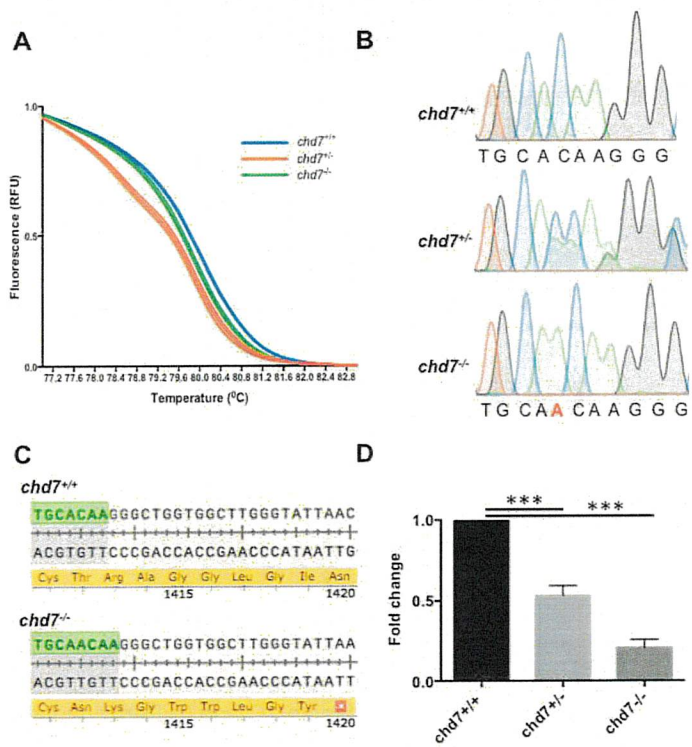

Figure 3.1: Genotyping by HRM and Sanger sequencing.

(A) HRM analysis shows shifting melting temperature curves (3 representatives) for the heterozygotes and homozygotes as compared to the wildtype curve. (B) Sanger sequencing revealed a 1-nucleotide insertion mutation (in red), and (C) Translation resulted in a premature stop codon (white *). (D) Real-time qPCR analysis of RNAs from 3 dpf larvae (in triplicate with N=5) shows a significant decrease of *chd7* mRNA expression in both *chd7*$^{+/-}$ and *chd7*$^{-/-}$ compared to wild-type (*** p<0.0001).

3.2 The *chd7*-mutants had a decreased survival and many morphological defects

First, survival and general morphology of *chd7*$^{+/-}$ and *chd7*$^{-/-}$ fish were assessed and compared to their wildtype *chd7*$^{+/+}$ siblings. The body axis of the homozygote (*chd7*$^{-/-}$) mutants showed to be slightly curved (**Figure 3.2A**). No major difference was observed between heterozygote fish compared to wildtype. Furthermore, the head of *chd7*$^{-/-}$ mutants was abnormal; smaller and deformed as compared to the wild-type (**Figure 3.2B** and **Figure 3.2E**; p<0.0001). The survival was significantly reduced in the *chd7*$^{-/-}$ larvae. Specifically after 9 dpf, the life span of the mutants shows a sharp decline as compared to both heterozygotes and wildtypes (**Figure 3.2D**). A small fraction of the mutants also displayed pericardial edema (**Figure 3.2C and 3.2F**).

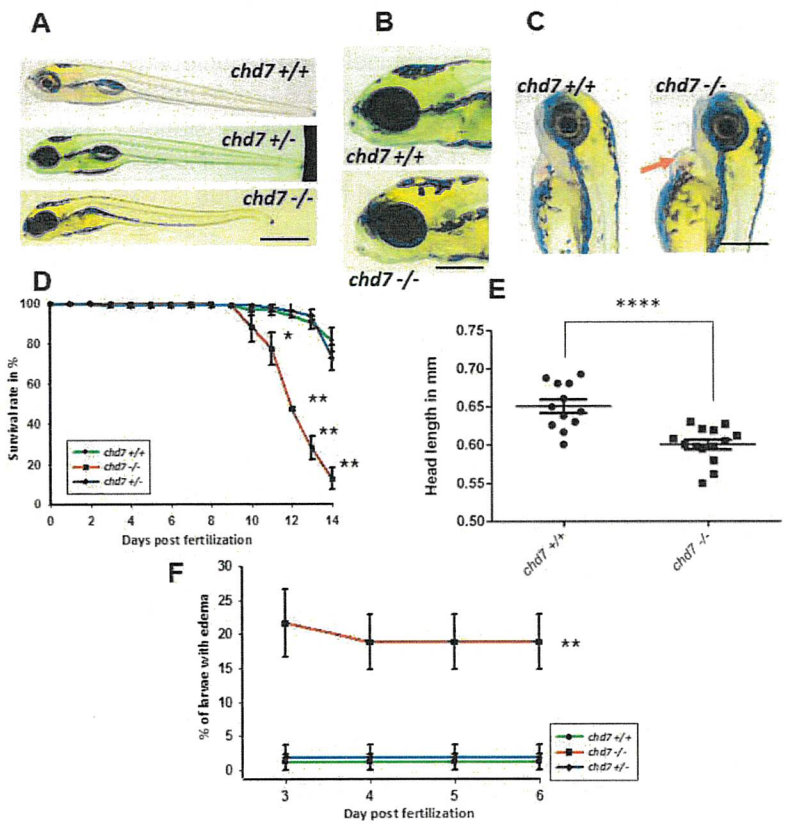

Figure 3.2: Gross morphology, survival and head size are affected in the *chd7*$^{-/-}$ larvae.
(A) The *chd7*-mutants are shorter than wildtypes and the body axis of the *chd7*$^{-/-}$ larvae is curved. (B) Head structure and size are abnormal in the *chd7*$^{-/-}$, larvae. (C and F) Pericardial edema was observed in some of the *chd7*$^{-/-}$ larvae, (** p=0.005; one way ANOVA) (red arrow point to the heart anomaly). (D) Survival plot of the life span of the *chd7*$^{+/+}$, *chd7*$^{+/-}$ and *chd7*$^{-/-}$ larvae within 14 dpf, * denotes p<0.05 and ** p<0.001; one way ANOVA . Red graph line represents *chd7*$^{-/-}$ larvae, blue *chd7*$^{+/-}$ *and green chd7*$^{+/+}$. (E) Head length is significantly reduced in *chd7*$^{-/-}$ compared to the *chd7*$^{+/+}$ larvae (P<0.0001, Student's t test), n=12 for *chd7*$^{+/+}$ and n=15 for *chd7*$^{-/-}$. For survival and gross morphology assessments, the N (batch) number for both *chd7*$^{+/+}$ and *chd7*$^{-/-}$ larvae was 5 and each batch contained n-number of at least 30 larvae. For *chd7*$^{+/-}$ larvae N=3 and n=18. Scales on images represent 200 µm. Error bars represent standard error of the mean (SEM).

3.3 Cranio-facial defects were observed in the *chd7*-mutants

Cranio-facial dysmorphism is a consistent phenotype in CS patients, we thus sought to explore this in the *chd7*$^{-/-}$ Zebrafish. To do so, an Alcian Blue staining was performed on 6dpf wild-type and mutant fish. Several structural defects of the cartilage were observed in *chd7*$^{-/-}$ compared to wildtype larvae. First, the ethmoid plate in the *chd7*$^{-/-}$ larvae showed to have a mild to severe cleft (**Figure 3.3A(i)**). This might correspond to the cleft palates, observed in CS patients. Furthermore, the angle at the ceratohyal cartilage was significantly larger in *chd7*$^{-/-}$ larvae compared to *chd7*$^{+/+}$ larvae (**Figure 3.3Aii**). Interestingly, the Meckel's cartilage, which is homologous to the human lower jaw, was found to be dysmorphic in the majority of the *chd7*$^{-/-}$ larvae (**Figure 3.3B**). Moreover, the pharyngeal arches appeared to be shorter in severe cartilage structural phenotype mutants and were not as clearly stained as in the wildtypes (**Figure 3.3A(i)**).

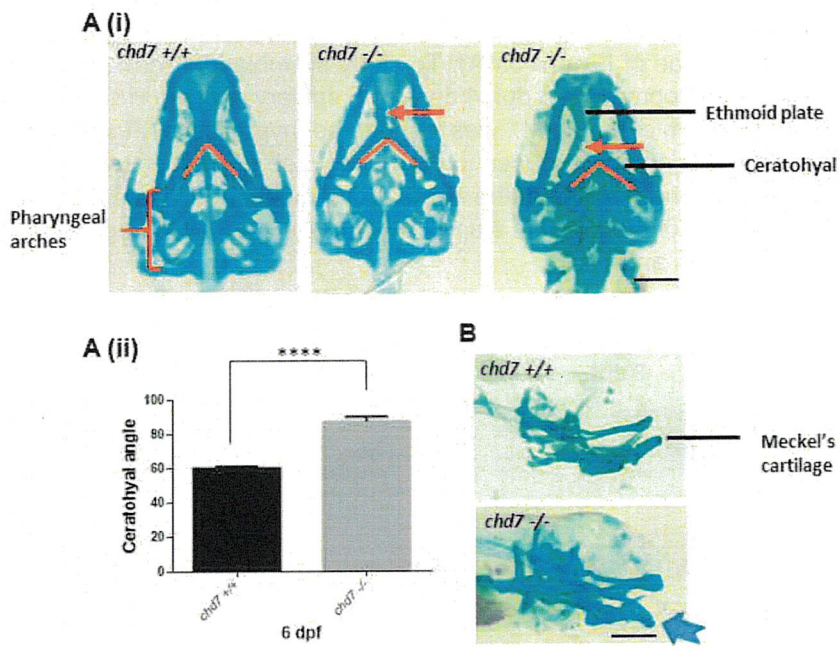

Figure 3.3: Cranio-facial cartilage defects in *chd7*-mutant fish.
(Ai) The *chd7*$^{-/-}$ larvae have cleft ethmoid plate (indicated by the red arrow), enlarged ceratohyal angle (angle made by the red lines) and weakly stained pharyngeal arches. (Aii) Abnormal morphology of the Meckel's cartilage in the *chd7*$^{-/-}$ larvae (blue arrowhead). (B) Plot of the average ceratohyal angle measurements in *chd7*$^{-/-}$ and *chd7*$^{+/+}$ larvae at 6 dpf. ($P<0.0001$, Student's t- test). Scales on images represent 200 µm. Ceratohyal angle of 12 larvae per genotype was measured.

3.4 Defects of the swimbladder development in *chd7*-mutants

A very consistent phenotype that we surprisingly observed in the majority of homozygote mutants is that they fail to develop a swimbladder (**Figure 3.4**). The swimbladder is an air-filled organ that functions to maintain buoyancy in the water and to be efficient with energy when descending or ascending in the water ("ZFIN Anatomy Ontology: swimbladder," n.d.). This organ is proposed to be homologous to the mammalian lung (Cass, Servetnick, & McCune, 2013). The swimbladder development starts as early as 36 hpf with epithelial bud outgrowth. Then 8-10 epithelial cells surround a lumen and the end of the epithelial budding takes place around 48 hpf. Then an additional mesenchymal layer surrounds the epithelial lumen. The third (mesothelium) layer, develops at 60 hpf and at 65 hpf the mesenchyme differentiates into smooth muscle cells. Moreover, the epithelial budding of a next anterior chamber starts at 64 hpf. Hegdehog (Hh) signaling is required in the early development for the specification of swimbladder epithelial and mesenchymal cells (Winata et al., 2009). The swimbladder starts developing around 2 dpf and gets inflated with air at 4-5 dpf. However, in around 70% of the *chd7*$^{-/-}$, there was no developed and inflated swimbladder even at 8 dpf (**Figure 3.4B**). Although some mutants do develop a swimbladder, they appeared smaller than that of the *chd7*$^{+/+}$ larvae (7 dpf larvae of **Figure 3.4A**). To study swimbladder formation in more detail, we first assessed its development at 3 dpf, 4 dpf and 5 dpf larvae using H&E staining. At 3 dpf, the swimbladder epithelium of the *chd7*$^{-/-}$ *was* found to be hypoplastic (**Figure 3.4C**). At 4 dpf, the swimbladder size was notably reduced in the mutant zebrafish suggesting an abnormality at the level of the enlargement phase of the three above-mentioned layers (**Figure 3.4C**). At 5 dpf, which marks the end of the inflation stage, the mutants also failed to properly inflate their swimbladder (**Figure 3.4A** and **3.4C**).

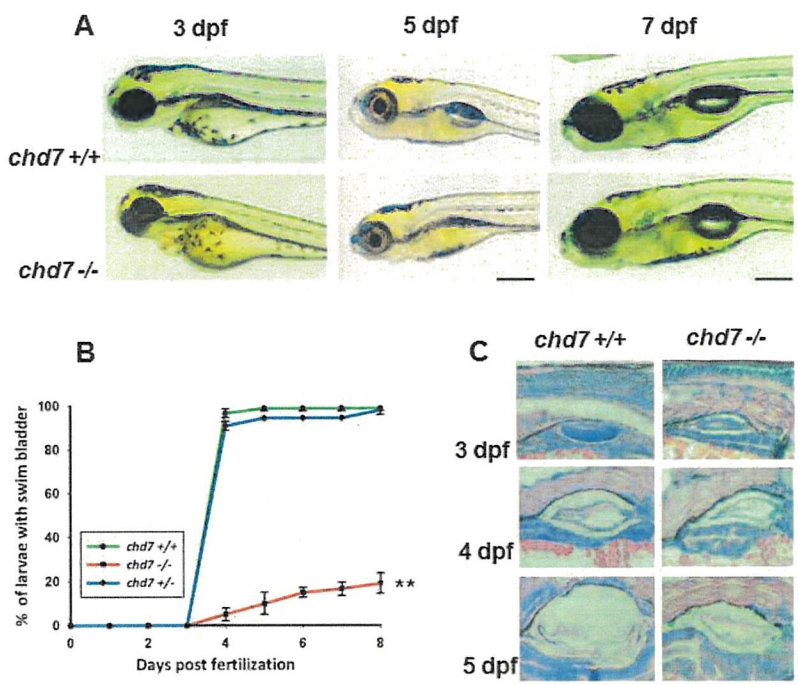

Figure 3.4: Images of the swimbladder region in *chd7*$^{+/+}$ and *chd7*$^{-/-}$ larvae and assessment of the swimbladder by H&E staining.
(A) Images of 3, 5 and 7 dpf *chd7*$^{-/-}$ and *chd7*$^{+/+}$ fish, showing the swimbladder. Wildtypes inflate the swimbladder by 5 dpf, while the mutants do not. The swimbladddder in the *chd7*-mutants is smaller in size even if it does inflate, shown in 7 dpf larvae. (B) Graph plot of percentage of fish with a swimbladder (** $p<0.001$; one way ANOVA). (C) H&E staining shows the hypoplasia of the swimbladder at 3, 4 and 5 dpf in the *chd7*-mutants. Red graph line represents the *chd7*$^{-/-}$, blue and green line the *chd7*$^{+/-}$ and the *chd7*$^{+/+}$ fish respectively. N=3 and n=30. Scales represent 200µm.

3.4.1 qRT-PCR of *Wnt*-related swimbladder specific genes

We have observed that the morphogenesis and the structure of the swimbladder is disrupted in the *chd7*-mutant zebrafish. As previous studies have demonstrated, a proper cross talk between the Hedge hoc *Hh* and the *wnt* developmental pathways is crucial for a normal development of the three different tissue layers of the swimbladder (Winata et al., 2009; Yin, Korzh, Winata, Korzh, & Gong, 2011). Thus, it seemed interesting to see whether the mutation of *chd7* affects the expression of member genes of the *wnt* and *Hh* pathway, that are also expressed in the swimbladder. The expression of *sox2*, *wif1* and *ctnnb1* were assessed using quantitative Real Time-Polymerase Chain Reaction (qRT-PCR). The gene *sox2* is one of the earliest genes expressed in the epithelial layer of the swim bladder (Yin et al., 2011). The results showed that the expression of *wif1* is significantly upregulated and the expression of beta catenin (*ctnnb1*) is significantly downregulated in the *chd7*$^{-/-}$ embryos (**Figure 3.5B** and **3.5C**). The latter is among the cardinal genes in the *wnt* signaling pathway. It can also be used as a measure of *Wnt* signaling activity as an accumulation of *ctnnb1* and its translocation to the nucleus marks activated *Wnt* signaling (Reya & Clevers, 2005). The gene *wif1* is a *Hh* target gene and inhibitor of the *Wnt* pathway (Yin, Korzh, & Gong, 2012a). The other assessed gene *sox2* shows a strong tendency of having an increased fold change as compared to the relative wildtype expression. However, this change was not significant (**Figure 3.5A**) and should be investigated further with for instance more biological replicates. Overall, These results indicate that *chd7* is most likely involved in *Wnt*/β-catening and/or the *Hh* developmental pathways, which is here manifested in the upregulation of the gene *wif1* and downregulation of *ctnnb1* in the *chd7* mutant embryos.

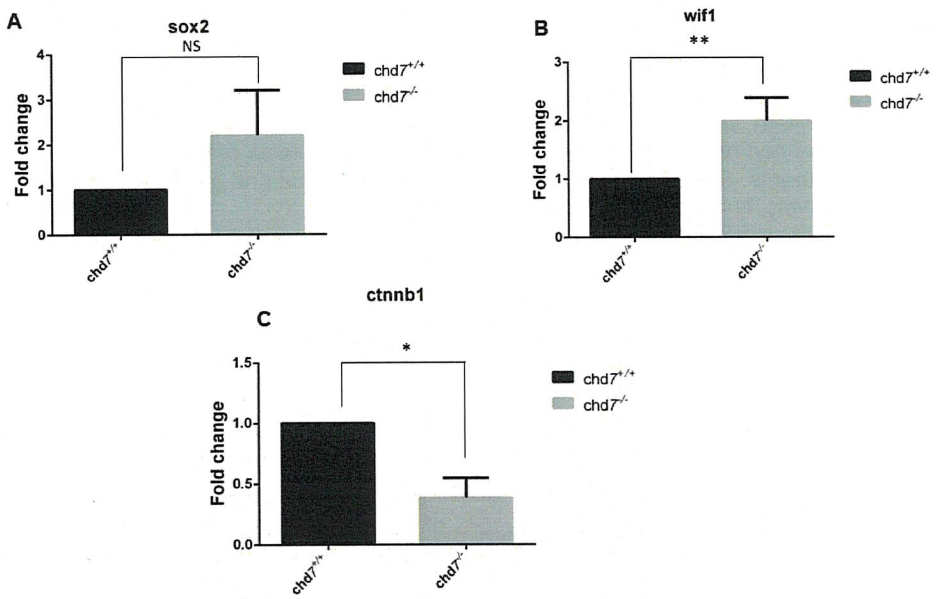

Figure 3.5: Expression levels of *Wnt* and *Hh*-related genes by qRT-PCR. Relative fold change in the expression level of genes *sox2*, *wif1* and *ctnnb1* in *chd7*$^{-/-}$ embryos relative to the expression in *chd7*$^{+/+}$ embryos. * denotes P<0.02; **P<0.005 (unpaired t-test).

3.5 The *chd7*-mutant zebrafish are hyperactive particularly in the dark

Because, sleeping disorders, nighttime hyperactivity, OCD and autistic like behaviors are present in most of the CS patients (Hartshorne et al., 2009; Hartshorne, Hefner, et al., 2005), we wanted to see if our model had any behavioral phenotype. In order to assess behavioral abnormalities in *chd7*$^{-/-}$ larvae, their locomotor activity was quantified in light-dark cycles using the Daniovision tracking device. Compared to wild-type and *chd7*$^{+/-}$ larvae, *chd7*$^{-/-}$ fish were significantly hyperactive (**Figure 3.6A**). This hyperactive phenotype was particularly prominent during dark cycles (**Figure 3.6B**). These results are also consistent with other zebrafish autism models which show hyperactivity during dark cycles (Hoffman et al., 2016).

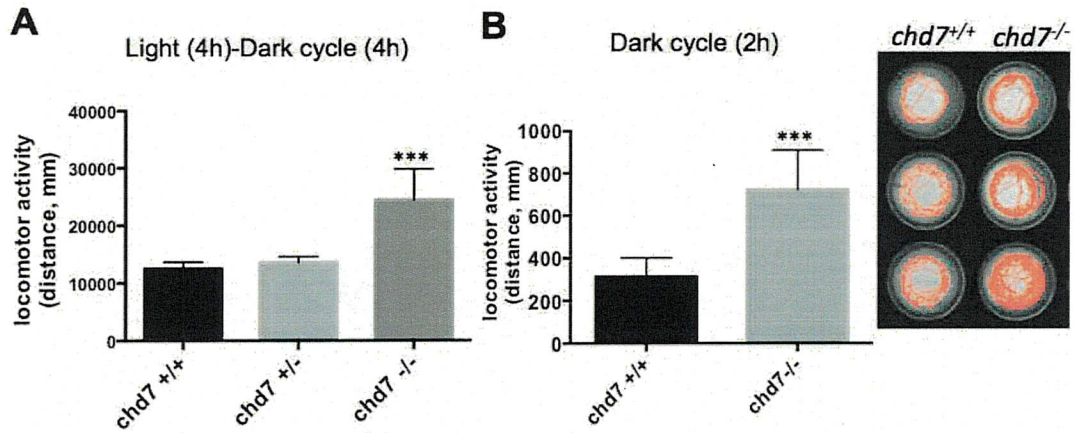

Figure 3.6: Mutant *chd7*$^{-/-}$ fish are hyperactive
(A) Swimming distance of 5-dpf larvae was automatically captured by the DanioVision tracking device across two 4-hr light/4-hr light cycles. Mutant *chd7*$^{-/-}$ larvae displayed hyperactive swimming compared to *chd7*$^{+/-}$ larvae and wildtypes (N=3, n=24; ***p<0.0001) with N batch number and n number of larvae per batch. (B) This phenotype was more prominent in the dark as depicted in the bar graph (*left*) and representative tracking images (*right*) (*** p<0.0001).

3.6 Cranial nerve abnormalities in the *chd7*$^{-/-}$ zebrafish

Developmental defects of the central nervous system and in specific of the cranial nerves are frequently observed in CS patients. We next studied the neuronal network development by anti-acetylated tubulin immuno-fluorescence labeling. Acetylated α-tubulin marks early axon scaffolds (Lowery, De Rienzo, Gutzman, & Sive, 2009). At 28 hpf, we observed the neuronal network of the cranial nerves and the commissural axons. And at 48 hpf, we could assess the sophisticated brain neuronal network of the optic tectum region and the ocular nerves, which develop from the trigeminal ganglia and are a more anterior extensions of it.

At the age of 28 hpf, the cranial neurons showed to have abnormal clustering network as well as defective migration patterns in the *chd7*$^{-/-}$ embryos when compared to the wildtypes (**Figure 3.7**). In particular the clustering of the trigeminal ganglia seems to be affected by the loss of function of *chd7* (**Figure 3.7A**). The intensity of axonal projects also seems to be reduced in the mutants. Specifically the commissural axons scaffolds in the Dorsolateral Cluster (DRC) as well as in the Supra-Optic Tract (SOT) are reduced in number and show distorted and truncated branching network in the *chd7*$^{-/-}$ embryos (**Figure 3.7B**). Furthermore later in development, at 48 hpf, we observed the neuronal network in the optic tectum to be affected in *chd7*$^{-/-}$ compared to *chd7*$^{+/+}$ fish. Particularly, the neuronal network in the mutants appeared less dense and decreased in area (**Figure 3.7C**). The ocular nerves seem also to be aberrantly clustered and have distorted migration in the *chd7*-mutants as observed at 48 hpf (orange arrows in **Figure 3.7D**).

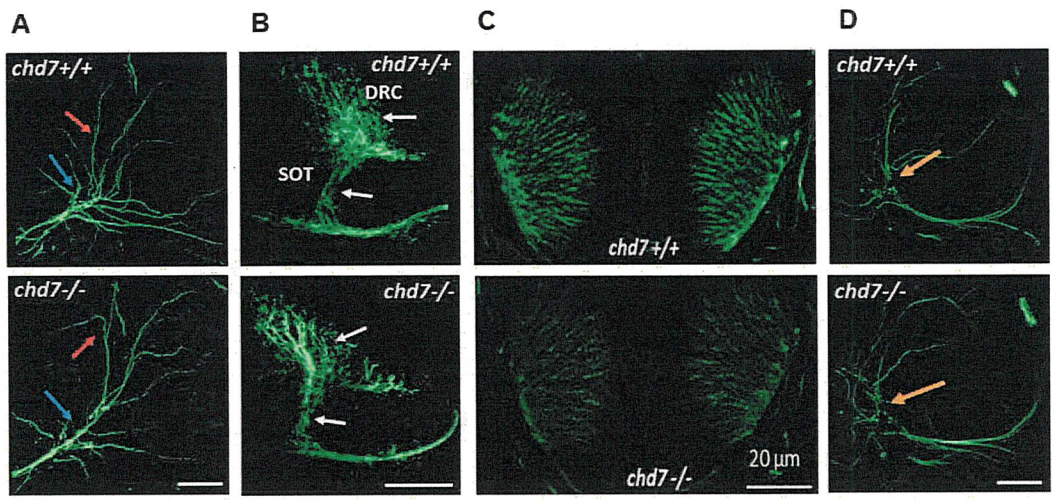

Figure 3.7: Visualization of the neuronal network in zebrafish larvae.
(A) The clustering network of the trigeminal ganglia and the branching of the cranial nerves are abnormal in the *chd7*$^{-/-}$ mutants. Red arrows point to the distorted branching and the blue arrows to the abnormal clustering of the point of origins of the axons. (B) Commissure axons are truncated and show a reduced network in the *chd7*$^{-/-}$ mutants. commissural axon scaffolds in Dorsolateral Cluster (DRC) and Supra-Optic Tract (SOT) seem to be decreased in the *chd7*$^{-/-}$ mutants (white arrows). (C) The optic tectum had a reduced area and network in the *chd7*$^{-/-}$ embryos. (D) The ocular nerves also show aberrant network (orange arrow) and branching in the mutant. N=3 and n= at least 10 for all of the acetyl-tubulin immuno-stainings. Scales are 50 µm unless mentioned otherwise.

CHAPTER 4: RESULTS OF THE SCREENING OF SMALL MOLECULES THAT POTENTIALLY AMELIORATE CS RELATED PHENOTYPES

4.1 A high-throughput screening of FDA-approved molecules in *C. elegans chd-7* mutant

Dr. Patten in collaboration with Dr. Parker (CRCHUM) recently demonstrated the power of combining worm (*C. elegans*) and zebrafish *in vivo* genetic models for drug screening for human diseases such as amyotrophic lateral sclerosis (ALS) (Patten et al., 2016; Patten et al., 2017). We sought to perform a similar rapid chemical genetic screen approach to potentially identify compounds that can ameliorate/rescue CS-related phenotypes.

As part of a collaborative project, Dr. Parker's lab described a deletion of about 700 bp in the *chd-7* gene of *C. elegans* (**Figure 4.1A**) in the mutant line *chd-7*(*gk290*) acquired from the *Caenorhabditis* Genetics Center. Homozygosity of *gk290* leads to significant impairment of the swimming locomotion of the worm when compared to WT animals (**Figure 4.1B**) and they have a lifespan significantly ($p<0.0001$) shorter than WT (**Figure 4.1C**). Using this model, Parker's lab exploited the impaired locomotion phenotype to perform a comprehensive drug screen with 3850 FDA-approved compounds in the Biomol Natural Products, Microsource Discovery Spectrum, Prestwick Commercial Products and Sigma Lopac sets. Forty-nine substances were found to have beneficial effects that could partially correct the impaired locomotion of *chd-7*(*gk290*) worms. From all positive substances, two that improved swimming movement particularly well were chosen for further investigation: Fisetin and Ephedrine (**Figure 4.2A**). Both compounds were able to increase lifespan of *chd-7*(*gk290*) worms significantly (**Figure 4.2B**), with Fisetin showing the most potent effect. Fisetin and Ephedrine were then further validated in the *chd7* zebrafish mutant line (**Figure 4.2A**).

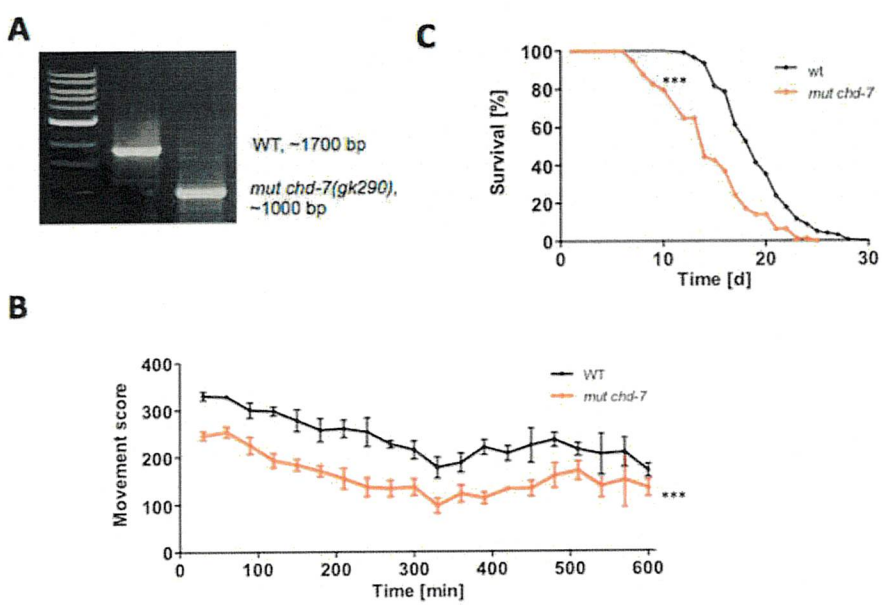

Figure 4.1: Characterization of a *C. elegans chd-7* mutant. (A) *C. elegans* mutant carried a deletion mutation of the gene *chd-7* , leading to a loss of function. (B) Movement scores of mutant strains (red line) shown as average of three measurements compared to N2 wildtype (WT; black line). (C) Survival rate of mutant strains (red line) over 30 days compared to N2 wildtype. *** denotes p<0.0001, N=3 and n=30. (Courtesy of Dr. Kathrin Schmeisser – data from a collaboration of Dr. Patten's and Dr. Parker's lab)

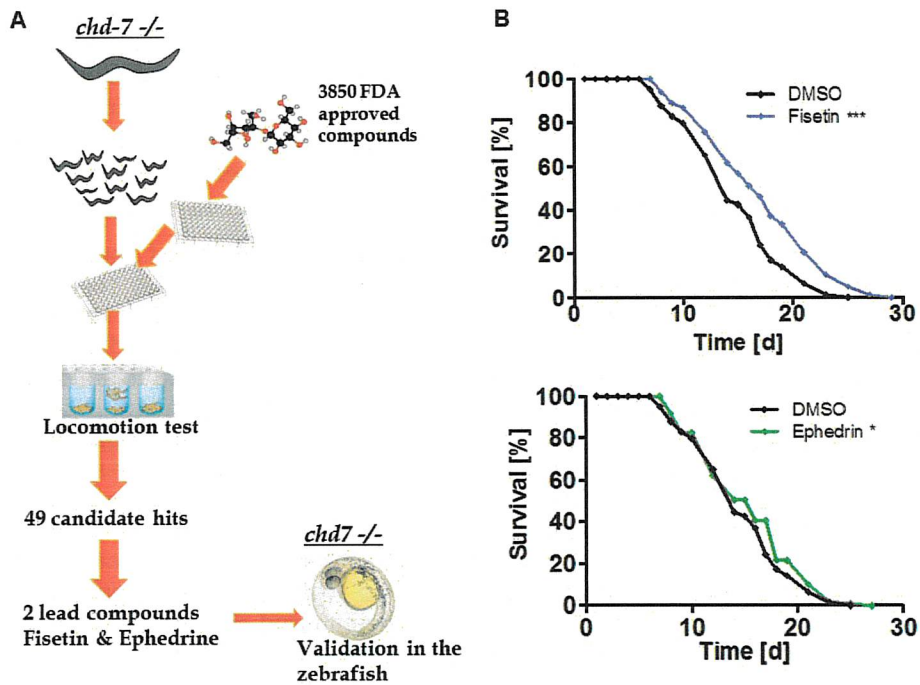

Figure 4.2: Schematic of the initial high-throughput drug screening in the *C. elegans chd-7* mutant and integration of the *C. elegans* and the zebrafish system for drug discovery.
(A) *C. elegans* carrying a deletion mutation of the gene *chd-7* were used for a screening of large amount of FDA approved chemicals. Their locomotion was used as outcome read out. The two lead compounds, Fisetin and Ephedrine were further screened in the *chd7*-mutant zebrafish. (B) Fisetin and Ephedrine could significantly improve the life span of the *chd-7*$^{-/-}$ *C. elegans*. *** denotes p<0.0001, * p<0.05, N=3 and n=30.

4.2 Validation of the lead compounds in the *chd7*-mutant zebrafish

Fisetin and Ephedrine were tested at different concentrations (2, 5,10, 20 and 40 µM). The safe and potent concentration of 10 µM was used for each drug and in each screening. Impaired behavioral phenotype, neuronal network defects, pericardial edema, survival and swimbladder development were used as outcome measures.

4.2.1 Treatment with Fisetin or Ephedrine rescues the hyperactivity phenotype

To confirm the neuroprotective properties of Fisetin and Ephedrine, they were tested in our *chd7*$^{-/-}$ zebrafish larvae, which show an abnormal hyperactivity behavioral phenotype particularly in dark cycles. Mutant *chd7* fish treated with either Fisetin or Ephedrine showed a significant reduction ($P<0.001$ and $P<0.05$ respectively) of hyperactivity in swimming response, as assessed by distance swam during dark cycles (**Figure 4.3**). The compounds had no effects on *chd7*$^{+/+}$ (WT) fish.

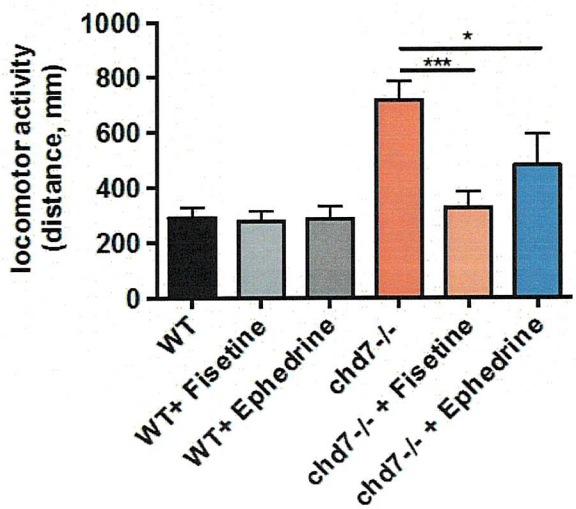

Figure 4.3: Fisetin and Ephedrine ameliorate hyperactivity phenotype in *chd7*-mutant fish. Distance swam were assessed in the dark with or without treatment. ***denotes $p<0.001$, *denotes $p<0.05$. N=3 and n=24 larvae.

4.2.2 The neuronal network development is ameliorated upon treatment with Fisetin or Ephedrine

We next sought to assess the effect of the Fisetin and Ephedrine treatment on neuronal network development. To our surprise, compared to non-treated *chd7*-mutants, Fisetin treated *chd7*$^{-/-}$ larvae displayed a better neuronal network development. This is manifested in a more organized clustering network of the trigeminal neurons (at 28h) as well as a more dense and bigger area of the optic tectum brain region (at 48 hpf). **Figure 4.4A** (orange arrows) depicts that the general clustering of the trigeminal glia is ameliorated upon treatment with Fisetin and Ephedrine. Similarly, the commissural axons' development was also partially rescued in both treatment groups. The commissural axons seem more branched and organized in both Fisetin and Ephedrine treated group (yellow arrows in **Figure 4.4B**). The optic tectum also had an improved density as well as organization in both treatment groups of *chd7*$^{-/-}$ larvae (**Figure 4.4C**). Overall, both Fisetin and Ephedrine seem to have a positive effect on the CNS defects.

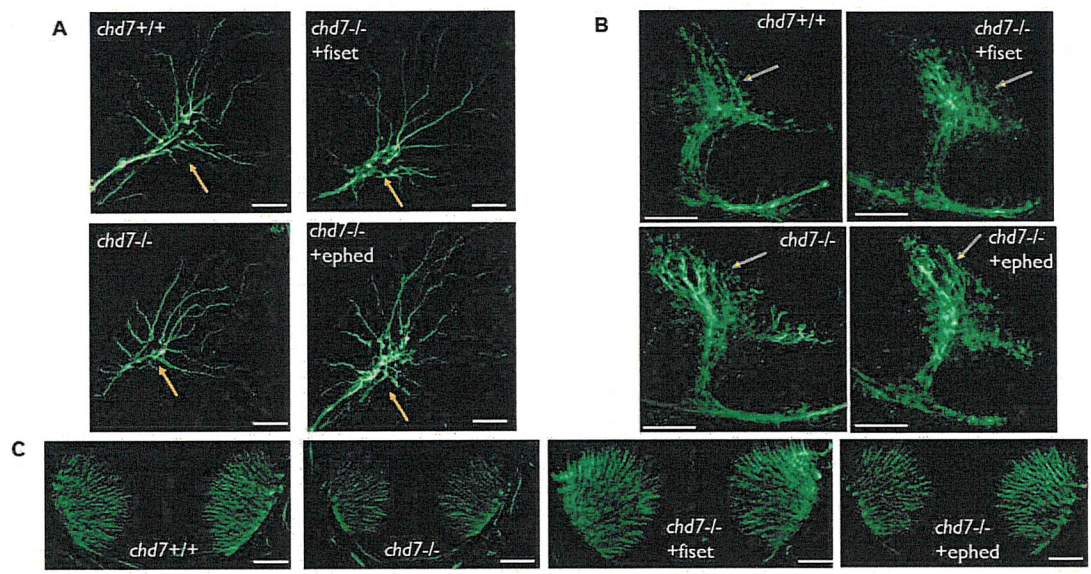

Figure 4.4: Representative confocal images of acetylated α-tubulin staining in 28 and 48 hpf zebrafish embryos with or without treatment of Fisetin or Ephedrine.
(A) The trigeminal ganglia in wildtype and *chd7*$^{-/-}$ treated and not treated larvae, the orange arrows point to the clustering network of the trigeminal nerves (B) Commissural neurons of the Fisetin treated and untreated *chd7*$^{-/-}$, yellow arrows point to the network and branching of the dorsolateral axonal scaffold which seems to be ameliorated in the treated *chd7*$^{-/-}$ embryos. (C) Images of the optic tectum brain region in the *chd7*$^{-/-}$ larvae with and without treatment of Fisetin or Ephedrine. For each treated and untreated group N=3 and n=10. Scales represent 50 µm.

4.2.3 Treatment with both Fisetin or Ephedrine limits pericardial edema rate

Pericardial edema was another outcome measure we used for the drug screenings. It was monitored between the 3rd day of development to the 6th day. Interestingly treatment with both Fisetin and Ephedrine seems to be beneficial against pericardial edema ($p<0.0001$; unpaired t-test). The dose response test of the drugs at the chosen concentration did not show any increase of edema in wildtype treatment groups, hence it was not included in the graph plot. The rate of edema in both treated groups is lower than in the non-treated group. More specifically, the edema in the Ephedrine group is as low as in the wildtype groups (see **Figure 4.5A** and **Figure 3.2C** and **3.2D**). Thus, Ephedrine seems more potent to rescue the pericardial edema in the *chd7*$^{-/-}$ larvae than Fisetin.

4.2.4 The survival and swimbladder development of the *chd7*-mutant zebrafish are not improved upon drug treatment

We did not observe any noticeable effect on the swimbladder development or the survival upon treatment with both of the target drugs. However, as observed from the trend of the graphs (**Figure 4.5B**), it seems that Ephedrine delays the sharp decline in survival after 10 dpf. The swimbladder development of the drug treated mutants seems to start later than non-treated *chd7*$^{-/-}$ larvae (**Figure 4.5C**). However, in the Fisetin treated larvae, on average 30% end up inflating a swimbladder between the 7th and 8th day post fertilization. On average, slightly more Fisetin and Ephedrine treated larvae develop and inflate a swimbladder than the non-treated mutants, but the difference is not significant. These data suggest that the drugs most likely exert their effect specifically in the neuronal and brain developmental pathways. Thus, they cannot rescue or ameliorate other developmental defects related to CS.

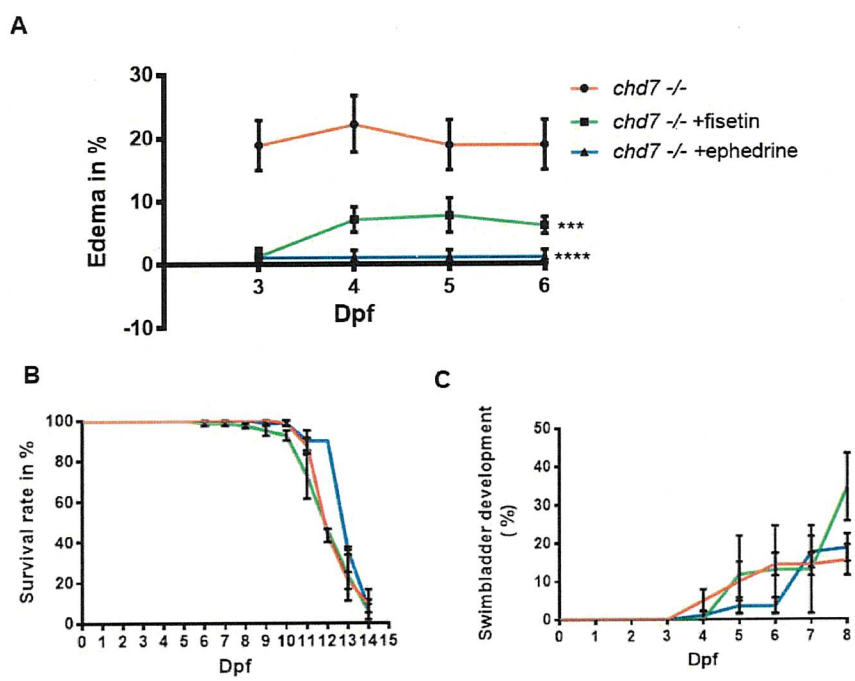

Figure 4.5: Plots of edema, survival and swimbladder development with and without treatment of Fisetin and Ephedrine.
(A) Pericardial edema rate is reduced in both Fisetin or Ephedrine treated larvae (**** and *** denote $p<0.0001$; unpaired t-test). (B) The survival is not ameliorated upon treatment with Fisetin or Ephedrine. (C) Treatment with Fisetin or Ephedrine does not ameliorate the swimbladder development. For each treated and untreated group N=3 and n=30 larvae. Red lines represent non-treated *chd7*$^{-/-}$ larvae, green line Fisetin treated *chd7*$^{-/-}$ larvae and blue line Ephedrine treated *chd7*$^{-/-}$ larvae. Error bars represent SEM.

CHAPTER 5: DISCUSSION AND CONCLUSION

5.1 The relevance of a *chd7*-mutant zebrafish line

There is a growing demand for biologically relevant systems to link gene discovery to pharmacological screens (Hoffman et al., 2016). Small animal models have proven to be useful to study mechanisms of complex disorders. The *drosophila*, *C. elegans* and zebrafish have been utilized to study various diseases and to screen for compounds that can rescue disease phenotypes (Giacomotto & Ségalat, 2010). The zebrafish is a unique simple vertebrate model for its use as a high or medium-throughput drug screening tool. In contrast to *in vitro* models, a whole organism is beneficial to also assess adverse effects of target compounds as well as the desired effects simultaneously (Giacomotto & Ségalat, 2010).

In this study, we have successfully established a *chd7* zebrafish mutant line, and to our knowledge it is the first one. This mutant line recapitulates CS related developmental defects and using this line, we screened target compounds as potential therapeutics to ameliorate or rescue the CS related features. Furthermore, this line will be very useful to study the role of CHD7 in CS pathogenesis as well as normal neuronal development. Moreover, the CRISPR-Cas9 induced a frameshift mutations in the zebrafish line, reflecting one of the most prevalent *CHD7* mutations in human patients which is also a frameshift leading to dysfunctional protein product (M C J Jongmans et al., 2006). However, seven out of the ten first identified mutation are heterozygous *CHD7* mutations that lead to early stop-codon (Vissers et al., 2004a). In our model, we did not observe any abnormal phenotypes in heterozygous *chd7*$^{+/-}$ fish. It is very plausible that this could be due to the presence of maternal mRNA effect as numerous research indicates the importance of the maternal mRNA during early zebrafish development (Shao et al., 2017; Mishima & Tomari, 2016).

The CRISPR induced mutation in our model targeted the ATPase/helicase domain of the zebrafish *chd7* and putatively led to a dysfunctional CHD7 protein product. We could not perform Westernblot to assess the protein, because there is no antibody available against the zebrafish *Chd7*. However, qPCR could confirm that *chd7* expression is significantly reduced in the mutants, both heterozygotes and homozygotes (**Figure 3.1D**). In contrast to the haploinsufficiency of *CHD7* in human patients (Zentner, Hurd, et al., 2010), the CS-related phenotypes were not evident in the heterozygote *chd7*-mutant fish. We hypothesize that there is some compensatory mechanisms in this mutant line. This can be studied further by generating other CRISPR/Cas 9 *chd7* mutant zebrafish lines, targeting other region (s) of the gene and studying the heterozygotes.

5.2 Summary of findings

We observed several defects that correspond to the human CS phenotypes in the *chd7*-mutant fish. We monitored the survival of the mutants as compared to their wildtype siblings, and observed their morphological development using bright field microscopy (Chapter 3). The lifespan of the homozygote mutants was significantly decreased, specifically from 9 dpf on, as compared to the lifespan of the heterozygotes and wildtypes. They had curvature of the body. and showed several defects in the network and organization of the cranial nerves and the optic tectum brain region. Furthermore, the swimbladder, was consistently lacking in the mutants and fails to inflate. Mutants exhibited a smaller and malformed head and cranio-facial cartilage. Craniofacial structures of the mutants ranged from mildly to severely malformed.

Measurements of the Meckel's cartilage, which corresponds to the lower jaw in humans, showed a significant increase in the mutants. These defects are consistent to the craniofacial malformation in human patients (Bajpai et al., 2010). More specifically, most of the CS patients have a square-shaped face next to facial palsy and asymmetry (Damien Sanlaville & Verloes, 2007). Furthermore, the mutant larvae were also hyperactive during the dark exposure, consistent to reports of sleeping disorders, nighttime hyperactivity and autistic like behaviors in most of the CS patients (Hartshorne et al., 2009; Hartshorne, Hefner, et al., 2005).

The abnormal swimming behavior was initially used as a robust and unbiased screening of the bioactive compounds. Lead compounds were tested on the neuronal network developmental defects, edema, swimbladder development as well as survival. They were potent in ameliorating the neuronal defects and the abnormal swimming behavior of the *chd7* mutants. Furthermore, the compounds also decreased the rate of pericardial edema. However, they did not improve swimbladder development and survival (Chapter 4). These findings suggest that their protective mechanism is likely restricted to the neuro-developmental pathway.

The swimbladder is a gas filled organ and is important for the zebrafish survival as it serves as a buoyancy regulator (Robertson, McGee, Dumbarton, Croll, & Smith, 2007). Despite having different functions and structure, the swimbladder and mammalian lungs are known to be analogous organs. A study claims that the most crucial difference between the two Air filled Organs (AO's) is that the lung develops from a ventral invagination, while the swimbladder develops from a dorsal invagination. Furthermore, this study showed that a set of genes expressed in the tetrapod lungs are also co-expressed in the zebrafish swimbladder (Cass et al., 2013). There is not much known about the involvement of the lung development in CS, however it is known that lung atresia is among the death causes in CS patients and Chd7 is highly expressed in the lung epithelium in mice, during fetal development (Sporik, Dinwiddie, & Wallis, 1997; Bosman et al., 2005). Thus, the involvement of the lungs might be a neglected topic in the study of CS pathology.

It was intriguing that in the swimbladder was absent in most of the *chd7*-mutant larvae. *Wnt* signaling was shown to play a crucial role in the swimbladder development and the proper development of this organ was perturbed upon down or upregulation of the *Wnt* signaling. Thus, a proper level of this signaling is required for the optimum development of the swimbladder (Yin et al., 2011; Yin, Korzh, & Gong, 2012). A proper cross talk between the *Wnt* and *Hh* pathways is required for a normal development of the swimbladder (Yin et al., 2011). Thus, we wanted to see whether the mutation of *chd7* affects the expression level of the *Wnt* and *Hh* signaling related genes, *sox2, ctnnb1* and *wif1*. The gene *sox2* is the earliest epithelial marker of the swimbladder. Many *SOX* family genes are known to modulate the canonical *WNT/B-catenin* signaling in normal development as well as in diseases (Yin et al., 2011; Kormish, Sinner, & Zorn, 2009). Furthermore, transcription factor Sox2 is known to physically interact with Chd7 (Engelen et al., 2011). Thus, an adequate interaction/feedback loop between the *sox2* and *Wntl β-catenin* signaling is required for a proper development of the swimbladder. Perhaps it will give more insight if more sox2 pahtway related genes are investigated in the future. The gene *wif1* was shown to be an important link of *Hh* and *Wnt*-pathway. WIF1 is a secreted protein which is maintained by Hh signaling. And WIF1 functions as a negative feedback loop to inhibit Wnt signaling (Yin et al., 2012b).

We aimed to find out why the swimbladder was consistently lacking in the *chd7*- mutants and the qRT-PCR outcomes point out that the members of the canonical *Wnt* signaling might indeed be adversely affected in the *chd7*-mutant fish. Although the genes we investigated (*sox2, ctnnb1* and *wif1)* are also expressed in other organs during early development, their expression is also important for the swimbladder development. The expression of gene *wif1* was significantly upregulated ($P<0.005$) and the expression of gene *ctnnb1* was significantly

downregulated in the *chd7*-mutants (P<0.02). The expression of *sox2* was increased in the mutants, but not significantly (P=0.0536) the expression of *sox2* is probably increased in the mutants (Chapter 3 **Figure 3.5A**). The downregulation of ctnnb1 in the mutant might be due to being bound to other proteins like sox2 or simply degraded by the ubiquitin pathway, because of general inhibition of the Wnt signaling, which were shown by Kormish et al. (Kormish et al., 2009). Looking at our results, the inhibition is likely partly due to upregulation of *wif1.* Furthermore, *ctnnb1* is regulated by multiple pathways and other proteins (Yin et al., 2011), where chd7 also might exert its effect. Thus, we can speculate from our results that protein chd7 possibly modulates the expression of member genes of the *Hh* and/or the *Wnt* signaling pathways to affect the *Wnt* signaling activity. Further assessment of the expression of more *Wnt* and *Hh* related genes in the *chd7*$^{-/-}$ is required to be conclusive about this. Gene *sox2* was not significantly affected by the *chd7* mutation, but shows a tendency of upregulation which should be further investigated by for instance increasing the biological replicates. As a future perspective and to ascertain the perturbation of the wnt signaling in the *chd7*$^{-/-}$ fish, a chemical agonists of wnt such as 6 Bromoindirubin-3'-oxime (BIO) (Xu et al., 2017) could be tested for possibly leading to more swimbladder development in the mutants by enhancing wnt signaling. . Another possible test is knocking down *wif1* in an attempt to upregulate the wnt-signaling and rescue the swimbladder phenotype in the chd7$^{-/-}$ mutants.

5.3 Our stable *chd7*-mutant line reflects the cranial nerve manifestations in CS

Our *chd7*- mutant model reflects most of CS phenotypes, particularly in terms of CNS defects. More specifically, the trigeminal ganglia also named 5th ganglia in zebrafish, are frequently affected in our model, corresponding to the cranial nerve V manifestation in human CS patients (Hudson & Blake, 2016). Trigeminal nerve is hypothesized to contribute to the feeding difficulties in CS and is among the major causes of mortality. These nerve bundles are also involved in innervation of chewing muscles and transmitting sensory information from the face structures to the brain (Kim D. Blake et al., 2008; Williams, 2005).

So far, many studies have shown the role of CHD7 in neuronal development, including axon morphology (E. A. Hurd, Poucher, Cheng, Raphael, & Martin, 2010; Aramaki et al., 2007). Furthermore, morpholino KD of *chd7* in the zebrafish led to disruption of the cranial motor neurons' organization as well as defects in the organization and clustering of the 5th trigeminal ganglion (Patten et al., 2012). Similar phenotypes of the trigeminal ganglia are observed in the current study. There is less axonal branching, and some cranial nerves seem to be missing or have aberrant neuronal migration and projection to the telencephalon, in the mutant. Furthermore, there seems to be a defect in migration of both cranial and commissural neurons in the *chd7*-mutant. Also the neuronal network in the optic tectum is affected in the *chd7*-mutant. The zebrafish optic tectum receives sensory input from mainly the retina but also from other sensory modalities (A. W. Thompson, Vanwalleghem, Heap, & Scott, 2016; Pietri et al., 2017). Its major role is thus detecting sensory stimuli, processing them and generating the adequate motor response such as pray capture (Pietri et al., 2017; Krauzlis, Lovejoy, & Zénon, 2013).

5.4 Our zebrafish model is comparable to other models of CS

Similar to our *chd7*-mutant model, craniofacial cartilage defects were observed in *chd7* MO KD zebrafish model of CS (Asad et al., 2016). The *chd7* KD zebrafish also had a missing lower jaw. Moreover, cranial ganglia were absent in at 24 hpf morphant embryos. Additionally, the expression of transcription factor *sox2* was significantly reduced in the *chd7* morphants (Asad et al., 2016). Interestingly, the expression of *sox2* seems increased in our mutants. This could perhaps be explained by the putative knock-out of *chd7* in our model, while *chd7* was knocked down in the morphants of Asad et al.

CHARGE syndrome was modelled in *Xenopus* embryos by downregulating *Chd7* expression or overexpressing its catalytically inactive ATPase mutant. The major feature of CS were observed in these models including, coloboma, microphthalmia, malformation of Meckel's cartilage, malformation of the craniofacial cartilage and heart defects. Additionally, in both the inactive ATPase mutants and the KD embryos, the cell migration to the pharyngeal arches was perturbed (Bajpai et al., 2010).

Homozygosity for *Chd7* loss-of-function leads to embryonic lethality in the mouse models, whereas heterozygous *Chd7*-mutant mice reflected most of CS phenotypes. Mice with heterozygous gene trapped *Chd7* loss of function had different degrees of circling behavior, head bobbing, reflecting vestibular disfunction in human patients (Elizabeth A. Hurd et al., 2007). This phenotype is also similar to the abnormal swimming behavior in our zebrafish model. Furthermore, the gene trapped mice ESCs were tagged with LacZ reporter and the researchers could track the cells that developed from them in the mice. They observed that both the homozygous $Chd7^{Gt/Gt}$ and the heterozygous $Chd7^{Gt/+}$ mice had abnormal growth and development of the organs involved in CS such as the eye, ear, pituitary, heart, brain and craniofacial structures (Elizabeth A. Hurd et al., 2007).

An earlier study of Bosman et al. showed that all 9 ENU mutant mice, identified to carry variable *Chd7* mutations, had circling and bobbing behavior. The mutations found in the ENU mice also lead to premature stop-codons in several domains of the protein. These mice models thus also reflect the human mutations and are similar to our model. Further, the ENU mice had other variably penetrant defects in the heart, ear and craniofacial tissue. One of the first discovered mutant, called *Wheels*, had abnormally extended circadian period and abnormal response to light (Bosman et al., 2005). We can similarly speculate that our zebrafish model might have abnormal circadian rhythm, as observed in their dark-time hyperactivity. This phenotype in the models might recapitulate the reported nighttime hyperactivity, OCD and autistic-like behaviors in human patients (Hartshorne et al., 2009; Hartshorne, Hefner, et al., 2005). The hyperactivity in our model is similar to the swimming behaviour observed in an ASD-related study of Hoffman et al. This likely reflects that there is a disturbance between the excitatory and inhibitory network in our model (Hoffman et al., 2016). Further analysis would shed light on mechanisms of autistic symptoms in CS and ASD in general. One possibility is studying the balance of GABAergic and glutamatergic neurons, which are often abnormal in ASD-patients (Hoffman et al., 2016).

5.5 This study can contribute to the acceleration of drug discovery for CS-related phenotypes

Working towards a rapid drug discovery goal, the first objective of my MSc project was generating a stable *chd7* zebrafish mutant line to model CS. Through our drug screen approach (Chapter 4), we identified two compounds that can potentially be used as effective drugs for CS. Although our lead compounds did not rescue all the defects completely or ameliorate the survival, they proved to be promising to treat the neurological developmental defects. Altogether, Fisetin and Ephedrine are probably beneficial to rescue the neuronal defects in the zebrafish model of CS. Additionally, both of the drugs also limit the rate of pericardial edema in the *chd7*$^{-/-}$ larvae. Screening both Fisetin and Ephedrine together would help determine whether they potentiate or synergize each other's' effect without having damaging effects.

We think that the drugs are not potent in rescuing every defect in our zebrafish model, such as the swimbladder development because their mechanism of work might be limited to the neuronal developmental pathway. Similarly, the life span of the treated mutants did not improve either, because there are probably multiple developmental pathways affected by the *chd7* loss of function. This is reflective of the complex pathogenesis of CS, where many organs and systems are affected (M C J Jongmans et al., 2006). There is to date no medical treatment to help the patients cope with their neurobehavioral difficulties. Our study hopefully accelerates the discovery of a pharmaceutical treatment to ameliorate the difficulties such as attention deficit, OCD and night time hyperactivity that are frequently present in CS patients. The treatment in combination with the different therapeutic approaches (D. Brown, 2005) might be very promising for a better quality of life of CS patients.

The first lead compound, Fisetin is a polyphenol flavonoid which is found as a plant pigment in various fruits and vegetables including, apples, strawberry, persimmon, grape, onion and cucumber. Fisetin has antioxidant and anticarcinogenic properties (Khan, Syed, Ahmad, & Mukhtar, 2013). Fisetin is gaining attention because of its pleiotropic effects in several biological systems (Syed et al., 2011). It was shown to be neuroprotective in various models of Huntington's disease and its mechanisms were linked to activating the Extracellular signal-Regulated Kinase (ERK) signaling cascade. The scientific interest in Fisetin is justified, because there is only a few compounds available that activate the ERK pathway (Maher et al., 2011). The same pathway might link the neuroprotective effect of Fisetin in our study. Another study found that Fisetin might also exert its effect on the wnt/β-catenin pathway by interfering with the cooperation between T-cell Factor-2 (TCF2) and β-catenin. The same study demonstrated that Fisetin has chemopreventive and anti-tumor activities (Syed et al., 2011). Thus, perhaps the neuroleptic/neuroprotective effects of Fisetin in our zebrafish chd7-mutants can be explained by the ERK activation and its ineffectiveness in the swimbladder development could be partly explained by its inhibitory effect on the *Wnt*-pathway.

Ephedrine is currently in use for treating hypotension that occurs during general anesthesia. It showed to lead to better postoperative neurological outcome that its equivalent phenylephrine. Ephedrine led to higher rates of ipsilateral cerebral tissue oxygen saturation (Aliane et al., 2017). Ephedrine is an agonist of α and β adrenergic receptors. So, it acts on the sympathetic nervous system (McMacken et al., 2018).

Together with Ephedrine, the selective β2 adrenergic agonist Salbutamol is being used to treat neuromuscular junction (NMJ) disorders such as Congenital Myasthenic Syndromes (CMS). Salbutamol treatment reduced defects in motor axon pathfinding in the zebrafish. Treatment with the Cyclic Adenosine Monophosphate (cAMP) activator Forskolin leads to same effects

as Salbutamol treatment. This indicates that sympathomimetics might positively affect neuromuscular synaptogenesis via binding to β2 receptors and activating the cAMP-pathway (McMacken et al., 2018). Ephedrine also showed to lead to better outcomes of the neuronal branching and migration as well as in treating the abnormal swimming activity in our model of CS. I suppose the same mechanism can be proposed for Ephedrine as salbutamol, as they are currently being used to treat the same NMJ disorder and are both agonists of the adrenergic receptors.

5.6 Perspectives

The stable *chd7*-mutant created in this study does not only allow for screening of compounds on the motor behavior, but also on other defects related to CS such as craniofacial dysmorphism and heart problems (pericardial edema in the fish). Furthermore, this stable *chd7*-mutant like can be utilized to study the involvement of *chd7* in CS pathogenic mechanisms as well as in normal developmental pathways. Because CHD7 binds to thousands of enhancer sites in a tissue specific and developmental stage specific manner, further research is required to study whether CHD7 has similar or different roles in different cell types (Donna M. Martin, 2010). More importantly, this line also allows the study of CHD7 involvement in the development of different neuron or interneuron sub-types, such as the GABAergic system. The study of the GABAergic system has already been started by one of the PhD student of the lab, Priyanka Jamadagni. As CHD7 is also involved in myelin sheath development, it is also a possible to study this process in the mutant by applying immunohistochemistry or in situ hybridization of myelin markers such as N-ethylmaleimide sensitive factor (NSF). The zebrafish nsf is expressed in the cells of the developing trigeminal ganglia, anterior spinal cord and forebrain as early as 14 somites stage and is essential for the proper organization of the myelin sheath (Woods, Lyons, Voas, Pogoda, & Talbot, 2006).

As mentioned earlier, this transgenic line offers a tool to study the complex mechanisms of *chd7* in CS pathogenesis as well as in normal development. CHD7 is involved in transcriptional reprogramming in cooperation with tissue specific complexes. For example, it synergistically cooperates with PBAF in early neural crest cells and renders them multipotent and migratory (Bajpai et al., 2010). There are many unanswered questions about the pathogenic mechanisms of CHARGE syndrome; whether the defects in the affected organs arise from increased cell death, reduced proliferation or premature cellular differentiation (Elizabeth A. Hurd et al., 2007).

Last but not least, the FDA-approved chemicals Ephedrine and Fisetin seem effective in suppressing the hyperactivity and ameliorating neuronal connections as well as network. Thus, next to being a possible remedy to the neuronal symptoms in CS, they might as well be repurposed to treat other neurobehavioral disorders such as ASD. The drugs were proven to be neuroleptic and suppress the ASD related behavior, hyperactivity in dark or nighttime. As ASD is also disorder of social interactions (Hoffman et al., 2016), the compounds could be tested on adult fishes' social behavior such as mating. Moreover, because these chemicals have already been labeled safe by the FDA, it is less time consuming to advance to clinical testing after validating them on higher mammalian models (Tamplin et al., 2012).

5.7 General conclusion and Significance of my work

In this Master's thesis, we developed a stable zebrafish line with *chd7*$^{-/-}$ mutation to model CHARGE syndrome and we characterized relevant CS-phenotypes. We also used our model as a robust tool for drug discovery. The stable transgenic line faithfully replicates most of the important features of CS, including CNS defects -manifested in abnormal neuronal development and hyperactivity-, heart defects and cranio-facial defects. Another striking and consistent phenotype of the *chd7*$^{-/-}$ zebrafish mutants is lack of swimbladder development and inflation. The model gives us a good starting point to study in which developmental pathways *chd7* is involved and how its loss of function leads to the defects observed in several organs and body systems. These findings will be included in two manuscripts that are currently in preparation.

With this study, we have tried to reproduce the pathogenesis of the complex birth defect CS. Despite observing many CS related phenotypes in our homozygote chd7 mutant zebrafish, we did not observe a relevant difference in from the wildtypes in the heterozygote mutants. As mentioned earlier, the mutations in human CS are autosomal dominant. Thus, we would expect some defects in the heterozygote mutant also. Perhaps, if the heterozygotes were also studied in more detail, such as with Alcian blue and Acetyle-tubulin staining, we could have shown some mild forms of the defects that were evident in the homozygotes.

Furthermore, another possible molecular studies of proliferation and cell death could have been studied to determine whether the *chd7*-mutation leads to more cell death or perhaps less cell proliferation that underly the different defects observed. But, because of time limitations, that could not be done by me. I am certain that it will be among the future experiments of the lab with this stable *chd7*-mutant line.

Following the initial high-throughput screenings in the *C. elegans*, the zebrafish model was used to test the lead compounds on the other phenotypes related to CS such as hyperactivity, neurodevelopmental defects, heart defects and the swimbladder development which we are not certain of how it connects to CS. Therefore, the zebrafish model can be used to test all the initial compounds of the chemical libraries on the rest of the phenotypes relevant for CS. The lead compounds have potential to treat the CNS related CS features and these compounds can be translated into preclinical trials. Overall, my thesis sets the groundwork to better understand CS pathogenesis and to accelerate the therapeutic development. My aspiration is that the lead compounds can be used to treat CS-related phenotypes or even ASD-related neurobehavioral anomalies one-day.

CHAPTER 6: REFERENCES

Ahmad, Y., Boisvert, F.-M., Gregor, P., Cobley, A., & Lamond, A. I. (2009). NOPdb: Nucleolar Proteome Database--2008 update. *Nucleic Acids Research*, *37*(Database), D181–D184. https://doi.org/10.1093/nar/gkn804

Al, S. T., Cottrell, D. A., & Hughes, C. V. (n.d.). Dental findings associated with the malformations of CHARGE. *Pediatric Dentistry*, *24*(1), 43–6. Retrieved from http://www.ncbi.nlm.nih.gov/pubmed/11874058

Aliane, J., Dualé, C., Guesmi, N., Baud, C., Rosset, E., Pereira, B., ... Schoeffler, P. (2017). Compared effects on cerebral oxygenation of ephedrine vs phenylephrine to treat hypotension during carotid endarterectomy. *Clinical and Experimental Pharmacology and Physiology*, *44*(7), 739–748. https://doi.org/10.1111/1440-1681.12759

Amatruda, J. F., Shepard, J. L., Stern, H. M., & Zon, L. I. (2002). Zebrafish as a cancer model system. *Cancer Cell*, *1*(3), 229–31. https://doi.org/10.1016/S1535-6108(02)00052-1

Anichtchik, O., Sallinen, V., Peitsaro, N., & Panula, P. (2006). Distinct structure and activity of monoamine oxidase in the brain of zebrafish (Danio rerio). *The Journal of Comparative Neurology*, *498*(5), 593–610. https://doi.org/10.1002/cne.21057

Aramaki, M., Kimura, T., Udaka, T., Kosaki, R., Mitsuhashi, T., Okada, Y., ... Kosaki, K. (2007). Embryonic expression profile of chickenCHD7, the ortholog of the causative gene for CHARGE syndrome. *Birth Defects Research Part A: Clinical and Molecular Teratology*, *79*(1), 50–57. https://doi.org/10.1002/bdra.20330

Asad, Z., Pandey, A., Babu, A., Sun, Y., Shevade, K., Kapoor, S., ... Sachidanandan, C. (2016a). Rescue of neural crest-derived phenotypes in a zebrafish CHARGE model by Sox10 downregulation. *Human Molecular Genetics*, *25*(16), 3539–3554. https://doi.org/10.1093/hmg/ddw198

Asad, Z., Pandey, A., Babu, A., Sun, Y., Shevade, K., Kapoor, S., ... Sachidanandan, C. (2016b). Rescue of neural crest-derived phenotypes in a zebrafish CHARGE model by Sox10 downregulation. *Human Molecular Genetics*, *25*(16), 3539–3554. https://doi.org/10.1093/hmg/ddw198

Ata, H., Clark, K. J., & Ekker, S. C. (2016). The zebrafish genome editing toolkit. *Methods in Cell Biology*, *135*, 149–170. https://doi.org/10.1016/BS.MCB.2016.04.023

Bailey, J., Oliveri, A., & Levin, E. D. (2013). Zebrafish model systems for developmental neurobehavioral toxicology. *Birth Defects Research Part C: Embryo Today: Reviews*, *99*(1), 14–23. https://doi.org/10.1002/bdrc.21027

Bajpai, R., Chen, D. A., Rada-iglesias, A., Zhang, J., Xiong, Y., Chang, C., ... Wysocka, J. (2010). CHD7 cooperates with PBAF to control multipotent neural crest formation, *463*(7283), 958–962. https://doi.org/10.1038/nature08733.CHD7

Balow, S. A., Pierce, L. X., Zentner, G. E., Conrad, P. A., Davis, S., Sabaawy, H. E., ... Scacheri, P. C. (2013). Knockdown of fbxl10/kdm2bb rescues chd7 morphant phenotype in a zebrafish model of CHARGE syndrome. *Developmental Biology*, *382*(1), 57–69. https://doi.org/10.1016/j.ydbio.2013.07.026

Basson, M. A., Echevarria, D., Petersen Ahn, C., Sudarov, A., Joyner, A. L., Mason, I. J., ... Martin, G. R. (2008). Specific regions within the embryonic midbrain and cerebellum require different levels of FGF signaling during development. *Development*, *135*(5), 889–898. https://doi.org/10.1242/dev.011569

Basson, M. A., & van Ravenswaaij-Arts, C. (2015). Functional Insights into Chromatin Remodelling from Studies on CHARGE Syndrome. *Trends in Genetics*, *31*(10), 600–611. https://doi.org/10.1016/J.TIG.2015.05.009

Batsukh, T., Schulz, Y., Wolf, S., Rabe, T. I., Oellerich, T., Urlaub, H., ... Pauli, S. (2012). Identification and Characterization of FAM124B as a Novel Component of a CHD7 and CHD8 Containing Complex. *PLoS ONE*, *7*(12), e52640. https://doi.org/10.1371/journal.pone.0052640

Bergman, J. E. H., Janssen, N., Hoefsloot, L. H., Jongmans, M. C. J., Hofstra, R. M. W., & van Ravenswaaij-Arts, C. M. A. (2011a). CHD7 mutations and CHARGE syndrome: the clinical implications of an expanding phenotype. *Journal of Medical Genetics*, *48*(5), 334–342. https://doi.org/10.1136/jmg.2010.087106

Bergman, J. E. H., Janssen, N., Hoefsloot, L. H., Jongmans, M. C. J., Hofstra, R. M. W., & van Ravenswaaij-Arts, C. M. A. (2011b). CHD7 mutations and CHARGE syndrome: the clinical implications of an expanding phenotype. *Journal of Medical Genetics*, *48*(5), 334–342. https://doi.org/10.1136/jmg.2010.087106

Bergman, J. E. H., Janssen, N., van der Sloot, A. M., de Walle, H. E. K., Schoots, J., Rendtorff, N. D., ... Hofstra, R. M. W. (2012). A novel classification system to predict the pathogenic effects of CHD7 missense variants in CHARGE syndrome. *Human Mutation*, *33*(8), 1251–1260. https://doi.org/10.1002/humu.22106

BLAKE, K. D., & BROWN, D. (1993). CHARGE association looking at the future - the voice of a family support group. *Child: Care, Health and Development*, *19*(6), 395–409. https://doi.org/10.1111/j.1365-2214.1993.tb00744.x

Blake, K. D., Davenport, S. L. H., Hall, B. D., Hefner, M. A., Pagon, R. A., Williams, M. S., ... Graham, J. M. (1998). CHARGE Association: An Update and Review for the Primary Pediatrician. *Clinical Pediatrics*, *37*(3), 159–173. https://doi.org/10.1177/000992289803700302

Blake, K. D., Hartshorne, T. S., Lawand, C., Dailor, A. N., & Thelin, J. W. (2008). Cranial nerve manifestations in CHARGE syndrome. *American Journal of Medical Genetics Part A*, *146A*(5), 585–592. https://doi.org/10.1002/ajmg.a.32179

Blake, K. D., & Prasad, C. (2006). CHARGE syndrome. *Orphanet Journal of Rare Diseases*, *1*(1), 34. https://doi.org/10.1186/1750-1172-1-34

Blustajn, J., Kirsch, C. F. E., Panigrahy, A., & Netchine, I. (2008). Olfactory anomalies in CHARGE syndrome: imaging findings of a potential major diagnostic criterion. *AJNR. American Journal of Neuroradiology*, *29*(7), 1266–9. https://doi.org/10.3174/ajnr.A1099

Bosman, E. A., Penn, A. C., Ambrose, J. C., Kettleborough, R., Stemple, D. L., & Steel, K. P. (2005). Multiple mutations in mouse Chd7 provide models for CHARGE syndrome. *Human Molecular Genetics*, *14*(22), 3463–3476. https://doi.org/10.1093/hmg/ddi375

Braasch, I., Gehrke, A. R., Smith, J. J., Kawasaki, K., Manousaki, T., Pasquier, J., ... Postlethwait, J. H. (2016). The spotted gar genome illuminates vertebrate evolution and facilitates human-teleost comparisons. *Nature Genetics*, *48*(4), 427–437. https://doi.org/10.1038/ng.3526

Brown, C. B., Feiner, L., Lu, M. M., Li, J., Ma, X., Webber, A. L., ... Epstein, J. A. (2001). PlexinA2 and semaphorin signaling during cardiac neural crest development. *Development (Cambridge, England)*, *128*(16), 3071–80. Retrieved from http://www.ncbi.nlm.nih.gov/pubmed/11688557

Brown, D. (2005). CHARGE syndrome ?behaviors?: Challenges or adaptations? *American Journal of Medical Genetics Part A*, *133A*(3), 268–272. https://doi.org/10.1002/ajmg.a.30547

Busa, T., Legendre, M., Bauge, M., Quarello, E., Bretelle, F., Bilan, F., ... Philip, N. (2016). Prenatal findings in children with early postnatal diagnosis of CHARGE syndrome. *Prenatal Diagnosis*, *36*(6), 561–567. https://doi.org/10.1002/pd.4825

Cass, A. N., Servetnick, M. D., & McCune, A. R. (2013). Expression of a lung developmental cassette in the adult and developing zebrafish swimbladder. *Evolution & Development*, *15*(2), 119–132. https://doi.org/10.1111/ede.12022

Chang, N., Sun, C., Gao, L., Zhu, D., Xu, X., Zhu, X., ... Xi, J. J. (2013). Genome editing with RNA-guided Cas9 nuclease in zebrafish embryos. *Cell Research*, *23*(4), 465–72. https://doi.org/10.1038/cr.2013.45

Chen, X., Xu, H., Yuan, P., Fang, F., Huss, M., Vega, V. B., ... Ng, H.-H. (2008). Integration of External Signaling Pathways with the Core Transcriptional Network in Embryonic Stem Cells. *Cell*, *133*(6), 1106–1117. https://doi.org/10.1016/J.CELL.2008.04.043

Chen, Y.-C., Priyadarshini, M., & Panula, P. (2009). Complementary developmental expression of the two tyrosine hydroxylase transcripts in zebrafish. *Histochemistry and Cell Biology*, *132*(4), 375–381. https://doi.org/10.1007/s00418-009-0619-8

Choanal Atresia Causes, Symptoms, Diagnosis, Treatment and Prevention. (n.d.). Retrieved August 29, 2018, from https://www.medindia.net/patients/patientinfo/choanal-atresia.htm

Christian Roberts, 11, born with Charge syndrome is able to grin after new surgery | Daily Mail Online. (n.d.). Retrieved July 3, 2018, from http://www.dailymail.co.uk/femail/article-2529481/A-smile-best-Christmas-gift-Boy-11-born-facial-paralysis-finally-able-grin-groundbreaking-surgery.html

Daubresse, G., Deuring, R., Moore, L., Papoulas, O., Zakrajsek, I., Waldrip, W. R., ... Tamkun, J. W. (1999). The Drosophila kismet gene is related to chromatin-remodeling factors and is required for both segmentation and segment identity. *Development (Cambridge, England)*, *126*(6), 1175–87. Retrieved from http://www.ncbi.nlm.nih.gov/pubmed/10021337

Davenport, S. L. H., Hefner, M. A., & Thelin, J. W. (1986). CHARGE syndrome. Part I. External ear anomalies. *International Journal of Pediatric Otorhinolaryngology*, *12*(2), 137–143. https://doi.org/10.1016/S0165-5876(86)80071-4

Dodé, C., & Hardelin, J.-P. (2010). Clinical genetics of Kallmann syndrome. *Annales d'Endocrinologie*, *71*(3), 149–157. https://doi.org/10.1016/j.ando.2010.02.005

Dürr, H., Flaus, A., Owen-Hughes, T., & Hopfner, K.-P. (2006). Snf2 family ATPases and DExx box helicases: differences and unifying concepts from high-resolution crystal structures. *Nucleic Acids Research*, *34*(15), 4160–7. https://doi.org/10.1093/nar/gkl540

Eissenberg, J. C. (2001). Molecular biology of the chromo domain: an ancient chromatin module comes of age. *Gene*, *275*(1), 19–29. https://doi.org/10.1016/S0378-1119(01)00628-X

Engelen, E., Akinci, U., Bryne, J. C., Hou, J., Gontan, C., Moen, M., ... Poot, R. A. (2011). Sox2 cooperates with Chd7 to regulate genes that are mutated in human syndromes. *Nature Genetics*, *43*(6), 607–611. https://doi.org/10.1038/ng.825

Feng, W., Kawauchi, D., Körkel-Qu, H., Deng, H., Serger, E., Sieber, L., ... Liu, H.-K. (2017). Chd7 is indispensable for mammalian brain development through activation of a neuronal differentiation programme. *Nature Communications*, *8*, 14758. https://doi.org/10.1038/ncomms14758

Feng, W., Khan, M. A., Bellvis, P., Zhu, Z., Bernhardt, O., Herold-Mende, C., & Liu, H.-K. (2013). The Chromatin Remodeler CHD7 Regulates Adult Neurogenesis via Activation of SoxC Transcription Factors. *Cell Stem Cell*, *13*(1), 62–72. https://doi.org/10.1016/j.stem.2013.05.002

Fernell, E., Olsson, V.-A., Karlgren-Leitner, C., Norlin, B., Hagberg, B., & Gillberg, C. (2007). Autistic disorders in children with CHARGE association. *Developmental Medicine & Child Neurology*, *41*(4), 270–272. https://doi.org/10.1111/j.1469-8749.1999.tb00597.x

Fujita, K., Ogawa, R., Kawawaki, S., & Ito, K. (2014). Roles of chromatin remodelers in maintenance mechanisms of multipotency of mouse trunk neural crest cells in the formation of neural crest-derived stem cells. *Mechanisms of Development*, *133*, 126–145. https://doi.org/10.1016/J.MOD.2014.05.001

Fulcoli, F. G., Huynh, T., Scambler, P. J., & Baldini, A. (2009). Tbx1 Regulates the BMP-Smad1 Pathway in a Transcription Independent Manner. *PLoS ONE*, *4*(6), e6049. https://doi.org/10.1371/journal.pone.0006049

Giacomotto, J., & Ségalat, L. (2010). High-throughput screening and small animal models, where are we? *British Journal of Pharmacology*, *160*(2), 204–216. https://doi.org/10.1111/j.1476-5381.2010.00725.x

Goldsmith, J. R., & Jobin, C. (2012). Think small: zebrafish as a model system of human pathology. *Journal of Biomedicine & Biotechnology*, *2012*, 817341. https://doi.org/10.1155/2012/817341

Gregory, L. C., Gevers, E. F., Baker, J., Kasia, T., Chong, K., Josifova, D. J., ... Dattani, M. T. (2013a). Structural pituitary abnormalities associated with CHARGE syndrome. *The Journal of Clinical Endocrinology and Metabolism*, *98*(4), E737-43. https://doi.org/10.1210/jc.2012-3467

Gregory, L. C., Gevers, E. F., Baker, J., Kasia, T., Chong, K., Josifova, D. J., ... Dattani, M. T. (2013b). Structural Pituitary Abnormalities Associated With CHARGE Syndrome. *The Journal of Clinical Endocrinology & Metabolism*, *98*(4), E737–E743. https://doi.org/10.1210/jc.2012-3467

Guyot, J. P., Gacek, R. R., & DiRaddo, P. (1987). The temporal bone anomaly in CHARGE association. *Archives of Otolaryngology--Head & Neck Surgery*, *113*(3), 321–4. Retrieved from http://www.ncbi.nlm.nih.gov/pubmed/3814379

Haldipur, P., & Millen, K. J. (2013). Deficits in early neural tube identity found in CHARGE syndrome. *ELife*, *2*, e01873. https://doi.org/10.7554/eLife.01873

Hall, J. A., & Georgel, P. T. (2007). CHD proteins: a diverse family with strong tiesThis paper is one of a selection of papers published in this Special Issue, entitled 28th International West Coast Chromatin and Chromosome Conference, and has undergone the Journal's usual peer review proces. *Biochemistry and Cell Biology*, *85*(4), 463–476. https://doi.org/10.1139/O07-063

Hanchate, N. K., Giacobini, P., Lhuillier, P., Parkash, J., Espy, C., Fouveaut, C., ... Dodé, C. (2012). SEMA3A, a gene involved in axonal pathfinding, is mutated in patients with Kallmann syndrome. *PLoS Genetics*, *8*(8), e1002896. https://doi.org/10.1371/journal.pgen.1002896

Harris, T. W., Chen, N., Cunningham, F., Tello-Ruiz, M., Antoshechkin, I., Bastiani, C., ... Stein, L. D. (2004). WormBase: a multi-species resource for nematode biology and genomics. *Nucleic Acids Research*, *32*(Database issue), D411-7. https://doi.org/10.1093/nar/gkh066

Hartshorne, T. S., Grialou, T. L., & Parker, K. R. (2005). Autistic-like behavior in CHARGE syndrome. *American Journal of Medical Genetics Part A*, *133A*(3), 257–261. https://doi.org/10.1002/ajmg.a.30545

Hartshorne, T. S., Hefner, M. A., & Davenport, S. L. H. (2005). Behavior in CHARGE syndrome: Introduction to the special topic. *American Journal of Medical Genetics Part A*, *133A*(3), 228–231. https://doi.org/10.1002/ajmg.a.30541

HARTSHORNE, T. S., HEUSSLER, H. S., DAILOR, A. N., WILLIAMS, G. L., PAPADOPOULOS, D., & BRANDT, K. K. (2009). Sleep disturbances in CHARGE syndrome: types and relationships with behavior and caregiver well-being. *Developmental Medicine & Child Neurology*, *51*(2), 143–150. https://doi.org/10.1111/j.1469-8749.2008.03146.x

He, D., Marie, C., Zhao, C., Kim, B., Wang, J., Deng, Y., ... Lu, Q. R. (2016). Chd7 cooperates with Sox10 and regulates the onset of CNS myelination and remyelination. *Nature Neuroscience*, *19*(5), 678–689. https://doi.org/10.1038/nn.4258

Hefner, M. (1999). *Diagnosis, Genetics and Prenatal Diagnosis in CHARGE*. Retrieved from http://www.chargesyndrome.org/wp-content/uploads/2016/05/Diagnosis-Genetics-and-Prenatal-Diagnosis.pdf

Ho, L., Ronan, J. L., Wu, J., Staahl, B. T., Chen, L., Kuo, A., ... Crabtree, G. R. (2009). *An embryonic stem cell chromatin remodeling complex, esBAF, is essential for embryonic stem cell self-renewal and pluripotency DEVELOPMENTAL BIOLOGY. PNAS March* (Vol. 31). Retrieved from http://www.pnas.org/content/pnas/106/13/5181.full.pdf

Hoffman, E. J., Turner, K. J., Fernandez, J. M., Cifuentes, D., Ghosh, M., Ijaz, S., ... Giraldez, A. J. (2016). Estrogens Suppress a Behavioral Phenotype in Zebrafish Mutants of the Autism Risk Gene, CNTNAP2. *Neuron*, *89*(4), 725–33. https://doi.org/10.1016/j.neuron.2015.12.039

Hudson, A., & Blake, K. (2016). Newly Emerging Feeding Difficulties in a 33-Year-Old Adult With CHARGE Syndrome. *Journal of Clinical Medicine Research*, *8*(1), 56–8. https://doi.org/10.14740/jocmr2288w

Hurd, E. A., Capers, P. L., Blauwkamp, M. N., Adams, M. E., Raphael, Y., Poucher, H. K., & Martin, D. M. (2007). Loss of Chd7 function in gene-trapped reporter mice is embryonic lethal and associated with severe defects in multiple developing tissues. *Mammalian Genome*, *18*(2), 94–104. https://doi.org/10.1007/s00335-006-0107-6

Hurd, E. A., Poucher, H. K., Cheng, K., Raphael, Y., & Martin, D. M. (2010). The ATP-dependent chromatin remodeling enzyme CHD7 regulates pro-neural gene expression and neurogenesis in the inner ear. *Development*, *137*(18), 3139–3150. https://doi.org/10.1242/dev.047894

Hwang, W. Y., Fu, Y., Reyon, D., Maeder, M. L., Kaini, P., Sander, J. D., ... Marechal, A. (2013). Heritable and Precise Zebrafish Genome Editing Using a CRISPR-Cas System. *PLoS ONE*, *8*(7), e68708. https://doi.org/10.1371/journal.pone.0068708

Ingham, P. W. (1983). Differential expression of bithorax complex genes in the absence of the extra sex combs and trithorax genes. *Nature*, *306*(5943), 591–593. https://doi.org/10.1038/306591a0

Issekutz, K. A., Graham, J. M., Prasad, C., Smith, I. M., & Blake, K. D. (2005). An epidemiological analysis of CHARGE syndrome: Preliminary results from a Canadian study. *American Journal of Medical Genetics Part A*, *133A*(3), 309–317. https://doi.org/10.1002/ajmg.a.30560

Janssen, N., Bergman, J. E. H., Swertz, M. A., Tranebjaerg, L., Lodahl, M., Schoots, J., ... Hoefsloot, L. H. (2012). Mutation update on the CHD7 gene involved in CHARGE syndrome. *Human Mutation*, *33*(8), 1149–1160. https://doi.org/10.1002/humu.22086

Jao, L.-E., Maddison, L., Chen, W., & Burgess, S. M. (2008). Using retroviruses as a mutagenesis tool to explore the zebrafish genome. *Briefings in Functional Genomics & Proteomics*, *7*(6), 427–43. https://doi.org/10.1093/bfgp/eln038

Jiang, Y., Yuen, R. K. C., Jin, X., Wang, M., Chen, N., Wu, X., ... Scherer, S. W. (2013). Detection of Clinically Relevant Genetic Variants in Autism Spectrum Disorder by Whole-Genome Sequencing. *The American Journal of Human Genetics*, *93*(2), 249–

263. https://doi.org/10.1016/j.ajhg.2013.06.012

Jongmans, M. C. J., Admiraal, R. J., van der Donk, K. P., Vissers, L. E. L. M., Baas, A. F., Kapusta, L., ... van Ravenswaaij, C. M. A. (2006). CHARGE syndrome: the phenotypic spectrum of mutations in the CHD7 gene. *Journal of Medical Genetics*, *43*(4), 306–14. https://doi.org/10.1136/jmg.2005.036061

Jongmans, M. C. J., Hoefsloot, L. H., van der Donk, K. P., Admiraal, R. J., Magee, A., van de Laar, I., ... van Ravenswaaij, C. M. A. (2008). Familial CHARGE syndrome and theCHD7 gene: A recurrent missense mutation, intrafamilial recurrence and variability. *American Journal of Medical Genetics Part A*, *146A*(1), 43–50. https://doi.org/10.1002/ajmg.a.31921

Jongmans, M., van Ravenswaaij-Arts, C., Pitteloud, N., Ogata, T., Sato, N., Claahsen-van der Grinten, H., ... Hoefsloot, L. (2009). *CHD7* mutations in patients initially diagnosed with Kallmann syndrome - the clinical overlap with CHARGE syndrome. *Clinical Genetics*, *75*(1), 65–71. https://doi.org/10.1111/j.1399-0004.2008.01107.x

Kabashi, E., Brustein, E., Champagne, N., & Drapeau, P. (2011). Zebrafish models for the functional genomics of neurogenetic disorders. *Biochimica et Biophysica Acta (BBA) - Molecular Basis of Disease*, *1812*(3), 335–345. https://doi.org/10.1016/j.bbadis.2010.09.011

Kaliakatsos, M., Giannakopoulos, A., Fryssira, H., Kanariou, M., Skiathitou, A.-V., Siahanidou, T., ... Tzetis, M. (2010). Combined microdeletions and CHD7 mutation causing severe CHARGE/DiGeorge syndrome: clinical presentation and molecular investigation by array-CGH. *Journal of Human Genetics*, *55*(11), 761–763. https://doi.org/10.1038/jhg.2010.95

Kalueff, A. V, Stewart, A. M., & Gerlai, R. (2014). Zebrafish as an emerging model for studying complex brain disorders. *Trends in Pharmacological Sciences*, *35*(2), 63–75. https://doi.org/10.1016/j.tips.2013.12.002

Känsäkoski, J., Fagerholm, R., Laitinen, E.-M., Vaaralahti, K., Hackman, P., Pitteloud, N., ... Tommiska, J. (2014). Mutation screening of SEMA3A and SEMA7A in patients with congenital hypogonadotropic hypogonadism. *Pediatric Research*, *75*(5), 641–4. https://doi.org/10.1038/pr.2014.23

Kari, G., Rodeck, U., & Dicker, A. P. (2007). Zebrafish: An Emerging Model System for Human Disease and Drug Discovery. *Clinical Pharmacology & Therapeutics*, *82*(1), 70–80. https://doi.org/10.1038/sj.clpt.6100223

Karlsson, J., von Hofsten, J., & Olsson, P.-E. (2001). Generating Transparent Zebrafish: A Refined Method to Improve Detection of Gene Expression During Embryonic Development. *Marine Biotechnology*, *3*(6), 0522–0527. https://doi.org/10.1007/s1012601-0053-4

Khan, N., Syed, D. N., Ahmad, N., & Mukhtar, H. (2013). Fisetin: a dietary antioxidant for health promotion. *Antioxidants & Redox Signaling*, *19*(2), 151–62. https://doi.org/10.1089/ars.2012.4901

Kim, H.-G., Kurth, I., Lan, F., Meliciani, I., Wenzel, W., Eom, S. H., ... Layman, L. C. (2008). Mutations in CHD7, encoding a chromatin-remodeling protein, cause idiopathic hypogonadotropic hypogonadism and Kallmann syndrome. *American Journal of Human Genetics*, *83*(4), 511–9. https://doi.org/10.1016/j.ajhg.2008.09.005

Kim, K. H., & Roberts, C. W. M. (2013a). CHD7 in charge of neurogenesis. *Cell Stem Cell*, *13*(1), 1–2. https://doi.org/10.1016/j.stem.2013.06.010

Kim, K. H., & Roberts, C. W. M. (2013b). CHD7 in Charge of Neurogenesis. *Cell Stem Cell*, *13*(1), 1–2. https://doi.org/10.1016/j.stem.2013.06.010

Kokel, D., Bryan, J., Laggner, C., White, R., Cheung, C. Y. J., Mateus, R., ... Peterson, R. T. (2010). Rapid behavior-based identification of neuroactive small molecules in the zebrafish. *Nature Chemical Biology*, *6*(3), 231–237. https://doi.org/10.1038/nchembio.307

Kormish, J. D., Sinner, D., & Zorn, A. M. (2009). Interactions between SOX factors and Wnt/β-catenin signaling in development and disease. *Developmental Dynamics*, *239*(1), NA-NA. https://doi.org/10.1002/dvdy.22046

Krauzlis, R. J., Lovejoy, L. P., & Zénon, A. (2013). Superior Colliculus and Visual Spatial Attention. *Annual Review of Neuroscience*, *36*(1), 165–182. https://doi.org/10.1146/annurev-neuro-062012-170249

Lalani, S. R., Hefner, M. A., Belmont, J. W., & Davenport, S. L. (1993a). *CHARGE Syndrome. GeneReviews(®)*. University of Washington, Seattle. Retrieved from http://www.ncbi.nlm.nih.gov/pubmed/20301296

Lalani, S. R., Hefner, M. A., Belmont, J. W., & Davenport, S. L. (1993b). *CHARGE Syndrome. GeneReviews®*. University of Washington, Seattle. Retrieved from http://www.ncbi.nlm.nih.gov/pubmed/20301296

Lalani, S. R., Safiullah, A. M., Molinari, L. M., Fernbach, S. D., & Martin, D. M. (2004). SEMA3E mutation in a patient with CHARGE syndrome. *J Med Genet*, *41*, 94. https://doi.org/10.1136/jmg.2003.017640

Layman, W., Hurd, E., & Martin, D. (2010). Chromodomain proteins in development: lessons from CHARGE syndrome. *Clinical Genetics*, *78*(1), 11–20. https://doi.org/10.1111/j.1399-0004.2010.01446.x

Layman, W. S., Hurd, E. A., & Martin, D. M. (2010). Chromodomain proteins in development: Lessons from CHARGE syndrome. *Clinical Genetics*, *78*(1), 11–20. https://doi.org/10.1111/j.1399-0004.2010.01446.x

Lin, A. E., Siebert, J. R., & Graham, J. M. (1990). Central nervous system malformations in the CHARGE association. *American Journal of Medical Genetics*, *37*(3), 304–310. https://doi.org/10.1002/ajmg.1320370303

Liu, L., Yu, T., Wang, L., Mo, X., & Yu, Y. (2014). A novel CHD7 mutation in a Chinese patient with CHARGE syndrome. *Meta Gene*, *2*, 469–478. https://doi.org/10.1016/J.MGENE.2014.06.002

Lowery, L. A., De Rienzo, G., Gutzman, J. H., & Sive, H. (2009). Characterization and classification of zebrafish brain morphology mutants. *Anatomical Record (Hoboken, N.J. : 2007)*, *292*(1), 94–106. https://doi.org/10.1002/ar.20768

Maher, P., Dargusch, R., Bodai, L., Gerard, P. E., Purcell, J. M., & Marsh, J. L. (2011). ERK activation by the polyphenols fisetin and resveratrol provides neuroprotection in multiple models of Huntington's disease. *Human Molecular Genetics*, *20*(2), 261–270. https://doi.org/10.1093/hmg/ddq460

Markaki, M., & Tavernarakis, N. (2010). Modeling human diseases in Caenorhabditis elegans. *Biotechnology Journal*, *5*(12), 1261–1276. https://doi.org/10.1002/biot.201000183

Martin, D. M. (2010). Chromatin Remodeling in Development and Disease: Focus on CHD7. *PLoS Genetics*, *6*(7), e1001010. https://doi.org/10.1371/journal.pgen.1001010

Martin, D. M., Sheldon, S., & Gorski, J. L. (2001). CHARGE association with choanal atresia and inner ear hypoplasia in a child with a de novo chromosome translocation t(2;7)(p14;q21.11). *American Journal of Medical Genetics*, *99*(2), 115–9. Retrieved from http://www.ncbi.nlm.nih.gov/pubmed/11241468

McMacken, G., Cox, D., Roos, A., Müller, J., Whittaker, R., & Lochmüller, H. (2018). The

beta-adrenergic agonist salbutamol modulates neuromuscular junction formation in zebrafish models of human myasthenic syndromes. *Human Molecular Genetics*, *27*(9), 1556–1564. https://doi.org/10.1093/hmg/ddy062

Mishima, Y., & Tomari, Y. (2016). Codon Usage and 3′ UTR Length Determine Maternal mRNA Stability in Zebrafish. *Molecular Cell*, *61*(6), 874–885. https://doi.org/10.1016/j.molcel.2016.02.027

Morgan, D., Bailey, M., Phelps, P., Bellman, S., Grace, A., & Wyse, R. (1993). Ear-nose-throat abnormalities in the CHARGE association. *Archives of Otolaryngology--Head & Neck Surgery*, *119*(1), 49–54. Retrieved from http://www.ncbi.nlm.nih.gov/pubmed/8417743

Murphey, R. D., Stern, H. M., Straub, C. T., & Zon, L. I. (2006). A Chemical Genetic Screen for Cell Cycle Inhibitors in Zebrafish Embryos. *Chemical Biology & Drug Design*, *68*(4), 213–219. https://doi.org/10.1111/j.1747-0285.2006.00439.x

Neale, B. M., Kou, Y., Liu, L., Ma'ayan, A., Samocha, K. E., Sabo, A., ... Daly, M. J. (2012). Patterns and rates of exonic de novo mutations in autism spectrum disorders. *Nature*, *485*(7397), 242–245. https://doi.org/10.1038/nature11011

O'Roak, B. J., Vives, L., Girirajan, S., Karakoc, E., Krumm, N., Coe, B. P., ... Eichler, E. E. (2012). Sporadic autism exomes reveal a highly interconnected protein network of de novo mutations. *Nature*, *485*(7397), 246–250. https://doi.org/10.1038/nature10989

Okuno, H., Renault Mihara, F., Ohta, S., Fukuda, K., Kurosawa, K., Akamatsu, W., ... Okano, H. (2017). CHARGE syndrome modeling using patient-iPSCs reveals defective migration of neural crest cells harboring CHD7 mutations. *ELife*, *6*. https://doi.org/10.7554/eLife.21114

Panula, P., Sallinen, V., Sundvik, M., Kolehmainen, J., Torkko, V., Tiittula, A., ... Podlasz, P. (2006). Modulatory Neurotransmitter Systems and Behavior: Towards Zebrafish Models of Neurodegenerative Diseases. *Zebrafish*, *3*(2), 235–247. https://doi.org/10.1089/zeb.2006.3.235

Patten, S. A., Aggad, D., Martinez, J., Tremblay, E., Petrillo, J., Armstrong, G. A. B., ... Drapeau, P. (2017). Neuroleptics as therapeutic compounds stabilizing neuromuscular transmission in amyotrophic lateral sclerosis. *JCI Insight*, *2*(22). https://doi.org/10.1172/jci.insight.97152

Patten, S. A., Armstrong, G. A. B., Lissouba, A., Kabashi, E., Parker, J. A., & Drapeau, P. (2014). Fishing for causes and cures of motor neuron disorders. *Disease Models & Mechanisms*, *7*(7), 799–809. https://doi.org/10.1242/dmm.015719

Patten, S. A., Jacobs-McDaniels, N. L., Zaouter, C., Drapeau, P., Albertson, R. C., Moldovan, F., ... Zohar, Y. (2012). Role of Chd7 in Zebrafish: A Model for CHARGE Syndrome. *PLoS ONE*, *7*(2), e31650. https://doi.org/10.1371/journal.pone.0031650

Patten, S. A., Parker, J. A., Wen, X.-Y., & Drapeau, P. (2016). Simple animal models for amyotrophic lateral sclerosis drug discovery. *Expert Opinion on Drug Discovery*, *11*(8), 797–804. https://doi.org/10.1080/17460441.2016.1196183

Pauli, S., Bajpai, R., & Borchers, A. (2017). CHARGEd with neural crest defects. *American Journal of Medical Genetics Part C: Seminars in Medical Genetics*. https://doi.org/10.1002/ajmg.c.31584

Pauli, S., Pieper, L., Häberle, J., Grzmil, P., Burfeind, P., Steckel, M., ... Michelmann, H. (2009). Proven germline mosaicism in a father of two children with CHARGE syndrome. *Clinical Genetics*, *75*(5), 473–479. https://doi.org/10.1111/j.1399-0004.2009.01151.x

Payne, S., Burney, M. J., McCue, K., Popal, N., Davidson, S. M., Anderson, R. H., & Scambler, P. J. (2015). A critical role for the chromatin remodeller CHD7 in anterior

mesoderm during cardiovascular development. *Developmental Biology*, *405*(1), 82–95. https://doi.org/10.1016/j.ydbio.2015.06.017

Pazin, M. J., & Kadonaga, J. T. (1997). SWI2/SNF2 and related proteins: ATP-driven motors that disrupt protein-DNA interactions? *Cell*, *88*(6), 737–40. Retrieved from http://www.ncbi.nlm.nih.gov/pubmed/9118215

Peterson, C. L., Dingwall, A., & Scott, M. P. (1994). Five SWI/SNF gene products are components of a large multisubunit complex required for transcriptional enhancement. *Proceedings of the National Academy of Sciences of the United States of America*, *91*(8), 2905–8. Retrieved from http://www.ncbi.nlm.nih.gov/pubmed/8159677

Phillips, J. B., & Westerfield, M. (2014). Zebrafish models in translational research: tipping the scales toward advancements in human health. *Disease Models & Mechanisms*, *7*(7). Retrieved from http://dmm.biologists.org/content/7/7/739?ijkey=30193e2a63fcf262770cc725af6770b0c558eefa&keytype2=tf_ipsecsha

Pietri, T., Romano, S. A., Pérez-Schuster, V., Boulanger-Weill, J., Candat, V., & Sumbre, G. (2017). The Emergence of the Spatial Structure of Tectal Spontaneous Activity Is Independent of Visual Inputs. *Cell Reports*, *19*(5), 939–948. https://doi.org/10.1016/j.celrep.2017.04.015

Rafferty, S. A., & Quinn, T. A. (2018). A beginner's guide to understanding and implementing the genetic modification of zebrafish. *Progress in Biophysics and Molecular Biology*. https://doi.org/10.1016/J.PBIOMOLBIO.2018.07.005

Reya, T., & Clevers, H. (2005). Wnt signalling in stem cells and cancer. *Nature*, *434*(7035), 843–850. https://doi.org/10.1038/nature03319

Robertson, G. N., McGee, C. A. S., Dumbarton, T. C., Croll, R. P., & Smith, F. M. (2007). Development of the swimbladder and its innervation in the zebrafish,Danio rerio. *Journal of Morphology*, *268*(11), 967–985. https://doi.org/10.1002/jmor.10558

Saleem, S., & Kannan, R. R. (2018). Zebrafish: an emerging real-time model system to study Alzheimer's disease and neurospecific drug discovery. *Cell Death Discovery*, *4*(1), 45. https://doi.org/10.1038/s41420-018-0109-7

Samarut, É., Lissouba, A., Drapeau, P., Wittwer, C., Thomas, H., Vossen, R., ... Moreno-Mateos, M. (2016). A simplified method for identifying early CRISPR-induced indels in zebrafish embryos using High Resolution Melting analysis. *BMC Genomics*, *17*(1), 547. https://doi.org/10.1186/s12864-016-2881-1

Samarut, É., Swaminathan, A., Riché, R., Liao, M., Hassan-Abdi, R., Renault, S., ... Drapeau, P. (2018). γ-Aminobutyric acid receptor alpha 1 subunit loss of function causes genetic generalized epilepsy by impairing inhibitory network neurodevelopment. *Epilepsia*, *59*(11), 2061–2074. https://doi.org/10.1111/epi.14576

Sanlaville, D., Etchevers, H. C., Gonzales, M., Martinovic, J., Clément-Ziza, M., Delezoide, A.-L., ... Attié-Bitach, T. (2006). Phenotypic spectrum of CHARGE syndrome in fetuses with CHD7 truncating mutations correlates with expression during human development. *Journal of Medical Genetics*, *43*(3), 211–217. https://doi.org/10.1136/jmg.2005.036160

Sanlaville, D., & Verloes, A. (2007). CHARGE syndrome: an update. *European Journal of Human Genetics*, *15*(4), 389–399. https://doi.org/10.1038/sj.ejhg.5201778

Schnetz, M. P., Bartels, C. F., Shastri, K., Balasubramanian, D., Zentner, G. E., Balaji, R., ... Scacheri, P. C. (2009a). Genomic distribution of CHD7 on chromatin tracks H3K4 methylation patterns. *Genome Research*, *19*(4), 590–601. https://doi.org/10.1101/gr.086983.108

Schnetz, M. P., Bartels, C. F., Shastri, K., Balasubramanian, D., Zentner, G. E., Balaji, R., ...

Scacheri, P. C. (2009b). Genomic distribution of CHD7 on chromatin tracks H3K4 methylation patterns. *Genome Research*, *19*(4), 590–601. https://doi.org/10.1101/gr.086983.108

Schnetz, M. P., Handoko, L., Akhtar-Zaidi, B., Bartels, C. F., Pereira, C. F., Fisher, A. G., ... Scacheri, P. C. (2010a). CHD7 Targets Active Gene Enhancer Elements to Modulate ES Cell-Specific Gene Expression. *PLoS Genetics*, *6*(7), e1001023. https://doi.org/10.1371/journal.pgen.1001023

Schnetz, M. P., Handoko, L., Akhtar-Zaidi, B., Bartels, C. F., Pereira, C. F., Fisher, A. G., ... Scacheri, P. C. (2010b). CHD7 Targets Active Gene Enhancer Elements to Modulate ES Cell-Specific Gene Expression. *PLoS Genetics*, *6*(7), e1001023. https://doi.org/10.1371/journal.pgen.1001023

Shao, M., Wang, M., Liu, Y.-Y., Ge, Y.-W., Zhang, Y.-J., & Shi, D.-L. (2017). Vegetally localised Vrtn functions as a novel repressor to modulate *bmp2b* transcription during dorsoventral patterning in zebrafish. *Development*, *144*(18), 3361–3374. https://doi.org/10.1242/dev.152553

Shimono, K., Shimono, Y., Shimokata, K., Ishiguro, N., & Takahashi, M. (2005). Microspherule Protein 1, Mi-2β, and RET Finger Protein Associate in the Nucleolus and Up-regulate Ribosomal Gene Transcription. *Journal of Biological Chemistry*, *280*(47), 39436–39447. https://doi.org/10.1074/jbc.M507356200

Siebert, J. R., Graham, J. M., & MacDonald, C. (1985). Pathologic features of the CHARGE association: Support for involvement of the neural crest. *Teratology*, *31*(3), 331–336. https://doi.org/10.1002/tera.1420310303

Sporik, R., Dinwiddie, R., & Wallis, C. (1997). Lung involvement in the multisystem syndrome CHARGE association. *Eur Respir J ©ERS Journals Ltd Eur Respir J*, *10*(10), 1354–1355. https://doi.org/10.1183/09031936.97.10061354

Srinivasan, S., Dorighi, K. M., & Tamkun, J. W. (2008). Drosophila Kismet regulates histone H3 lysine 27 methylation and early elongation by RNA polymerase II. *PLoS Genetics*, *4*(10), e1000217. https://doi.org/10.1371/journal.pgen.1000217

Steffen, P. A., & Ringrose, L. (2014). What are memories made of? How Polycomb and Trithorax proteins mediate epigenetic memory. *Nature Reviews Molecular Cell Biology*, *15*(5), 340–356. https://doi.org/10.1038/nrm3789

Stern, H. M., & Zon, L. I. (2003). Cancer genetics and drug discovery in the zebrafish. *Nature Reviews Cancer*, *3*(7), 533–539. https://doi.org/10.1038/nrc1126

Steventon, B., Mayor, R., & Streit, A. (2014). Neural crest and placode interaction during the development of the cranial sensory system. *Developmental Biology*, *389*(1), 28–38. https://doi.org/10.1016/j.ydbio.2014.01.021

Stokes, D. G., & Perry, R. P. (1995). DNA-binding and chromatin localization properties of CHD1. *Molecular and Cellular Biology*, *15*(5), 2745–53. Retrieved from http://www.ncbi.nlm.nih.gov/pubmed/7739555

Sulston, J. E., Schierenberg, E., White, J. G., & Thomson, J. N. (1983). The embryonic cell lineage of the nematode Caenorhabditis elegans. *Developmental Biology*, *100*(1), 64–119. Retrieved from http://www.ncbi.nlm.nih.gov/pubmed/6684600

Syed, D. N., Afaq, F., Maddodi, N., Johnson, J. J., Sarfaraz, S., Ahmad, A., ... Mukhtar, H. (2011). Inhibition of human melanoma cell growth by the dietary flavonoid fisetin is associated with disruption of Wnt/β-catenin signaling and decreased Mitf levels. *The Journal of Investigative Dermatology*, *131*(6), 1291–9. https://doi.org/10.1038/jid.2011.6

Tamplin, O. J., White, R. M., Jing, L., Kaufman, C. K., Lacadie, S. A., Li, P., ... Zon, L. I. (2012). Small molecule screening in zebrafish: swimming in potential drug therapies.

Wiley Interdisciplinary Reviews: Developmental Biology, *1*(3), 459–468. https://doi.org/10.1002/wdev.37

Tellier, A. L., Cormier-Daire, V., Abadie, V., Amiel, J., Sigaudy, S., Bonnet, D., ... Lyonnet, S. (1998). CHARGE syndrome: report of 47 cases and review. *American Journal of Medical Genetics*, *76*(5), 402–9. Retrieved from http://www.ncbi.nlm.nih.gov/pubmed/9556299

Tellier, A. L., Lyonnet, S., Cormier-Daire, V., de Lonlay, P., Abadie, V., Baumann, C., ... Munnich, A. (1996). Increased paternal age in CHARGE association. *Clinical Genetics*, *50*(6), 548–50. Retrieved from http://www.ncbi.nlm.nih.gov/pubmed/9147897

Thelin, J. W., & Fussner, J. C. (2005). Factors related to the development of communication in CHARGE syndrome. *American Journal of Medical Genetics Part A*, *133A*(3), 282–290. https://doi.org/10.1002/ajmg.a.30550

Thompson, A. W., Vanwalleghem, G. C., Heap, L. A., & Scott, E. K. (2016). Functional Profiles of Visual-, Auditory-, and Water Flow-Responsive Neurons in the Zebrafish Tectum. *Current Biology*, *26*(6), 743–754. https://doi.org/10.1016/j.cub.2016.01.041

Thompson, B. A., Tremblay, V., Lin, G., & Bochar, D. A. (2008). CHD8 is an ATP-dependent chromatin remodeling factor that regulates beta-catenin target genes. *Molecular and Cellular Biology*, *28*(12), 3894–904. https://doi.org/10.1128/MCB.00322-08

Tropepe, V., & Sive, H. L. (2003). Can zebrafish be used as a model to study the neurodevelopmental causes of autism? *Genes, Brain and Behavior*, *2*(5), 268–281. https://doi.org/10.1034/j.1601-183X.2003.00038.x

Ufartes, R., Schwenty-Lara, J., Freese, L., Neuhofer, C., Möller, J., Wehner, P., ... Pauli, S. (2018). Sema3a plays a role in the pathogenesis of CHARGE syndrome. *Human Molecular Genetics*, *27*(8), 1343–1352. https://doi.org/10.1093/hmg/ddy045

Van Battum, E. Y., Brignani, S., & Pasterkamp, R. J. (2015). Axon guidance proteins in neurological disorders. *The Lancet Neurology*, *14*(5), 532–546. https://doi.org/10.1016/S1474-4422(14)70257-1

van Ravenswaaij-Arts, C., & Martin, D. M. (2017). New insights and advances in CHARGE syndrome: Diagnosis, etiologies, treatments, and research discoveries. *American Journal of Medical Genetics, Part C: Seminars in Medical Genetics*, *175*(4), 397–406. https://doi.org/10.1002/ajmg.c.31592

Vissers, L. E. L. M., van Ravenswaaij, C. M. A., Admiraal, R., Hurst, J. A., de Vries, B. B. A., Janssen, I. M., ... van Kessel, A. G. (2004a). Mutations in a new member of the chromodomain gene family cause CHARGE syndrome. *Nature Genetics*, *36*(9), 955–957. https://doi.org/10.1038/ng1407

Vissers, L. E. L. M., van Ravenswaaij, C. M. A., Admiraal, R., Hurst, J. A., de Vries, B. B. A., Janssen, I. M., ... van Kessel, A. G. (2004b). Mutations in a new member of the chromodomain gene family cause CHARGE syndrome. *Nature Genetics*, *36*(9), 955–957. https://doi.org/10.1038/ng1407

Wade, P. A., Jones, P. L., Vermaak, D., Veenstra, G. J., Imhof, A., Sera, T., ... Wolffe, A. P. (1998). Histone deacetylase directs the dominant silencing of transcription in chromatin: association with MeCP2 and the Mi-2 chromodomain SWI/SNF ATPase. *Cold Spring Harbor Symposia on Quantitative Biology*, *63*, 435–45. Retrieved from http://www.ncbi.nlm.nih.gov/pubmed/10384308

White, R. M., Sessa, A., Burke, C., Bowman, T., LeBlanc, J., Ceol, C., ... Zon, L. I. (2008). Transparent Adult Zebrafish as a Tool for In Vivo Transplantation Analysis. *Cell Stem Cell*, *2*(2), 183–189. https://doi.org/10.1016/j.stem.2007.11.002

Williams, M. S. (2005). Speculations on the pathogenesis of CHARGE syndrome. *American*

Journal of Medical Genetics Part A, *133A*(3), 318–325. https://doi.org/10.1002/AJMG.A.30561

Winata, C. L., Korzh, S., Kondrychyn, I., Zheng, W., Korzh, V., & Gong, Z. (2009). Development of zebrafish swimbladder: The requirement of Hedgehog signaling in specification and organization of the three tissue layers. *Developmental Biology*, *331*(2), 222–236. https://doi.org/10.1016/j.ydbio.2009.04.035

Woodage, T., Basrai, M. A., Baxevanis, A. D., Hieter, P., & Collins, F. S. (1997a). Characterization of the CHD family of proteins. *Proceedings of the National Academy of Sciences of the United States of America*, *94*(21), 11472–7. Retrieved from http://www.ncbi.nlm.nih.gov/pubmed/9326634

Woodage, T., Basrai, M. A., Baxevanis, A. D., Hieter, P., & Collins, F. S. (1997b). Characterization of the CHD family of proteins. *Proceedings of the National Academy of Sciences of the United States of America*, *94*(21), 11472–7. https://doi.org/10.1073/PNAS.94.21.11472

Woods, I. G., Lyons, D. A., Voas, M. G., Pogoda, H.-M., & Talbot, W. S. (2006). nsf Is Essential for Organization of Myelinated Axons in Zebrafish. *Current Biology*, *16*(7), 636–648. https://doi.org/10.1016/j.cub.2006.02.067

Xu, J., Zhang, R., Zhang, T., Zhao, G., Huang, Y., Wang, H., & Liu, J.-X. (2017). Copper impairs zebrafish swimbladder development by down-regulating Wnt signaling. *Aquatic Toxicology*, *192*, 155–164. https://doi.org/10.1016/j.aquatox.2017.09.018

Yin, A., Korzh, S., Winata, C. L., Korzh, V., & Gong, Z. (2011). Wnt Signaling Is Required for Early Development of Zebrafish Swimbladder. *PLoS ONE*, *6*(3), e18431. https://doi.org/10.1371/journal.pone.0018431

Yin, A., Korzh, V., & Gong, Z. (2012a). Perturbation of zebrafish swimbladder development by enhancing Wnt signaling in Wif1 morphants. *Biochimica et Biophysica Acta (BBA) - Molecular Cell Research*, *1823*(2), 236–244. https://doi.org/10.1016/j.bbamcr.2011.09.018

Yin, A., Korzh, V., & Gong, Z. (2012b). Perturbation of zebrafish swimbladder development by enhancing Wnt signaling in Wif1 morphants. *Biochimica et Biophysica Acta (BBA) - Molecular Cell Research*, *1823*(2), 236–244. https://doi.org/10.1016/J.BBAMCR.2011.09.018

Yu, T., Meiners, L. C., Danielsen, K., Wong, M. T., Bowler, T., Reinberg, D., … Basson, M. A. (2013). Deregulated FGF and homeotic gene expression underlies cerebellar vermis hypoplasia in CHARGE syndrome. *ELife*, *2*. https://doi.org/10.7554/eLife.01305

Zentner, G. E., Hurd, E. A., Schnetz, M. P., Handoko, L., Wang, C., Wang, Z., … Scacheri, P. C. (2010). CHD7 functions in the nucleolus as a positive regulator of ribosomal RNA biogenesis. *Human Molecular Genetics*, *19*(18), 3491–3501. https://doi.org/10.1093/hmg/ddq265

Zentner, G. E., Layman, W. S., Martin, D. M., & Scacheri, P. C. (2010a). Molecular and phenotypic aspects of CHD7 mutation in CHARGE syndrome. *American Journal of Medical Genetics. Part A*, *152A*(3), 674–86. https://doi.org/10.1002/ajmg.a.33323

Zentner, G. E., Layman, W. S., Martin, D. M., & Scacheri, P. C. (2010b). Molecular and phenotypic aspects of *CHD7* mutation in CHARGE syndrome. *American Journal of Medical Genetics Part A*, *152A*(3), 674–686. https://doi.org/10.1002/ajmg.a.33323

ZFIN Anatomy Ontology: swim bladder. (n.d.). Retrieved September 19, 2018, from https://zfin.org/ZFA:0000076

ZFIN The Zebrafish Information Network. (n.d.). Retrieved November 4, 2018, from http://zfin.org/